UNIVERSIDAD AUTÓNOMA DE MADRID

ALUMINIUM-AIR BATTERIES: STUDY OF COMMERCIAL ALUMINIUM ALLOYS AS ANODES

PhD candidate:

Mikel Pino Martinez

Directors:

Prof. Dr. Pilar Ocón Esteban

Prof. Dr. Enrique Fatás Lahoz

Index

ABSTRACT

Abstract

Due to the constant increase in electric demand of our society, new energy production, transport and storage systems will play a key role in a near future. Regarding to energy storage systems, electrochemical energy storage is a very interesting candidate because of the just one step conversion of electric energy in chemical energy and reversely.

A lot of electrochemical energy storage systems are commercially available nowadays. From primary alkaline batteries to large scale Li-ion cells, going through Ni-Cd, lead acid, Zn-air, etc. technologies. Every system presents some favourable properties as well as some drawbacks, and specific operation parameters. This makes each battery technology suitable for certain applications where other systems could not work so properly. The latter makes all these different technologies coexist at the same time, what is called “the energy storage mix”, and it results the most accurate approach for the supply of quite different and specific electronic devices, electric vehicles, large scale energy storage, etc.

However, due to the rapid technological progress, some medium-future applications could not be successfully energy supplied by the existing commercial technologies. And so, new electrochemical energy storage systems are needed to face the challenges ahead.

In this sense, metal-air battery systems have demonstrated the capability to storage big amounts of energy in low volume and weight, postulating themselves as one of the technologies that will shape “the mix” of the future. Inside this battery family, aluminium-air presents one of the higher gravimetric and volumetric specific energies, while being, aluminium, the fourth most abundant element in the Earth, and so, very cheap, easily available and expanded metal.

In this work the use of commercial aluminium alloys as anodes in metal-air battery systems is studied. This commercial alloys are worldwide used for very differentiated applications, and its presence is very common in our day-to-day. Food cans, vehicles, window frameworks, boats, etc. are made of Al alloys. So, the development of a high-

performance Al alloy based battery could be the way for a cheap and abundant energy supply.

Several alloys compositions have been tested, being the most remarkable ones the Al2024, Al7475 and Al1085, in different electrolyte formulations. The processes taking place in each electrolyte during the discharge of the battery have been studied, and different approaches explored trying to overcome the founded issues.

Four electrolyte formulation have been presented, three of them presenting alkaline pH electrolyte, and the resting one neutral pH. Inside the alkalines, KOH in low concentration and high concentration KOH gelled electrolytes have been explored, as well as a high concentration NaOH based electrolyte. The neutral pH electrolyte was NaCl based.

In low concentration KOH electrolyte, specific capacities of 120 $mAh \cdot g^{-1}$ were achieved with the Al2024 commercial alloy at discharging currents of 12.8 $mA \cdot cm^{-2}$. This system presented some issues related to the self-corrosion of aluminium that was found to compete with Al oxidation during discharge. So, when a current was applied, part of the aluminium anode mass began to oxidase to deliver electrons, while other part get corroded evolving hydrogen. As discharging current increased, more part of aluminium was oxidised, displacing the corrosion, and so, obtained specific capacities were higher.

Another pathway for KOH based electrolyte was the jellification of a high concentration solution. The obtained gel was quite sticky and flexible allowing a good adhesion to the electrodes. Al7475 obtained the best results on this electrolyte of 430 $mAh \cdot g^{-1}$ at maximum currents of 8.4 $mA \cdot cm^{-2}$. The limiting factor in this electrolyte was the accumulation of $Al(OH)_3$ between the gel-electrode interface that impeded the hydroxyl ion diffusion to the anode. The behaviour of the pure aluminium cladding of commercial alloys was studied, and it was concluded that for low current rates Al7475Clad anode performed better than the Al7475 without pure Al cover. However, at higher currents, the uncladded alloy could reach higher maximum currents as well as specific capacities. The latter was found to be because of the influence of galvanic pairs in the electrolyte due to the release of alloying metals during Al oxidation. This galvanic pairs get dissolved

at high currents, and due to the higher ease of alloyed aluminium to oxidise, Al7475 without pure Al protection layer performed better results as anode.

The third electrolyte was NaOH based, with a combination of some additives able to protect the Al surface from massive corrosion, as well as to complex the formed $Al(OH)_3$. In this electrolyte, huge specific capacities of 1400 $mAh \cdot g^{-1}$ were measured with the Al7475 alloy at currents of more than 80 $mA \cdot cm^{-2}$. This electrolyte formulation minimised the effect of galvanic pairs, and stimulated the displacement of self-corrosion in favour of Al oxidation, up to the point of completely inhibiting the hydrogen evolution at currents higher to 45 $mA \cdot cm^{-2}$. The effect of the distance between electrodes was also corroborated, increasing more than 300 mV the cell potential just by reducing to 1 cm the distance between anode and cathode.

The last electrolyte formulation was that of NaCl, with neutral pH. This electrolyte resulted very interesting because of the non-existence of self-corrosion reaction of Al in this media, so the anode could get immersed in the electrolyte without Al mass loss and hydrogen evolution. The main issue in this electrolyte was the partial solubility of the formed aluminium hydroxide that get adhered all over the anode forming a gel that impeded the correct functioning of the battery. To overcome this situation a carbon treatment for the anode was proposed, that minimised the adhesion of the formed gel, allowing it to precipitate, not impeding the reaction. With this treatment, high specific capacities of 1200 $mAh \cdot g^{-1}$ at 10 $mA \cdot cm^{-2}$ were obtained with Al7475 and Al1085.

INTRODUCTION

1. Introduction

1.1. Context: batteries and its history.

A battery is a device that converts the chemical energy contained in its active materials directly into electric energy through an electrochemical oxidation-reduction (redox.) reaction [1]. This type of reactions involves both, the transfer of electrons from one material to the other across an electric circuit and the ionic transport thought the electrolyte. In the case of a rechargeable, or secondary, battery the reverse of the process takes place for the recharge.

For referencing a single unit of a battery, the term “cell” is normally used, while a “battery” refers to one or more of this cells, connected in series or parallel, or both, with a final voltage and capacity output.

A cell is composed of three main components:

- The anode (or negative electrode), which is oxidized during the discharge of the cell for delivering electrons to the external circuit.
- The cathode (or positive electrode), which is reduced during the discharge of the cell by accepting electrons from the external circuit.
- The electrolyte, which provides the medium for the transfer of ions between the anode and the cathode.

So, a cell composed of a light, high voltage and high capacity anode-cathode materials pair will be the most favourable one. However, other factors like reactivity, cost, abundance, toxicity, etc. must be considered to define a functional anode-cathode pair [2]. An optimum electrolyte must fill some parameters like good ionic conductivity but not being electronically conductive, non-reactivity with electrode materials, non-variability with pressure and temperature changes, etc [3,4]. Most of the electrolytes

are aqueous solutions, but some technologies require the absence of water so, non-aqueous, molten salts or ionic liquid electrolytes are used.

Batteries are nowadays in full swing and they will play a key role in future technological developments, but the discovery of this electrochemical systems dates back to two centuries ago. In 1780, Luis Galvani was dissecting a frog affixed to a brass hook. When he touched its leg with his iron scalpel, the leg twitched. Galvani called that phenomenon "animal electricity" [5]. However, a friend of him, Alexandro Volta studied this event, and confirmed that the twitch occurred because of two different metals joined together by a moist intermediary [6]. In 1800, Volta presented the first battery, known as the "Voltaic pile", which was composed of coper and zinc plates separated by brine impregnated cardboard. This finding was the starting point for a lot of new developments related to the electrochemical generation of electricity. In 1836, john Frederic Daniell, presented the "Daniell cell" which was an improved version of the voltaic pile. Daniell used two electrolytes for the Zn and Cu electrodes separated by an earthenware to enable ion transport while not allowing liquids getting mixed [7]. This solved several issues related to hydrogen generation on the Zn side, etc. This pile could deliver long constant current discharges with a voltage of 1.1 V, and so, it soon became the industry standard for use, mostly in telecommunications sector [8].
In 1860, a variation of the Daniell cell came into the market. It was called gravity cell, because the separation of the Cu and Zn electrodes reaction products was made taking advantage of the different densities. This cell improved the maximum current available for the cell discharge because of the absence of physical separator, and resulted easier to maintain due to the simple reaction product separation.

Up to this point, all existing batteries were primary cells, and had to be drained once the electrode material was expended, but in 1859, Gaston Planté, invented the Lead-acid battery [9]. This battery was composed of a lead anode and a lead dioxide cathode connected by a sulfuric acid electrolyte. Even of the limited energy accumulated by weight and volume, the possibility to discharge at larger currents than other technologies and the relatively high voltage of 2 V, made this battery quite common for

different applications. After several design improvements, as pasted plate electrodes, tube electrodes or gel electrolytes, nowadays is still one of the most used batteries [10].

In 1866, Georges Leclanché invented a primary battery that consisted in an anode of zinc and a cathode of manganese dioxide pasted in a porous material, immersed in ammonium chloride. The voltage was 1.4 V and it was extended quickly for telecommunication applications [11]. 20 years later, Carl Gassner patented a variant of the Leclanché cell. The innovation was the use of plaster for solidifying the ammonium chloride electrolyte, and the addition of zinc chloride to displace the parallel reactions [12,13]. This cell was considered the first "dry cell", and became very famous because of the possibility to use it in any orientation, no leaches, no maintenance necessity, etc [14]. And so, this was the first mass-produced battery, by the company Columbia and named Columbia Dry Cell, and it gave rise to the invention of portable devices like the flashlight. To differentiate it from the Leclanché´s one, it was called the "Zn-Carbon" battery, because of the addition of carbon to the manganese dioxide to improve the electric conductivity of the cathode [15,16].

By the beginning of the 20th century, Waldemar Jungner, presented the first alkaline battery, based in nickel-cadmium electrochemistry. This rechargeable battery was robust and offered the possibility to storage more energy by weight and volume than its competitor lead-acid [17], but the cost of production was notably higher, so it was commonly used for maximum reliability applications, like emergency lighting, etc. At the same time, Jungner worked with the nickel-iron electrode pair, but he decided not to continue his investigation in favour of the Ni-Cd because of the best performance and reliability.

Some years later, Thomas Edison recovered this investigation and patented a Ni-Fe based battery, which had good market penetration, even if the objective of Edison was to become this battery a standard for electric vehicle and the appearance of the internal combustion engine dispelled his idea.

Until that time, most of portable devices were functioning by means of the Zn-Carbon primary cell, but by mid-century, common alkaline batteries appeared. They were composed of a manganese dioxide + carbon cathode, and the anode was replaced by

zinc powder to enhance the useful surface of the electrode, both immersed in an alkaline electrolyte [18]. With a potential of 1.5 V and better achievable current values, these batteries hit the market in 1960 and are still wildly used in common portable devices [19].

Based in the alkaline battery, new approached were invented like the mercury battery or the silver-oxide battery, which used mercury oxide or silver oxide respectively, instead manganese dioxide in the cathode side, with the same alkaline electrolyte (KOH). These cells presented high volumetric and gravimetric capacities so they were used mostly for button cells. But they had some issues like the toxicity in the case of the mercury based cell and the high cost of the silver, so, they get displaced from the market or used just for certain applications like silver-oxide for spacecraft, satellites, etc [20]. because of the high specific energy and energy density.

In 1970, a new commercial battery appeared as cheap replacement for the toxic Zn-HgO cell. It was also a Zn based battery, homologous to the Zn-Carbon battery, but with the difference that in this case, the cathode-can was opened to the atmosphere to let the oxygen enter. This battery was named Zn-air battery because of the use of oxygen from the air. The energy density and specific energy of this type of cells was very high because of the no-need to storage the cathode reactant, resulting in more space for the anode material [21]. They are still one of the most used primary button type cells, for energy supply in hearing aids, cameras, etc.

In 1980 a new variation of the Ni-Cd battery was presented, Ni-MHx rechargeable battery. This cell was based in the use of the hydrogen as anode, so a metal hydride was chosen for replacing the cadmium from the batteries [22]. The latter achieved a simpler manufacturing process, because of the toxicity of handling cadmium, and a reduction of the price. However, the cell did not result as reliable as Cd one, so its use was extended for consumer electronics mostly, and not as a replacement of its predecessor.

In 1970, first primary lithium cells came into the market, compared to other technologies, the ones with metallic lithium, offered a higher cell potential, up to 3 V, and high energy and power densities [23]. This type of cells is still common in designs

like CR2032 or CR2025 coin cells. But the most important use of lithium for batteries was discovered in the early 80s, when different groups of scientist discovered the possibility of the intercalation of lithium-ions in certain materials. The latter allowed the use of lithium ions, instead of metallic lithium, which get intercalated in a carbon-based anode [24,25] and a metallic oxide [26,27] based material cathode during charge and discharge. This finding solved issues related to the low stability of metallic lithium, the dendritic formation during charge, and other problems related to safety.

The voltage of the cell could go as high as 3.6 V (up to 5 V in current investigations [28]). The lightness of this cell compared to the lead-acid or Ni-Cd ones was notably higher, as well as the achievable power. In 1990, first commercial lithium-ion battery was presented by Sony, and most of the portable electronic devices were adapted to this technology. Some year later, different cathode materials were found, as well as the possibility of solidifying the electrolyte by confining it into a polymer. Lithium-ion batteries are nowadays one of the most used batteries, and the reference in energy storage systems for portable electronics, power tools, etc.

1.2. Present situation: batteries and challenges ahead.

The importance of batteries in actual society and in the global model of consumption is undeniable. Most of our working, living and relating habits are carried out through an electronic device powered by a battery. In this present situation, one common concern is the autonomy of the devices involved in our lives: how much battery is resting to my smartphone?, is my laptop´s battery enough to last for all the trip?, is my electric car going to arrive to my destiny without recharging the battery?, etc.

So, are the present battery technologies enough good for incoming technological advances? Even, are the present battery technologies enough good for present technologies? These questions can be answered by different points of view.

One of them, is to change the consumption pattern to make the actual energy storage systems valid for the applications where, with nowadays demands, are not enough.

Most of the commercial full electric vehicles, powered by Li-ion batteries, present an autonomy of 150 to a maximum of 450 km (high end vehicles), less than a half of the autonomy of diesel or gasoline cars [2,29].

But if we look at an average daily car travel of one person in Madrid for example, the travel is of about 50 to 60 km a day [30], and longest travels are normally related to holydays, or business trips, which normally takes from 3 to 4 weeks a year. So, some experts propose that the use of an EV based in actual battery technologies with an autonomy of 100 to 150 km would be enough to cover the average daily demand. And for uncommon travels a combustion engine car could be rented to have an enhanced autonomy.

This approach however, is not so successful for sectors like smartphones or laptops, where the actual battery technology can bring autonomies of just hours, while the energy consumption of these devices is expected to be higher and higher. Other sectors like the new concept of “Smart Grid” and “Smart City”, would not be efficiently energy supplied by the electrochemical based actual energy sources.

1.2.1. Sectors waiting for new battery technologies: Smart cities, hearing aids and large scale energy storage systems.

A Smart Grid is an electrical grid which includes a variety of electronic sensors and/or actuators to have a central control of the energy, from generation, distribution, storage, etc. to final consumption [31,32]. A sensor [33] is small electronic device that can read a variable every period, and to send that information via wireless to a central control station. An actuator [34] however, is not only able to read and send this information periodically, but also to act in the necessary processes to make the tendency of the monitored variable change. This intervention could be realized by predefined algorithms in the actuator, so the actuator would work itself, or by the commands send from the central control station to the device. The latter permits a flexible and real-time control of the energy in the grid, and so, a quite high adaptability in generation and consumption to achieve high energy efficiencies.

And so, a Smart City is a bounded area where different variables, including energy, are controlled and actuated through different sensors and actuators all over the area.

A Smart City brings the opportunity to manage the traffic of the place by acting on the traffic lights, or controlling the temperature of different spaces by re-counting the affluence of people, or even mapping the contamination of different areas to turn aside the traffic for not exceeding risk limits, etc. Then, a Smart City could be as "smart" as desired, acting over all the interesting variables for enhancing the global efficiency of a place [35].

So, how are all these sensors and actuators energy supplied? If we look at a scenario with thousands of sensors and actuators scattered all over the area, the necessary infrastructure to extend the grid to all of them would be non-cost-effective in all cases due to the offshoring of the different devices. So, the most accepted approach is the use of primary batteries [36]. But are the existing commercial technologies able to provide such high energy for long time is so low volumes?

Different experts fix the barrier of cost-effectivity in a battery that could reach an autonomy of at least 5 years, which matches with the maintenance period of these devices [36], and then, the substitution of the pile would be included in the maintenance program, cheapening notably the whole cost.

As in the case of the cited devices, others like hearing aids, where the volume of the entire device (including energy source) is a limiting factor, could be benefited by new battery technologies. Today's hearing aids work with a Zn-air button cell, able to provide a 4 to 5-day autonomy [21], so every month 6 to 8 cells must be expended. Some tries have been done with Li-ion rechargeable cells, which turn the autonomy to just 1 to 2 days [37], so every night the device must be charged next to the smartphone, to ensure the entire next day autonomy.

The use of hearing aids is commonly related to elderly people, which makes the necessity of changing or charging the battery every 2 to 5 days a tedious extra responsibility. For these applications, where the volume is a limiting factor, not only for hearing aids but also for a lot of medical instrumentation, cell autonomy is a limiting factor, so a priori, new cell technologies will be necessary in a nearly future.

Another remarkable sector where the development of new battery technologies could play a key role is that of large scale ESSs (energy storage systems).

Most of the called green energies present an important drawback: the intermittence. This makes the integration of large scale solar or wind-turbine farms difficult because of the inflexibility of the grid. The average energy generation mix of a European country is that where nuclear is continuously working, providing a constant amount of energy to the grid; the combustion and combined cycle centrals work adapted to the demand curve but still with a flat evolution during the hours of the day; and the renewable energy sources work when sun (day) or wind (mostly night) are available [38,39], see Figure 1.2.1.1 But also for satisfying the demand peaks, what is notoriously seen in the case of hydropower.

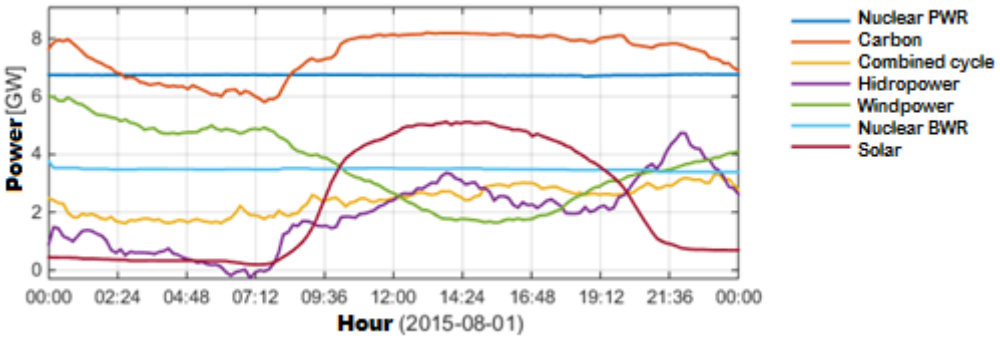

Fig. 1.2.1.1: Energy generation mix of a summer day in Spain by hours.

Due to the intermittency of the renewable energy sources, displacing the nuclear or thermal energy is not possible without energy storage to support solar and wind power. That is, during the night, a percentage of the wind power could be used to satisfy direct energy demand, and exceed for charging large-scale energy storage systems [40]. For, during the daylight produce solar energy with the background of the charged ESS. The latter could allow a higher renewable energy percentage in the mix, without the necessity to oversize the renewable installed power [41].

This large-scale ESSs are based mostly in three technologies [42], and each of them present some important drawbacks to be solved:

- The most suited technology for this task is the vanadium flow battery. A flow battery is like a conventional battery with the particularity that the active

materials instead of being “pasted” in electrodes, are suspended in two electrolytes (anolyte and catholyte), interconnected by an ion-exchange membrane. So, the capacity of the cell is as high as the amount of anolyte and catholyte stored in tanks outside the cell, while the power is as high as the area of the current collectors. The electrolytes are circulated by pumps, and the voltage of the battery depends of the cell stack number. The easy scalability of this battery and its high cyclability, up to 100,000 cycles [43], makes it suitable for large-scale energy storage. The main issue is the high price of the vanadium based electrolytes, which cost around 800 $/kWh (just electrolytes). Other electrochemical pairs like Zn/Br or Fe/Cr, are available for the flow technology but the maturity of development and the endurance are still low [44].

- Li-ion technology: These batteries are nowadays the standard for a lot of applications due to their capability to work in different power ranges, high deep of discharge and relatively high cycle life. For large-scale energy storage, Li-ion batteries can be stacked into series for developing packs with the final application voltage, and then these packs connected in parallel to get as much capacity as necessary. Li-ion battery based 20, 40 or 60 feet containers up to 3MWh are commercially available [45]. The deep of discharge of this battery is around 80% for a cycle life of 2,000 to 8,000 cycles depending on the Li technology. One of the main issues is the obligation to use associated electronics to control each cell, or module, voltage and temperature, to ensure a correct balance of the cells because of the explosion risk at high temperatures and under over-voltage. The second one is also the price, around 600 $/kWh (some technologies like Li titanate anode based cells are around 900 $/kWh), and the extra costs related to the more electronics needed when the system presents more cell connexions.

- Lead acid based battery packs: A large-scale ESS based in lead acid batteries is like that of Li-ion, but due to the lower energy density and deep of discharge (around 50-60%), the volume to supply 3MWh is about 3 times more than the one for Li-ion [46]. So even if the cost of the lead acid is less than 200 $/kWh, the

transport and infrastructure necessary to transport and install 3 containers instead of 1, makes the final cost raise up. Additionally, the cycle life of lead based batteries is 1,000 to 2,000 cycles so if we consider a daily charge-discharge, the lifetime of these batteries would be from 3 to 5 years, and more maintenance is needed compared to Li-ion battery packs [47].

Thus, even if the existing batteries can cover the necessities of large-scale energy storage, the volume, endurance and mostly costs are not suitable for a cost-effective expansion.

So, many experts believe that new battery technologies could be the solution for resolving the presented challenges.

A small overview of the existing commercial technologies, its working parameters and common applications is performed in the next point.

1.3. Commercial products: batteries and its parameters.

There is a great variety of commercial piles and accumulators into the market. Almost all discovered electrochemistry pairs are still used for some specific applications, while just few of them hoard most of the market. Roughly 3 rechargeable and 3 primary batteries can be highlighted from the others.

1.3.1. Commercial rechargeable batteries and its parameters.

If we look at the secondary batteries, lead acid, Ni-Cd and Li-ion technologies are the most used batteries [19]. Table 1.3.1.1 shows a comparison between the cited technologies in terms of capacity, voltage, power, working temperature, etc. In the table, the Ni-MHx battery is included, because, even if the appearance of the Li-ion battery partially replaced this technology, the medium-low price and lightness compared to lead acid makes it still useful for some applications as hybrid electric vehicles, cheap electronics, etc. In the collection, the lithium-ion technology is divided

in 3 types, which are the most common cathodes for these accumulators, but not the only ones.

The first commercial Li based battery was that with cobalt oxide as intercalation cathode. As can be seen, it presents the highest specific energy up to 180 $Wh \cdot kg^{-1}$, so it is the most common choice for applications like smartphones, laptops, and electronic devices in general [48]. The manganese oxide based cathode was commercialised later, even if it was the first intercalation material discovered. The main advantage of these batteries is the higher thermal stability, which increases the safety of this technology, and the huge admissible currents, even if the energy density is lower [49]. The latter, makes this battery the most used one for applications in power tools, electric vehicles, etc. In the last years, new cathodes have been developed by doping the manganese oxide structure with metals like nickel and cobalt, and higher specific capacities have been achieved without scarifying power [50].

Iron phosphate based Li-ion cell presents lower specific energy, a bit higher power and thermal stability compared to manganese based ones, but specially, they present 2 important advantages related to the cycle life [51] and the cost. Their main use is in cheap electronics or where a high cycle life/power ratio is needed regardless to the weight of the battery.

Two other types of Li based rechargeable cells are commercially available but are not included in the table because they are not still widespread, mostly because of the higher cost compared to its predecessors. The previously mentioned lithium titanate anode based cell (can be used with any of the mentioned cathodes), which sacrifices nominal voltage (2.4 V) and specific energy (80 $Wh \cdot kg^{-1}$ at most), for a very high cycle life up to 7,000 nominal cycles (up to 10,000 cycles in low working power conditions) [52]. And the second one is the aluminium-nickel-cobalt oxide based cathode, that presents the highest specific energy (up to 250$Wh \cdot kg^{-1}$), but the safety and thermal stability as well as the admissible power are less flattering.

The lead acid battery was the first discovered rechargeable cell [9,47], commercial since 1880. Due to its low specific energy, and therefore its high weight, it is used mostly for

stationary applications. But, at the beginning of its discovery, it has been used for powering electric vehicles, trains and other means of transport [53].

The main advantage of the lead acid battery is the simplicity regarding to the active materials, design, maintenance, etc. That´s what makes this battery so cheap, and consequently used around the world. There is a great variety of lead acid based cells, from Planté plate cells, to flat plate or tubular electrode cell, with gelled electrolyte or valve regulated (VRLA). The characteristics between them variate significantly, almost doubling the cycle life from flat plates to tubular gelled battery [54].

Even the more advantaged lead acid batteries result cheaper than the more basic lithium-ion or cadmium ones, and that's why it is the most sold battery [19]. Most of the stationary applications where the volume and the weight is not a handicap, use lead acid batteries, as in medium-scale energy storage systems, emergency powering in buildings, back-up power, etc. Additionally, it is the most used battery for automotive starting, lighting and ignition (SLI batteries) thanks to its relatively high power to weight ratio, and for vehicle propulsion in electric golf cars, submarines, electric assisted trains, etc.

The last presented rechargeable battery is the Ni-Cd cell, which´s more characteristic property is the reliability. Its electrodes are composed of a stainless steel current collector where the active material is supported. This support can be done by pasting the active material or by sintering.

Due to the unchanging properties of the current collector, this battery results infallible. The extended cycling of this battery can make the active material get detached (mostly in the case of pasted electrodes) which makes the capacity go down, but still without failure. And so, there are Ni-Cd batteries with more than 20 years still working with just a 10 or 20% of the nominal capacity but without failure [55,56].

The most important drawbacks of this cell are mostly: the existence of secondary reactions, also called memory effect; the high toxicity of cadmium; and so, the final cost, which is located between lead-acid and Li-ion, around 300 to 350 €·kWh^{-1}.

Table 1.3.1.1: Commercial rechargeable batteries and its working parameters

				Li-ion cathode technologies[4]		
Specifications	Lead acid[1]	Ni-Cd[2]	Ni-MHx[3]	Cobalt	Manganese	Phosphate
Voltage (V)	2	1.2		3.6	3.8	3.2
Specific capacity (Ah·kg^{-1})	15 - 20	37.5 - 68	50 - 100	40 - 50	26 - 36	28 - 37.5
Specific energy (Wh·kg^{-1})	30 - 50	45 - 80	60 - 120	130 - 180	100 - 135	90 - 120
Cycle life (DoD 80%)*	300 – 400	> 1,000	300 - 500	500 - 1,000		< 2,000
Internal resistance (mΩ/V)	< 10	< 30	< 50	< 30	< 20	< 15
Self-discharge/month (room temp. %)	5 - 15	20	30	< 5		
Discharge cut off-voltage (V)	1.7 - 1.8	1		2.5 - 3		2.8
Charge cut off-voltage (V)	2.4 (2.25 float)	1.45		4.2		3.6
Overcharge tolerance	High	Moderate	Low			
Fast charge time (hours)	8 - 16	1	2 - 4	2 - 4	< 1	
Peak load current (<1s)	5C	20C	5C	> 3C	> 30C	
Peak load current (>2s)	0.2C	1C	0.5C	< 1C	< 10C	
Charge temperature (ºC)	-20 - 50	0 - 45				
Discharge temperature (ºC)	-20 - 50	-20 - 65		-20 - 60		
Maintenance requirements	3 - 6 months (equalization)	30 - 60 days (discharge)	60 - 90 days (discharge)	none		
Safety requirements	Thermally stable	Thermally stable, fuses common		Protection circuit mandatory		
Time durability	> 15 years		> 10 years			
Toxicity	High		Low			
In use since	1880	1950	1990	1991	1996	1999

*DoD: deep of discharge

[1] [10,46,54,57] [2] [1,55,56] [3] [17,22,55] [4] [9,45,50]

Due to these properties, the Ni-Cd battery is the most used battery for applications related to safety, back-up, and for medical devices where the energy supply cannot fail. A great part of these cells market is related to transport communications, mostly planes and trains.

1.3.2. Commercial primary batteries and its parameters.

Once we have a brief overview of rechargeable commercial cells, let´s look at primary cells, its parameters and applications.

Primaries play an important role, especially when charging is impractical or impossible, such as in military combat, rescue missions and forest-fire services. Primary batteries also service pacemakers in heart patients, smart meters (sensors and actuators), animal-tracking, remote light beacons, as well as wristwatches, remote controls, electric keys and children's toys.

So, even if piles tend to get overshadowed by the media attention that rechargeable batteries receive, and they look like they are old technology on the way out, they are still the most consumed cells and essential for certain applications.

The main characteristic of these primaries compared to secondary batteries is the higher specific energy, as well as energy density, which makes possible to supply energy for portable devices taking up small volumes and without compromising the final weight of the device. Additionally, they present long storage time and readiness so they can be stored for up to twenty years, and when necessary, they are ready to be used [58].
As in the case of secondary ones, 3 main primary battery technologies occupy the mayor percentage of the market. Table 1.3.2.1 presents the main working parameters of these cells.

The well-known alkaline battery heated the market in the 1960s and displaced other technologies of that time. Compared to them, alkalines delivered near to the double

specific energy, and a similar potential of 1.5 V, with a cost-effective energy to cost ratio [59].

Nowadays is still the most used battery (near to the 50% of the primary and secondary cell sales in Europe were alkalines in 2014) for common applications from telecommunications to portable devices, remote controls, toys, flashlights, or consumer electronics.

The development of the Zn-air battery was promoted by two phenomena [21,60]: the new technique of using Zn powder instead of Zn sheets for the anode in alkaline piles, which permitted a higher use rate of the material and higher usable currents; and, the advances achieved in the field of fuel cells, which lead to the development of a small-size button cell air-cathode. This cathode is just a few hundred microns thick, so the rest of the volume of the cell (button cell in this case) can be filled with a Zn powder + KOH (alkaline electrolyte) paste.

This cell supplies a specific energy of 440 to 470 $Wh \cdot kg^{-1}$, which almost doubled that of its predecessor silver-oxide cell, but its power is lower than the other technologies, being used in discharges of 300 or 100 hours, and reaching maximum continuous current discharges of 20-30 hours (for preserving at least a 70% of the nominal capacity). This circumstance is due to a high internal resistance (around 8Ω/V, what supposes more than an order of magnitude more than other technologies) [61,62].

A lot of medical devices, hearing aids, smart meters, electrified fences, etc. are nowadays powered by Zn-air cells.

The main strength of these cells against other electrochemistry pairs is the high energy to cost ratio, what makes the energy accumulated in the Zn-air battery the cheapest commercial one. The drawbacks however, are the cited low power working range, the reduced operating temperatures, and the low self-life, which is reduced from 3 years to 6 months at the most once removed the protection lip.

Table 1.3.2.1: Commercial primary batteries and its working parameters

			Li primary cathodes technologies[3]		
Specifications	Alkaline[1]	Zn-air[2]	Manganese	Thionyl chloride	Iron sulphide
Nominal voltage (V)	1.5	1.4	3.3	3.6	1.5
Specific capacity (Ah·kg^{-1})	100 -115	300 - 330	80 - 85	150 - 190	200 - 230
Specific energy (Wh·kg^{-1})	150 - 180	440 - 470	260 - 280	550 - 680	310 - 350
Internal resistance (mΩ/V)	250 - 350	8000	< 200	600	< 100
Self-discharge/month (room temp. %)	< 0.3	< 0.5	< 0.1	< 0.01	< 0.1
Operating voltage (V)	1.2 - 1.4	1.2 - 1.3	2.8 - 3	3.4 - 3.5	1.3 - 1.5
Discharge cut off-voltage (V)	0.8	1.1	2.5	3	1
Peak load current (<1s)	C/2	C/10	1C	C/2	5C
Peak load current (>2s)	C/10	C/20	C/5	C/10	C/2
Discharge temperature (ºC)	-18 - 55	0 - 40	-30 - 65	-55 – 120	-40 - 60
Maintenance requirements	None				
Safety requirements	none		flammable	Highly flammable	Flammable
Time durability (years)	5 - 10	< 3	> 10	15 - 20	20
Toxicity	low			Highly toxic	medium
In use since	1965	1970	1985	1994	2002

[1] [1,18,59] [2] [21,57,61] [3] [23,63,64]

Another primary important batteries are those of metallic lithium. Li-MnO_2 cell, also referred as CR by the IEC (International Electrotechnical Commission), is the most popular consumer-grade primary lithium battery. It presents a nominal voltage around 3.3 V, and a specific capacity up to 280 $Wh \cdot kg^{-1}$. It offers the possibility to work in a higher temperature range to work at higher power [23,63]. It has been traditionally used as replacement for 2 in series alkaline battery packs making it cost-effective.
Most of electronic remote controls, keys, or hard drives use these cells but also, photo-cameras, automotive electronics, utility meters, etc.

Lithium-thionyl chloride cell is the higher specific energy electrochemical pair available commercially, going up to 680 $Wh \cdot kg^{-1}$, with a voltage of 3.6 V. Additionally, it can deliver energy in extremely high and low temperature conditions (from -55 to 120ºC) [65], what makes it play a key role in certain specific applications, like rescue equipment, outdoor utility metering, military radio communications, etc. On the other hand, it presents important issues related to security, due to the explosive and corrosive nature of its compounds. And, so the cost results high [66].

Lithium-iron disulphide presents a nominal voltage of 1.5 V, equal to that of alkaline cells. That´s why is also known as “voltage-compatible” lithium cell, and it was created as high power replacement for alkaline batteries [23,67]. However, the cost results much higher than alkalines, so it applications are limited to high power portable electronics as speakers, music players, etc. and mostly military applications.

The described lithium primary technologies although, represent just a small part of the existing variety of cathode materials, being more than 15 lithium based primary cells commercially available.

This brief overview of existing commercial batteries aims to be a little reference of which are the working parameters of actual technologies, to have a comparative framework where to locate the results of this work.

1.4. Metal-air battery: a deeper overview.

To present the aluminium-air system, a better understanding of the metal-air family system is necessary. Thus, we are going to move deep inside this technology to know which are the capabilities, the different types of systems and which research is been carried out in this area during the years.

A metal-air system is in broad strokes a junction between a metal with tendency to deliver electrons, and a catalyst able to facilitate the reduction reaction of oxygen (ORR) from the air. Both interconnected by an electrolyte that permits the movement of ions from one electrode to another. In the case of a secondary battery, the air cathode would include a bivalent catalyst also for the oxygen evolution reaction (OER) during the charge step of the battery [68].

Compared to any other battery technology, as for example lithium-ion, metal-air cells present the important advantage of the no-need to storage the cathode reactant, present free in the air. The latter permits a reduction of the volume of the cell for obtaining the same capacity, or an improvement in the stored energy for the same volume cell [69].

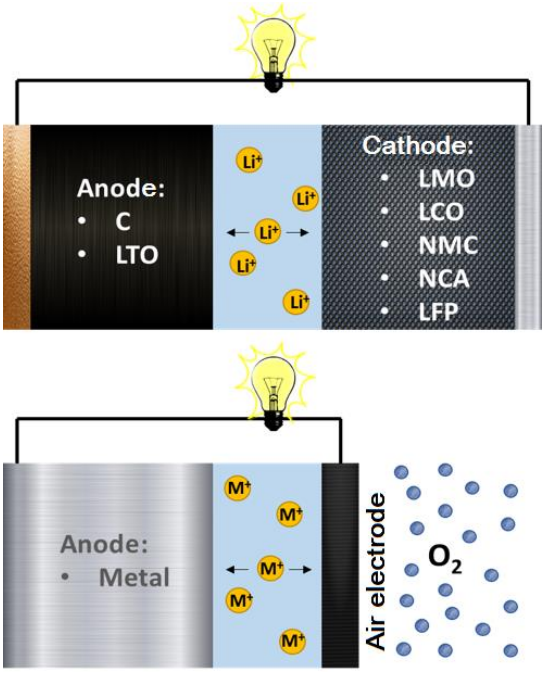

Fig. 1.4.1: Schematic comparison between lithium-ion and metal-air cells.

There are several kinds of metal air batteries based on different metal species and their reaction mechanisms. Fundamentally, metal-air batteries can be classified into two types per the used electrolyte. On one hand, there are systems using an aqueous electrolyte and, on the other hand, there are water sensitive systems which use an electrolyte with aprotic solvents or ionic liquid (or mixtures of both).

If we also look at the rechargeability of the cell, three types of systems can be differentiated: non-rechargeable or primary batteries, electrochemically rechargeable or secondary batteries, and mechanically rechargeable batteries. A mechanically rechargeable battery is a primary cell prepared so that its active materials get replaced once exhausted, for a new use of the battery.

Figure 1.4.2 presents a diagram of the most common metal-air cells classified by the used electrolyte and its rechargeability.

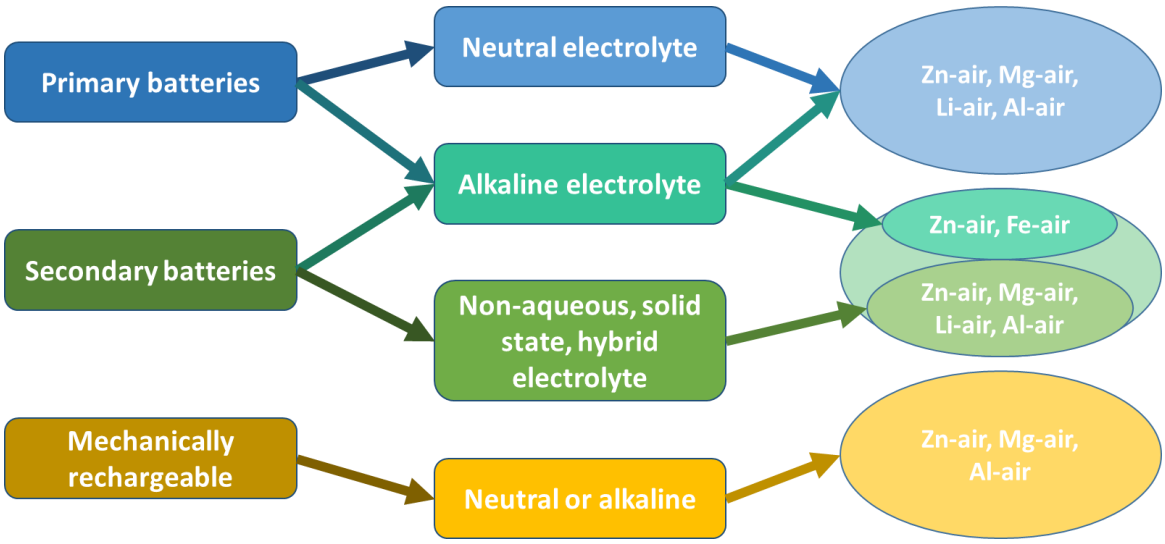

Fig. 1.4.2: listing of common metal-air systems as function of used electrolyte and recharging technology [60].

So, the equations involved in an aqueous electrolyte based metal-air battery are [70]:

$$\rightarrow Anode: \quad M^0 \leftrightarrow M^x + xe^- \qquad \textit{eq. 1.4.1}$$

$$\rightarrow Cathode: \quad \tfrac{1}{2}O_2 + H_2O + 2e^- \leftrightarrow 2OH^- \qquad \textit{eq. 1.4.2}$$

$$\rightarrow Overall: \quad M^0 + nO_2 + yH_2O \leftrightarrow M(OH)_x \qquad \textit{eq. 1.4.3}$$

In some cases, depending on the pH and the anode metal (M), an extra process occurs in the electrolyte:

$$\rightarrow Electrolyte: \quad M(OH)_x \leftrightarrow MO_z + yH_2O \qquad \textit{eq. 1.4.4}$$

And so:

$$\rightarrow Overall: \quad M^0 + nO_2 \leftrightarrow MO_z \qquad \textit{eq. 1.4.5}$$

If we look at the last overall reaction (see eq. 1.4.5), It is easy to understand why this technology results so attractive. If the oxygen involved in the process is directly consumed from the surrounding atmosphere (which is inexhaustible), the unique consumption of reactive is that of the anodic metal. And so, if a high theoretical specific energy metal is used, the resulting battery should present extremely high specific energy, just limited by the amount of metal anode.

But when we move to real systems, the appearance of parasitic reactions, issues related to the ORR and OER in the air cathode, electroplating of some metals during charge, as well as other challenges, make these systems not so easy to become successful developments.

In a non-aqueous system, the overall reaction of the cell is the same (see eq. 1.4.5), as well as the one in the anode (see eq. 1.4.1), but the reaction that takes place in the cathode results different [71,72]:

$$\rightarrow Cathode: \quad O_2 + e^- \leftrightarrow O_2^- \qquad \textit{eq. 1.4.6}$$

In the same way as before, the theoretical capacity of a cell is just limited by the weight of metal. But in practice, different challenges must be solved related to the reactivity of the superoxide, the existence of secondary reactions, the non-reversibility of some metallic oxides or dendritic formation of plated metal, etc.

For a better comprehension of the mentioned challenges, possible anodes and systems, and developments in cathodes are going to be expound, referring to the investigations

carried out by relevant researchers and some of the obtained results during the last years.

1.4.1. Anodes for metal-air batteries.

Several metals have been investigated since the last 5 decades for their use as anode material in metal-air batteries. As previously commented, the most appreciated and pursued parameters of these negative electrodes are a high theoretical gravimetric and volumetric capacity and a high oxidation potential against air (+0.40 *vs* SHE). The latter leads to a final cell with a high specific energy, as well as high energy density. Table 1.4.1.1 shows the theoretical open circuit potential (OCP), theoretical specific capacity by weight and volume, as well as idealized cell reaction of several metals coupled with air.

The theoretical gravimetric capacity values shown by any metal in the table are incredibly high, but in practice the weight of the whole system must be considered, including both electrodes, electrolyte and cell casing. Additionally, this technology tends to need an excess of electrolyte to ensure good functioning, and if we assume that the faradaic efficiency is not a 100%, the achievable final specific capacity results lower than a half of the presented theoretical one.

Even of these drawbacks, metals like aluminium, lithium or magnesium, could achieve final system specific capacities of 10 to 15 times that of commercial alkalines (see table 1.3.2.1).

Table 1.4.1.1: Metal-air battery anodes: cell reaction and theoretical values [1].

Anode	**Idealized cell reaction**	**OCP (V)[#]**	**Gravimetric capacity ($Ah \cdot kg^{-1}$)[#]**	**Volumetric capacity ($Ah \cdot L^{-1}$)[#]**
Ca	$2Ca + O_2 \rightarrow 2CaO$	3.11	1340	2050
Mg	$2Mg + O_2 \rightarrow MgO$	3.03	2200	3800
Li	$4Li + O_2 \rightarrow 2Li_2O$	2.98	3860	2060
Zn	$2Zn + O_2 \rightarrow 2ZnO$	1.86	820	5800
Al	$4Al + 3O_2 \rightarrow 2Al_2O_3$	2.75	2980	8100
Na	$4Na + O_2 \rightarrow Na_2O$	1.97	1160	1140
Fe	$3Fe + 2O_2 \rightarrow Fe_3O_4$	1.28	960	7500

[#]*Theoretical values*

Other metals like sodium or iron result quite interesting as anodes for rechargeable batteries. Even if the achievable capacities result not as high than the ones for other metals, the abundancy and low price of the compounds as well as a practical capacity up to 5 or 6 times that of actually commercial technologies make them suitable candidates for future developments.

Several tries have been carried out with calcium or even silicon as anode for metal-air batteries, but these metals present important difficulties to be solved. Professor Yair Ein-Eli from Thecnion (Israel Institute of technology) demonstrated the reversibility of a silicon-air based system, achieving capacities of 20 to 25 $mAh \cdot g^{-1}$ in discharges of 0.3 $mA \cdot cm^{-2}$ with voltage plateaus of 1.1-1.2 V [73,74]. In 1988 A.F. Sammells proposed the use of calcium as anode in a high- temperature metal-air battery operating at 850ºC [75]. Most recently, researchers of Massachusetts Institute of technology in collaboration with Wuhan university presented a calcium based primary flow battery [76] able to deliver 2.4 $Ah \cdot g^{-1}$. However, these systems are in the early stages of development and further efforts must be done for achieving suitable progress.

Let's look more in detail the most promising candidates as anodes for metal-air batteries:

Aluminium, which was the selected candidate for this work, is going to be presented more in deep in subsequent points.

1.4.1.1. Lithium:

This metal presents the highest theoretical gravimetric capacity thanks to its low molecular weight of just 7 $g \cdot mol^{-1}$ and ability to deliver one electron. Additionally, Li presents a high oxidation potential which permits a theoretical 2,98 V cell potential when coupled with oxygen. Most of the energy storage experts position Li-air cell as the most promising system for future application in electric mobility and portable electronics, which could achieve specific energies of 5 to 10 times these of commercial lithium-ion technologies [67].

Four types of Li-air systems can be differentiated as function of the used electrolyte, see figure 1.4.1.1.1: a) aqueous electrolyte type, b) aprotic/non-aqueous electrolyte type, c) mixed/ hybrid electrolyte type, and d) solid-state electrolyte type. All systems use lithium metal as the anode and oxygen gas as the cathode material, but their electrochemistry differs per the electrolyte.

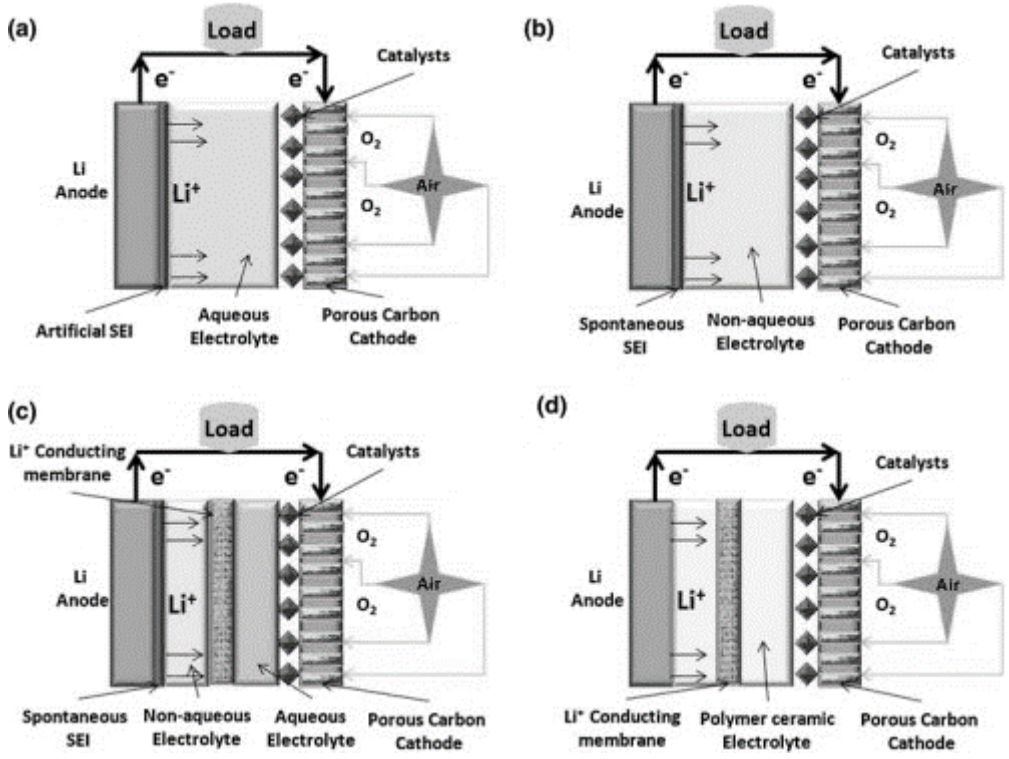

Fig. 1.4.1.1.1: Lithium-air battery types [77].

Aqueous systems have graved important research attendance because of its relatively high cell potential of 2-2.3 V, and practical specific energies of 1.3 and 1.4 $Wh \cdot g^{-1}$ in basic and acidic media respectively [78]. The most challenging point is the violent reactivity of metallic lithium when in contact with water, which leads to a constant corrosion and heat liberation in the cell. Thus, most of the investigations with aqueous electrolytes have focus in developing an artificial Solid Electrolytic interface (SEI) to prevent direct contact of water with lithium, while permitting Li-ion transport. Among different developments, ceramic LiSICON (Lithium-ion Superionic Conductor) family is the most remarkable one. Several mixed oxides like Li_x-M_y-GeO_4 or Li_x-M_y-$(PO_4)_3$, where M represents a metal from Zn, Ti, Si, etc., have demonstrated good Li ionic transport [79–

81], enough good to become commercial materials for battery research. Additionally, this system presents some advantages related to the cathodic side of the cell thanks to the developments carried out in fuel cells (air cathodes) which usually work in aqueous media. Cathode compositions and developments will be described later more in deep.

Another type of electrolyte for Li-air systems is the non-aqueous, which is composed of an organic solvent where a salt containing Li is dissolved. Most common solvents are propylene carbonate (PC), ethylene carbonate (EC), and dimethoxy ethane (DMEC), or in some cases mixtures between them [4,82,83]. In some cases, glymes or ethers are added as co-solvents to prevent evaporation, enhance oxygen solubility, etc. [84,85]. Usually mixed with salts like $LiBF_4$, LiPF6, $LiN(SO_2CF_3)$, and LiTFSI [77].
In these electrolytes, metallic lithium can be used without any protective layer. The main issue comes from the cathode of the battery. In organic media, the reaction between Li-ions and the reduced oxygen gives as product Li_2O and Li_2O_2. Li_2O is less desirable because its electrochemical oxidation is more difficult than Li_2O_2 one [86]. Additionally, the formation of amorphous Li_2O_2 would be more desirable because of a better O_2 conduction during the charge of the battery [87,88].
Achieved results are not easily comparable because differences in normalising specific capacity by the weight of catalyst in the cathode, adding or not carbon additive or adding or not binders and electric contacts [89]. Anyway, high capacity values have been reported of ~1000 $mAh \cdot g^{-1}_{carbon+catalyst}$ [90], being the maximum specific capacity of Li_2O_2 formation 1160 $mAh \cdot g^{-1}$. Cyclibility of this cell is still low, in the range of 20 to 50 cycles [91].

Hybrid electrolyte Li-air cells try to put in together the most favourable condition for negative and positive electrodes separately. That's it, a non-aqueous electrolyte in the anodic side, where metallic lithium can perform reversibly, and an aqueous electrolyte in the cathode side, where a lot of developments in bivalent air cathodes have been presented yet [92,93]. Both interconnected by a Li conducting membrane, normally NASICON (different ceramic composition than LiSICON), which presents good Li-ionic conductivity, as well as good intimate contact with both aprotic and aqueous solvents. Obtained results are scanty because of high internal resistance due to ceramic

conductor, as well as because of exchanging membrane surface saturation by reaction products.

And finally, solid-state electrolytes are also being investigated for developing a successful Li-air technology. In this case, the electrolyte is an ion-conducting solid, ceramic or polymeric. The main drawback of this technology is the low conductivity of the solid electrolyte [94], what restricts its use just for low power discharges. Other important issue is the incapability of the reaction product to get dissolved, which leads to the saturation of the air-cathode surface [94].

1.4.1.2. Magnesium:

Magnesium offers considerable arguments as anode for energy storage. Is the 5th more abundant element in Earth´s crust, it presents a high energy density as well as high electronegative potential, comparable to that of lithium, see Table 1.4.1.1., and additionally, the electrochemical processes related to its reversible plating/stripping have demonstrated the absence of dendrites formation (crystalline structure of some metals like Zn or Li, shaped like sharp tips). The latter permits the use of raw metal as anode, without fear of short-circuiting during charge of the battery due to the drilling of the separator by the dendrites [95].

Several electrolytes have been tested for their use in magnesium-air batteries or magnesium based anodes. Aqueous, or common polar solvents like carbonates or nitriles, coupled with magnesium containing salts such us perchlorates or tetrafluroborates [96] have demonstrated the formation of a passivating layer when in contact with metallic Mg. Unlike SEI (solid electrolyte interphase) in lithium based batteries, which permits good Li-ion transport and prevents electrolyte from further decomposition because highly reducing environment during Li plating [97], the passivating layer formed in magnesium surface presents low ionic transport, and induces electrolyte decomposition during charge [98,99]. Two main approaches have been explored to face this situation: the use of organo-magnesium reagents and solvents and the use of Mg-ion intercalation structures as anodes.

In the 1990s Gregory et al. [100] proposed several Grinard or organoborate reagents based electrolytes for reversible Mg platting/stripping. These reagents were commonly dissolved in organic solvents like THF, and even if they were inert towards cathode material, low chemical window (2V *vs* Mg), make them not suitable for battery application. 10 years later, Aurbach et al. reported the combination of organoborate salts with Al-based Lewis Acids [95], which presented enhanced chemical stability as well as faster electrochemical performance. Other salts like magnesium borohydrides, mixed together with lithium or aluminium bases salts, in dimethoxy-ethane (DME) presented also high efficiency Mg deposition/stripping, low oxidation potentials, as well as high potential window as Mohtadi et al. [101] demonstrated.

About intercalation anodes, Arthur et al. [102] firstly reported Mg-ion intercalation in different composition Bi and Sb alloys. Obtained specific capacity was near to 300 $mAh \cdot g^{-1}$, which decayed to 215 after a hundred cycles. Intercalation in Sn was also demonstrated [103] achieving capacities of 900 $mAh \cdot g^{-1}$, near to the theoretical value. However, these measurements were carried out at very low current rates of 0.005 C, while at 0.05 C the capacity obtained was just a 20%. The latter was due to the sluggish intercalation/extraction kinetics of Mg-ion [104], and to the pulverization process. This process takes place due to the volume expansion of the intercalation material when metal-ion get intercalated and volume depression when extracted, resulting in an anode material break off.

So, on the one hand, due to all these challenges related to the use of magnesium anodes, this technology still requires of major advances and research to become a practical metal-air rechargeable system. But, on the other hand, magnesium is a high-performance metal for primary or mechanically rechargeable metal-air batteries.
Several commercial magnesium based primary batteries have been developed, mostly for reserve energy or military applications. As previously commented, Mg exhibits high energy density as well as high voltage *vs* air cathode, the main issue is the evolution of hydrogen burbles during the operation of the cell, as well as the poor storageability of a partially discharged cell due to the corrosion [1]. Due to these drawbacks, most of magnesium-air battery developments have been focused on undersea applications by

using dissolved oxygen in seawater as cathode reactant. These batteries get activated once in contact with seawater (which acts as electrolyte), and can deliver 700 $Wh \cdot kg^{-1}$. Mg anodes are often alloyed with Al and Zn to prevent magnesium hydroxide formation in anode surface that could impede hydroxyl ion diffusion, and high surface, open structure air cathodes are used for ensuring seawater inlet. Because of the non-possibility to use more than one cell in series (owing to the high conductivity of the seawater), big scale batteries are used to provide enough energy and the voltage of the cell (1.2-1.6 V) is then rectified to higher values by a DC/DC converter.

1.4.1.3. Iron:

Iron has historically been used as anode for batteries due to its ease oxidation and ability to be electrodeposited form aqueous electrolytes, together with its low price and abundancy. Iron-nickel oxide cells patented by T.A. Edison is a good example of the latter. An iron-air battery is in broad stokes the evolution of the cited cell, where the Ni based cathode has been substituted by an air cathode, and some additives have been added to the alkaline electrolyte.

Compared to other metals, metallic dendrites are not formed during iron deposition, but on the other hand, hydrogen evolution, low efficiencies and self-corrosion in standby must be faced. The cell potential of this technology is 1.3 V (lower than Fe-Ni cells, 1.45 V), but it doubles the specific capacity of the cell described by Edison. In 1960s NASA developed a 20 Ah iron-air battery for transport applications with an energy density of 140 $Wh \cdot kg^{-1}$ [105] , able to charge-discharge for more than 200 cycles. This technology attracted fair commercial attention during the 1970s, during the oil crisis, by companies like Siemens or Matsushita, and Westinghouse Electric Corporation reported the acceptable performance characteristics of a state-of-the-art iron sintered electrode. They predicted an iron-air battery of 140 $Wh \cdot kg^{-1}$ and more than 1000 cycles performance at a sustainable manufacturing cost. More recently, several groups working in iron-air batteries reported energy densities of 110 $Wh \cdot kg^{-1}$ for more than 1000 cycles [106], or impressive 2000 cycles for 70 $Wh \cdot kg^{-1}$ by Narayanan et al. [107].

However, there is still no commercial product available due to some issues to be solve: Iron anode oxidation gives as result two differentiated plateaus during discharge, from Fe^0 to Fe^{2+} (1.3 V *vs* air cathode) and then to Fe^{3+} (1.15 V *vs* air cathode) [108]. The discharge product of this first reaction is $Fe(OH)_2$ (electrical isolator), which results insoluble in alkaline electrolytes, and it gives raise to it accumulation into electrode surface increasing discharge over-potential [109]. During the second plateau the iron hydroxide turns into iron oxide which results reversible during charge stage of the battery. Due to these complex discharge reactions, the ciclability of the cell gets compromised. Additionally, the charge efficiency of the iron electrode results low owing to a hydrogen evolution parallel reaction that consumes water [110], and once charged (metallic state) iron suffers from corrosion in alkaline media, which results in self-discharge of the battery during standby.

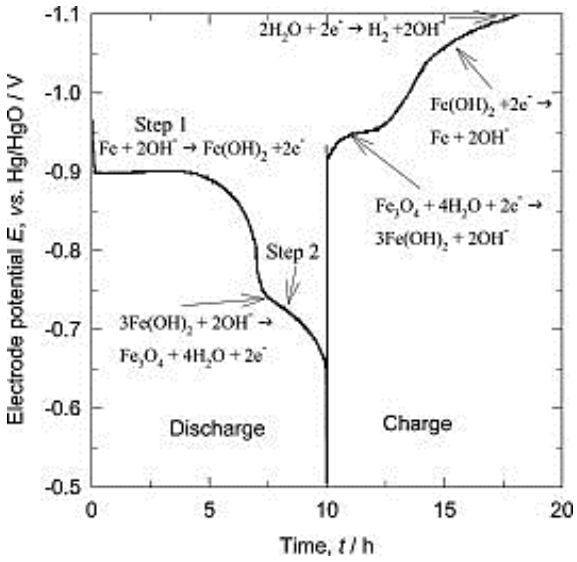

Fig. 1.4.1.3.1: Iron electrode performance vs Hg/HgO reference in KOH electrolyte [110].

To overcome the cited issues, several strategies have been focused by different research groups. For a better utilization of iron, nanoparticle size dispersions in carbonaceous materials have been used [111], as well as open carbon structures to prevent $Fe(OH)_2$ accumulation. Other strategies were the addition of salts like Bi_2S_3 or FeS, etc. to prevent hydrogen generation during charge, increasing significantly charge efficiency [112]. The latter resulted in are specific capacity of 786 $mAh \cdot g^{-1}$ (weight of iron) and cycling efficiency of 76% at the 30th cycle reported by Ito et al. and Hang et al. [113,114].

Compared to other metal-air systems, most of the challenges for a commercial iron-air system are located in the cathode side of the battery (later analysed). This is due to the previous developments in iron anodes for Fe-Ni technology from companies like Changhong Electric Co., Zapp Works Inc., etc.

1.4.1.4. Zinc:

As commented in the beginning of this introduction, Alexandro Volta invented the first battery, which was composed of a copper cathode and a zinc anode. Since this invention, metallic zinc has been the anode material for choice of many primary systems as zinc-carbon, zinc-manganese, alkaline cells, zinc-air, etc. [59]. Zn is an attractive metal for energy storage due to its low equivalent weight, high energy density, low price and toxicity, and additionally it is the most electropositive metal that results stable in aqueous and alkaline media without significant corrosion [62].

The latter makes Zn-air cells, together with Mg-air (underwater systems), the unique commercial metal-air batteries. Most of commercial cells used a gelled mixture of granulated Zn as anode. The morphology and particle size has been found to be important in achieving good electrical conductivity, for a better electrochemical performance. Several strategies have been studied for this purpose. Durkot et al. reported that a large proportion of fine Zn particles (<200 mesh) had increased high rate discharge [115], while Oyama et al. proposed a combination of coarse and fine particles as a good balance between high rate performance and corrosion resistance [116]. Other electrode configurations have been reported also, as Zn fibers by Zhang et al. [117] with enhanced behaviour in large-size Zn-air cell due to its low internal resistance, high surface area and good mechanical properties. Besides, Drillet et co-workers reported a foam like Zn electrode with high energy densities [118].

However, as the Zn active area increases, corrosion becomes more significant. The latter gives rise to electrolyte consumption and hydrogen evolution, and so, efficiency decay as well as battery life time shortening. Several strategies have been explored during the last century. A first try has been an amalgamation of zinc electrodes by using mercury, which nowadays is know that results toxic, and later other metals like Pb, Cd, Bi, Sn, In,

etc. has been used for this purpose [119]. Other treatments like surface coating with Al_2O_3, lithium salts, etc. were reported with satisfactory results [120].

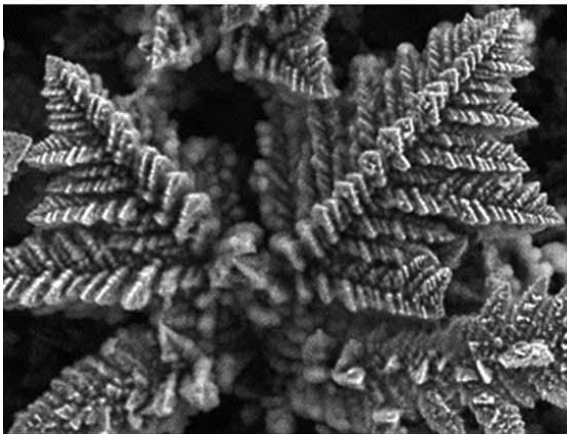

Fig. 1.4.1.4.1: Electroplated zinc dendrite SEM image [121].

These electrodes were suitable for primary Zn-air cells, but when tested in rechargeable cells several issues appeared. Zinc, unlike iron or magnesium, tend to form dendrites when electroplated in aqueous electrolytes. These dendrites grow perpendicularly to the electrode surface, going through the separator, and finally short circuiting anode and cathode. For solving this challenge, organic and inorganic additives to the anode or the electrolyte have been proposed by different groups, as well as Zn alloys. Vatsalarani et al. presented a polyaniline based surface coting to avoid dendrite formation [122]. Addition of calcium hydroxide or zincate demonstrated also an enhancement of cycle life of Zn electrodes [123], as well as other alkaline-earth metal hydroxides or citrates [124]. McBreen and co-workers investigated additions of Bi_2O_3, PbO, In_2O_3, etc. in the electrode for preventing dendrite formation during charge [125,126]. The latter generated a nanoscale electric conductor layer before the Zn deposition that distributed homogeneously charging current all over the electrode surface, permitting thin and compact zinc depositions. PEG (polyethylene glycol) and other organic polymers demonstrated also capability to partially suppress dendrite formation [127].

At this point, zinc is situated as the most promising anode for metal-air rechargeable batteries in a near future. Different experts consider that a successful development of Zn-air battery could be the key for the final implementation of the electric vehicle with large-range [2].

For this purpose, issues related with the reversibility of the air cathode, as well as novel cells designs must be solved and developed. These challenges are going to be explained more in detail in the next points.

1.4.2. Cathodes for metal-air batteries.

As explained before, metal-air batteries are composed, equal to a classic battery, of an anode, an electrolyte and a cathode. The main difference between metal-air batteries and other technologies is the fact that the cathode is an air electrode which is exposed to oxygen to make it reduce as main reactant of the cell.

This process was discovered by Leclanche in 1868, when he developed the MnO_2/Carbon electrode. He observed that the carbon cathode performed better when supporting carbon was saturated of oxygen, so he concluded that the MnO_2 was catalysing the oxygen reduction reaction (ORR). Since this discovery, many strategies have been carried out for the exploitation of oxygen as reactant in energy generation devices: metal-air batteries, fuel-cells, metal hydride-air batteries, etc.

In the 1930s, Heise and Schudmacher deepened in the finding of Leclanche and developed the first commercial air electrode [128]. They saturated carbon electrodes of oxygen and then treated their electrodes with wax to prevent flooding. These electrodes presented still low capacity and resulted bulky, but the research performed in fuel cells, gave rise to a new design of an air cathode.

This cathode was different from the previous MnO_2/Carbon based electrodes even if the composition was in brad strokes the same. It was a film of just 1 or 2 mm thick, where a mixture of carbon powder, manganese dioxide and a binder, was pressed into a metallic mesh. This electrode was not designed for being totally immersed in electrolyte, but to put together one of the faces with electrolyte and the opposite directly in contact with oxygen (from the atmosphere or from an oxygen flow).

This new electrode was called GDE (Gas Diffusion Electrode), and permitted the development of first “modern” metal-air cells some years later. In the 1970s first large size commercial zinc-air batteries appeared as a joining between alkaline cells and fuel cell air cathodes, and a few years later, this technology was found suitable for button cells constitution. Zn-air button cells for hearing aids, watches, and small devices hit the

market in 1976 and are still nowadays the most used batteries for certain applications [1].

The constitution of commercial air electrodes has not change too much form its first invention in 1970s. Nowadays several companies produce these electrodes for their use in commercial Zn-air batteries, and for R&D purpose. Electric Fuel Ltd., Gaskatel GmbH., Rayovac Corp., Gillette Corp., etc. have their own composition for their air cathodes, variating from the current collector metallic mesh composition or shape, to the employed catalyst for ORR, but the design of the cathode results the same:

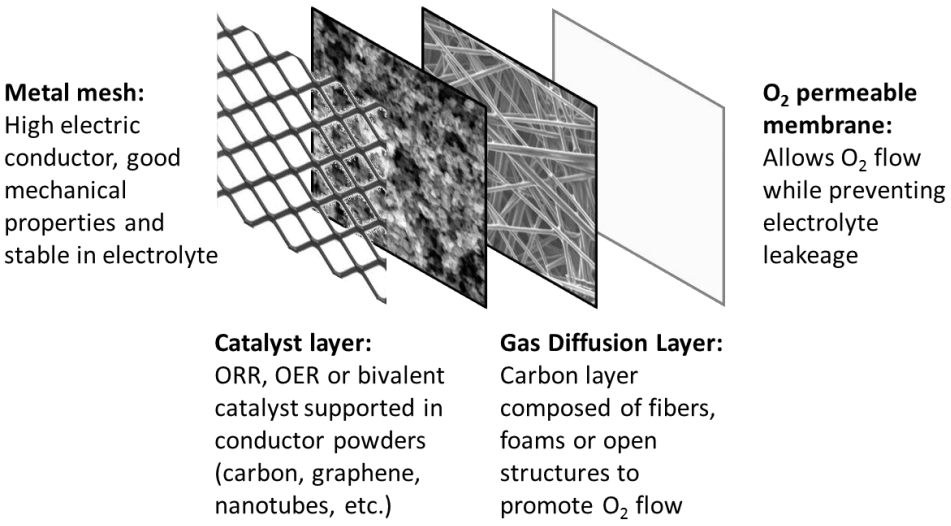

Fig. 1.4.2.1: Air cathode standard architecture.

Air cathodes in general are composed of four parts as represented in the figure 1.4.2.1:

- Metallic mesh: Even if carbon results a good electric conductor, when it gets in contact with electrolyte conductivity decays rapidly. That is due to the high porosity of the material which gets soaked. To ensure a good electrical conductivity of the cathode a metallic mesh is pressed directly in contact with the catalyst layer. The latter is also beneficial for improving mechanical resistance of the air electrode, mostly for medium or large-size cathodes. Different metals are used as current collectors as well as different shapes, as function of the specific needs of the electrochemical system. Most of the commercial air electrodes for Zn-air cells use nickel as current collector, due to a

good valance between electric conductivity, chemical resistance to alkaline environments and cost. But when chloride based, acid or non-aqueous electrolytes are used, nickel did not result enough stable, so other metals must be used. Several companies offer stainless steel mesh based cathodes, or even gold or silver plated mesh cathodes.

- Catalyst layer: Since the discovery of the use of oxygen as main cathodic reactant, millions of publications have explored the use of different catalyst, supports, etc. for their use in fuel cells or metal-air batteries. Among all known materials, platinum is the catalyst par excellence for ORR, the main issue is its high price due to low-abundancy. That is why other less precious materials have been explored. The most used catalyst for commercial air electrodes is MnO_2, due to its good performance to price ratio, even if it results in a low voltage and low power cathode, these parameters are enough for commercial Zn-air applications, as well as much cheaper than better catalysts. A table with a summary of different catalyst compositions reported by several groups and companies for metal-air battery cathodes is presented later.

  In addition to the employed catalyst, supports play a key role in the well-functioning of the electrode. High surface conductor materials (mostly carbons) are used to ensure a high number of catalytic points, when a good dispersion of the catalyst particles is obtained. Materials like carbon nanotubes, graphene, or graphite oxides have attracted lot of research attention in the last years due to its favourable conditions [91,129–131]. Some supports like graphene doped with nitrogen have even demonstrated good activity as catalyst for ORR.
- Gas diffusion layer: also known as GDL, it is the responsible of the contact between gas (oxygen), liquid (electrolyte) and solid (catalyst) to allow an efficient reduction of oxygen. This layer is composed of open structure materials, mostly carbon fibers or foams, to ensure a good distribution or the oxygen, while permitting a good contact with catalyst layer and surface wettability of electrolyte. A lot of research works have explored surface treatments for GDLs, to obtain a hydrophobic external face and an internal hydrophilic face [132].
- O_2 permeable membrane: This layer is normally a polytetrafluoroethylene (PTFE, the most famed brand is Teflon®) or woven plastic fibers based thin layer which

permits O_2 inlet and evacuation, while preventing electrolyte leakage to the outside; and humidity, CO_2 or any other impurity percolation.

Different patents from several companies define the better conditions for air electrodes fabrication. Most of them refer to a continuous production line, where a carbon GDL is firstly pasted or sprayed with a catalyst containing ink (a dispersion of catalyst particles, carbon powder, binder and solvent), and then the solvent is removed by hot air. Afterward, a PTFE solution is sprayed by both sides of the carbon GDL, a metallic mesh is placed in the catalyst containing face and a PTFE film in the contrary face, and finally, all together is pressed by a hot roll press machine at 120 to 150 ºC (some research works use higher temperatures (up to 300ªC) at laboratory scale for air cathode fabrication [133]).

1.4.2.1. Catalyst for air cathodes

The ORR in aqueous solutions can proceed by two pathways: direct four-electron pathway and a less efficient peroxide two-electron pathway [134]:

$$\rightarrow 4e^- \, pathway: \quad O_2 + 2H_2O + 4e^- \rightarrow 4OH^- \qquad \text{eq.1.4.2.1}$$

$$\rightarrow 2e^- \, pathway: \quad O_2 + H_2O + 2e^- \rightarrow HO_2^- + OH^- \qquad \text{eq.1.4.2.2}$$

$$HO_2^- + H_2O + 2e^- \rightarrow 3OH^- \qquad \text{eq.1.4.2.3}$$

In the direct four-electron pathway, oxygen directly reduces to OH^-. In the peroxide two electron pathway, an initial reduction to HO_2^- is followed by its reduction to OH^-. The peroxide pathway of the ORR is more common in alkaline solutions, while the direct four-electron pathway of the ORR proceeds by dissociative absorption on the metal catalyst surface, that is a complex process which usually requires expensive noble metals.

The most desirable reaction is that of four-electron pathway because of the high reactivity of HO_2^- molecule, that could attack electrode material, separator or cell casing. Most of the commercial GDEs contain MnO_2 as catalyst due to the low price and

availability of this compound, however it´s ORR activity is insufficient and it promotes the less efficient two-electron pathway. However, it is sufficiently active for hydrogen peroxide decomposition and stable in alkaline solution.

For a secondary metal-air battery, a bifunctional air cathode is necessary. This bivalent electrode has active components for both ORR and OER, and it results extremely desirable since it eliminates the replacement of the electrolyte and anode metal like in mechanically rechargeable metal-air batteries.

In this case, during charge step, the contrary reaction takes place in the air cathode: Oxygen Evolution Reaction (OER):

$$\rightarrow 4OH^- \rightarrow O_2 + 2H_2O + 4e^- \qquad \text{eq.1.4.2.4}$$

The OER restores the previously generated OH^- to original oxygen, which goes out through the PTFE membrane. That is why metal-air rechargeable batteries are also called “breathing” batteries, because of the oxygen inlet and outlet during discharge and charge.
A table with some representative catalyst for air cathodes is presented below.

Among different catalyst for air electrodes, manganese, cobalt and silver oxides are the most used materials because they present good price to performance ratio. For commercial Zn-air button batteries MnO_2 is normally used as catalyst but for more specific applications like military or aerospace Ag, Co or even Pt has been used.

Table 1.4.2.1: list of catalyst for air cathodes by group, composition, design and performance parameters.

Group / Company	**Catalyst Composition**	**Design**	**Performance**	**Ref.**
Rayovac Corp. (USA)	MnO_2 (20µm) + C (activated carbon) + PTFE	Standard*	1.15 V (vs Zn) at 150 mA·cm^{-2} in 30% KOH for 15h	1
C-Y Wu et al.	Ag/CNC (carbon nano-capsules)	Standard*	0.99 V (vs Zn) at 200 mA·cm^{-2} in 30% KOH	2
H. Meng et al.	AgW_2C/C	Standard*	200 mV (vs Hg/HgO) at 6 mA·cm^{-2} in 1M KOH	3
Gillette Corp. (USA)	MnO_2 + <10% $AgMnO_4$ + C + PTFE	GDL 30-70%PTFE; CL 10-30% PTFE	5% $AgMnO_4$ - 0.16 V (SHE) at 30mA·cm^{-2} in KOH 10% $AgMnO_4$ - 0.16 V (SHE) at 50mA·cm^{-2} in KOH	4
Luz Electric Fuel Ltd. (Israel)	Raney Silver catalyst +PTFE	C + PTFE on Ni mesh/foam	0.9 V (vs Zn) at 200 mA·cm^{-2} in KOH after 5h	5
Zinc air Power Corp. (USA)	Ag_2O + 10% $LaNiO_3$	Standard*	1.2 V (vs Zn) at 10 mA·cm^{-2} in KOH for 500h	6
Ovonic battery company Inc. (USA)	2.5% MnO_x + CoO_x/C	Standard*	0.1V (SHE) at 120 mA·cm^{-2} in KOH	7
M. Miura et al.	60% Mn_4N/C + PTFE	Standard*	0.8 V (RHE) at 300 mA·cm^{-2} in 9M NaOH (80ºC)	8
J.W. King et al.	$NiCo_2O_4$ spinel	Standard*	0.85 V (RHE) in 5M KOH	9
T. Hyodo et al.	1) $LaMnO_3$ perovskite 2) $LaCoO_3$ perovskite	Standard*	1) -160 mV (Hg/HgO) at 1200 mA·cm^{-2} 2) -160 mV (Hg/HgO) at 1000 mA·cm^{-2}	10
		Bifunctional electrodes		
Westinghouse Electric Corp. (USA)	1) $CuSO_4$ + $NiWO_4$ + WC + 20% Co 2) WC + Ag/C + FEP (polymer)	Hydrophilic CL + FEP sheet	-0.3V (Hg/HgO) at 100mA·cm^{-2} (decay to 40mA·cm^{-2} after 900h) in KOH	11
Y. Shimizu et al.	$La_{1-x}A_xFe_{1-y}Mn_yO_3$ (A = Sr, Ca)	-	-0.3 V (Hg/HgO) at 300 mA·cm^{-2} in 7M KOH	12
Y. Shimizu et al.	$La_{0.6}Ca_{0.4}Co_{0.8}Fe_{0.2}O_3$	-	-0.15 V (Hg/HgO) at 200 mA·cm^{-2} in NaOH	

[1] [135] [2] [136] [3] [137] [4] [138] [5] [139] [6] [140] [7] [141] [8] [142] [9] [143] [10] [144] [11] [145] [12] [146]

Other materials like perovskites or spinels have gained a lot of attention due to their high ORR activity and wild development for their use in other technologies like Li-ion batteries.

Bifunctional or bivalent air cathodes are nowadays one of the hottest topics in metal-air battery research. The use of a cathode for both ORR and OER could give raise to the development of high energy density batteries which could power the requirements of lots of applications in a near future.

These first 4 points of the introduction have summarized the history of the development of most common battery technologies, have propose some future scenarios where batteries will play a key role and have explain briefly what a metal-air battery is. Advantages of this technology compared to other commercial batteries have been presented, as well as existing anodes, electrolytes and cathodes. Now, we are going to move to the main scope of this work, which is aluminium-air technology. This battery is the unique metal-air battery still not presented, so, the next point is going to summarize the particular characteristics of this metal, as well as which relevant research has been carried out during last years in this scope and the motivation for choosing aluminium as anode.

1.5. Aluminium-air battery: discovery, commercial alloys and state of the art.

Aluminium is the third most abundant element in the earth´s crust, just after oxygen and silicon [147]. The latter coupled with the highest theoretical volumetric capacity, makes this metal one of the most promising anodes for energy storage electrochemical systems. The relatively high density of around 2.7 $g \cdot cm^{-3}$ and its trivalent ionic state makes the theoretical volumetric capacity of Al go up to 8.04 $Ah \cdot cm^{-3}$, more than two and three times that of magnesium and lithium respectively [148]. This unique property makes aluminium based batteries particularly interesting for their use in devices where available volume is limited or where minimal size is the most advantageous attribute for

energy supply, such us portable electronics, electric vehicles or domestic self-consumption. Moreover, the theoretical gravimetric capacity of Al it's comparable to that of lithium, 2.9 vs 3.8 Ah·cm^{-3}, resulting attractive also for applications where weight is a limiting factor.

1.5.1. Discovery and production.

Even of its widespread use all over the world, aluminium is a young metal since it was discovered in 1825 (just less than 200 years ago) by Hans Christian Oersted [149]. Some years later, Henry Sainte-Claire Deville obtained the first pure aluminium ingot by reduction of aluminium chloride with potassium, but the real revolution came with the discovery of the Hall-Héroult process by Martin Hall and Paul Héroult, and the Bayer procces by Karl Bayer in the late 1880s.

The Hall-Héroult process made possible the electrolysis of molten aluminium oxide (dissolved in cryolite) to obtain 99.8% pure metallic aluminium. This process was discovered at the same time (less than one year difference) in America and France so there is still some controversy about the real authorship.

This process is relatively simple [150]: it consists in a large size electrolytic cell or "pot" where aluminium oxide (alumina) is dissolved in molten cryolite (Na_3AlF_6) at 1000ºC. Cryolite is used as solvent because of the high melting temperature of alumina (2080ºC). In this "pot" a carbon anode and cathode are placed and when a 5 V potential and 1 to 3 A·cm^{-2} current density is applied aluminium salt electrolysis takes place. Molten aluminium and CO_2 are the result of the process (see equation 1.5.1.1) and liquid aluminium is extracted by density (aluminium drops to the bottom of the cube because of its higher density).

$$\rightarrow Al_2O_3 + \frac{3}{2}C \rightarrow 2Al + \frac{3}{2}CO_2 \qquad \text{eq.1.5.1.1}$$

This process was boosted to success thanks to the Bayer process, which refines Bauxite (one of the most abundant mineral, and the world´s main source of aluminium) to alumina, which is the main reactive for the Hall-Héroult process.

In broad strokes, Bayer process consists in a NaOH treatment to Bauxite to produce $Na[Al(OH)_4]$, which is then treated with water, crystalized and dried at 1000ºC to finally obtain aluminium oxide [151]. Over 90% of alumina produced worldwide is used for aluminium electrolysis by the Hall-Héroult process.

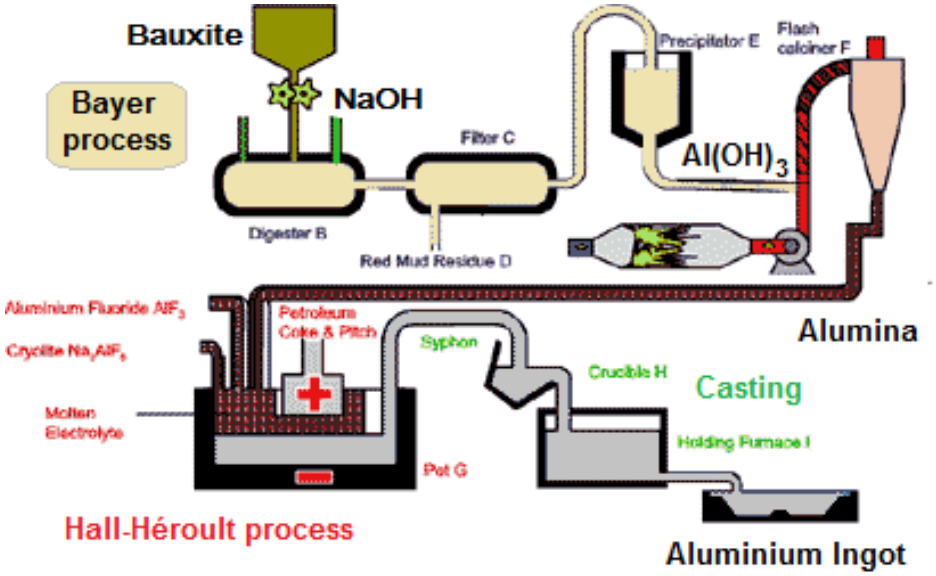

Fig. 1.5.1.1: Schematic diagram of aluminium industrial production (Bayer process + Hall-Héroult process) from Bauxite mineral.

As commented before, these two processes where discovered in the late 1880s. The latter coupled with a low cost of the electricity made aluminium one of the cheapest and used materials for applications like construction, automotive sector, aircraft, etc. In 1850 (before Hall-Héroult process) the production of aluminium was just some tens of kilos and it was more expensive than silver or gold, so much so that Emperor Napoleon III of France was said to have reserved his few sets of aluminium dinner plates and eating utensils for his most honoured guests.

The first aluminium large-size production plant (operating with the Hall-Héroult process) was installed in Pittsburgh in 1888 and it later became Alcoa Corporation which is still one of the biggest aluminium producers worldwide [152]. The production of aluminium in 2010 was 25 million of tonnes, and it is considered that the 75% of the Al produced form its discovery to nowadays is still in use. This is possible because of the high recyclability of this metal.

Aluminium is one of the most recycled metals due to its low melting point of around 660ºC (depending on the alloying elements), its ductility and malleability and its ability to resist corrosion during time. This corrosion resistance happens because the passivation process in the aluminium surface. The latter consists in the formation of an aluminium oxide passive layer of just microns of thickness in the Al surface that protects the intern metal form further corrosion [153]. This phenomenon makes this metal one of the most used for construction purpose, in windows, facades, body shells for cars or planes, boats, etc. And makes it last for long times without surface corrosion or degradation of its internal properties.

Aluminium recycling process is estimated to consume just a 5% of the energy consumed in "fresh" aluminium production from Bauxite [154]. Additionally, new alloys can be easily produced just by adding small quantities of other metals in the recycling process. It is calculated that near to 85% of "new purpose" aluminium comes from recycled metal, and just a 15% of fresh aluminium from Bauxite is added to the Al consumption chain every year [155]. The latter makes aluminium cost low and constant in time.

1.5.2. Commercial aluminium alloys.

From its discovery, a large industry is being created around aluminium because of its favourable properties for infinite purposes. Pure aluminium is a soft and brittle light grey metal which did not present good mechanical properties for construction or manufacturing of pieces. But, with the addition of small quantities of other metals these properties change significantly. For example, the addition of iron and silicon gives it strength for construction purposes, manganese makes is malleable and ductile, zinc or magnesium makes it more resistant to corrosion and harder, etc [156]. Because of this particular behaviour a great deal of commercial aluminium alloys is actually available for different uses.

There are two principal classifications, namely casting alloys and wrought alloys, both of which are further subdivided into the categories heat-treatable and non-heat-treatable. About 85% of aluminium is used for wrought products, for example rolled plate, foils and extrusions. Cast aluminium alloys yield cost-effective products due to the low melting point, although they generally have lower tensile strengths than wrought alloys.

Aluminium alloys are also classified as function of its alloying elements giving as result 8 series for wrought alloys and 9 series for casting alloys [157]. Every alloy from a series presents similar mechanical properties due to the prevalence of some alloying elements. Casting alloys are more limited in composition because of the need to add silicon to ensure good casting properties. Table 1.5.2.1 shows some characteristics of the wrought aluminium alloys series, major alloying elements and most remarkable alloys in the series. These thousands of aluminium alloys compositions have been formulated not only by aluminium producers but also by material science researches, and still every year new composition are included in these 8 series. Not all the alloys are commercially available, because of the high specialisation grade of its compositions, and some of them must be made to order.

The International Alloy Designation System is the most widely accepted naming scheme for wrought alloys. Each alloy is given a four-digit number, where the first digit indicates the major alloying elements, the second — if different from 0 — indicates a variation of the alloy, and the third and fourth digits identify the specific alloy in the series. For example, in alloy 3105, the number 3 indicates the alloy is in the manganese series, 1 indicates the first modification of alloy 3005, and finally 05 identifies it in the 3000 series [158].

- → 1000 series are essentially pure aluminium with a minimum 99% aluminium content by weight and can be work hardened.
- → 2000 series are alloyed with copper, can be precipitation hardened to strengths comparable to steel. Formerly referred to as duralumin, they were the most common aerospace alloys, but were susceptible to stress corrosion cracking and are increasingly being replaced by 7000 series in new designs.
- → 3000 series are alloyed with manganese, and can be work hardened, they present the higher strength to price ratio.
- → 4000 series are alloyed with silicon. Variations of Al-Si alloys intended for casting (and therefore not included in 4000 series) are also known as silumin.
- → 5000 series are alloyed with magnesium, and offer superb corrosion resistance, making them suitable for marine applications.

- → 6000 series are alloyed with magnesium and silicon. They are easy to machine, are weldable, and can be precipitation hardened, but not to the high strengths that 2000 and 7000 can reach.
- → 7000 series are alloyed with zinc, and can be precipitation hardened to the highest strengths of any aluminium alloy.
- → 8000 series are alloyed with other elements which are not covered by other series. Al-Li alloys are an example.

From these thousand compositions, 3000 series alloys are the most used aluminiums worldwide, and most concretely 3003 and 3004 alloys because its favourable tensile strength and corrosion resistance to price ratio. Most of worldwide food and drink cans are made of these aluminium alloys, as well as bigger multipurpose cans, window frames, roofing and sidings, etc [159].

When special corrosion protection is needed and the tensile strengths of some alloy compositions must be maintained, a process called Cladding is used. This Cadding process, also known as Alclad, trademark from Alcoa company, consists in the metallurgically bonding of a pure aluminium thin layer on the surface of a high-strength aluminium alloy core material [160]. This aluminium cladded alloy presents tensile strength as high as the alloy core material, for example Al 2024, while the highest possible corrosion protection of pure Al. The metallurgical bonding permits a thorough union between the alloy and the pure aluminium, so, no corrosion or pitting could be initiated between layers.

Table 1.5.2.1: Commercial aluminium alloys series, most remarkable alloys and characteristics. *Ref:* [157]

Al Alloy series	**Major alloying element**	**Remarkable characteristics**	**Most used alloys**
*1000**	High Al content (>99%**)	- High corrosion resistance - High brightness when polished - Can be work hardened	- 1050 – drawn tubes - 1060 – universal uses - 1145 – Al foils
*2000**	Cooper	- Referred as Duralumin - Can be precipitation hardened - Strengths comparable to steel	- 2024 – universal uses, aerospace - 2090 – aerospace, cryogenics - 2319 – bars and wires
*3000**	Manganese	- Good workability and moderate strength - Good corrosion resistance - Most worldwide used series, general purpose aluminium	- 3002 – heat exchangers - 3003/3004 – food and drink cans - 3105 – roofing and siding
*4000**	Silicon	- Variations of Al-Si alloys intended for casting - Very good welding properties - Used for aluminium forging and extrusion	- 4007 – welding wires - 4032 - forging
*5000**	Magnesium	- Very good corrosion resistance - Moderate strength - Good welding properties	- 5005 – chemical and food equipment - 5052 – marine parts/ boats - 5086 – welded pressure vessels
*6000**	Silicon + Magnesium	- Good corrosion resistance - Good machinability, weldability and formability - Most used for extrusions	- 6010 – multipurpose Al pieces - 606X – building and architecture - 6450 – automotive applications
*7000**	Zinc	- Higher strength aluminium - Good machinability - Heat treatable	- 7005 – Device shells - 7075 – aircraft wings - 7475 – aerospace fuselage
*8000**	Others (Sn, Li, V, etc.)	- Very specific alloys - Ultra-light weight alloys (lithium)	- 8030 – high electric conductivity - 8090 – lightweight aircraft

**1000, 2000, etc. series are sometimes also represented as 1XXX, 2XXX, etc.*

***by weight.*

1.5.3. Al-air battery, working principle.

In the same way than before presented metal-air batteries, Al-air battery is composed of an air cathode, and aluminium anode and an electrolyte between them. The overall theoretical reaction of a water electrolyte based Al-air battery is [1]:

$$\rightarrow \ 4Al + 3O_2 + 6H_2O \rightarrow 3Al(OH)_3 \qquad \textit{eq.1.5.3.1}$$

Being the single electrode reactions:

$$\rightarrow \text{ anode: } \ Al + 3OH^- \rightarrow Al(OH)_3 + 3e^- \qquad \textit{eq.1.5.3.2}$$

$$\rightarrow \text{ cathode: } \ O_2 + 2H_2O + 4e^- \rightarrow 4OH^- \qquad \textit{eq.1.5.3.3}$$

But when an alkaline electrolyte is used for Al-air battery, aluminium suffers from a self-corrosion parasite reaction, which makes reactions change as follows [161]:

$$\rightarrow \text{ anode: } \ Al + 4OH^- \rightarrow Al(OH)_4^- + 4e^- \qquad \textit{eq.1.5.3.4}$$

$$Al(OH)_4^- \rightarrow Al(OH)_3 + OH^- \qquad \textit{eq.1.5.3.5}$$

$$Al + 3H_2O + OH^- \rightarrow Al(OH)_4^- + H_2 \uparrow \qquad \textit{eq.1.5.3.6}$$

The oxidation of aluminium, due to the high hydroxyl concentration in an alkaline environment delivers one electron more to form $Al(OH)_4^-$, see equation 1.5.3.4, instead of $Al(OH)_3$, see equation 1.5.3.5. This aluminium hydroxide anion can stay as ion, which is soluble in the alkaline electrolyte or it can move to its more stable non-excited form. This reaction is sometimes called “electrolyte regeneration reaction”, and is common for other alkaline electrolyte based metal-air batteries like Zn or Fe-air [61].

Parallel to the oxidation of aluminium, a corrosion reaction takes place, see equation 1.5.3.6. This reaction is spontaneous, and starts immediately just by simple contact between aluminium and alkaline electrolyte, consuming Al mass and water, decreasing the pH and generating hydrogen. The latter makes the standby of an alkaline Al-air

battery impractical because of the loss of active species before starting the discharge. Additionally, due to this parasitic reaction that occurs not only at open circuit potential (OCP), but also during the discharge, the coulombic efficiency of the anode is notoriously decreased [153].

Thermodynamically, aluminium oxidation in alkaline media should exhibit a potential of -2.4 V *vs* SHE, and oxygen reduction reaction +0.3 V, so the theoretical cell voltage should be 2.7 V. However, due to the self-corrosion reaction which presents a much cathodic potential of -0.89 V *vs* SHE, a practical Al-air alkaline cell presents a potential between 1.5 to 2 V.

In sodium chloride electrolyte, neutral pH, the reaction of Al is not completely clear, because of the mixed species in the aluminium surface, combining metallic Al - Al_2O_3 - $Al(OH)_3$ - H_5AlO_4 - and other chlorinated complex species. Taking the latter into account, the most extended and accepted reaction is described as follows [162]:

$$\rightarrow \ 2Al + 6H_2O \ \rightarrow 2Al(OH)_3 + \ 3H_2 \uparrow \ + 3e^- \qquad \textit{eq. 1.5.3.7}$$

So, contrary to what happens in alkaline media, in saline electrolyte, the hydrogen generation does not take place because of a parasitic reaction, but because of the main oxidation of Al anode. However, during cell standby (aluminium immersion in the electrolyte at OCP) there is not hydrogen evolution or mass loss [69].

This hydrogen generation is always thermodynamically favourable at potentials were aluminium dissolution occurs, so H_2 gas may evolve during battery operation.

The potential of Al in saline media is thermodynamically limited to -1.66 V *vs* SHE, what makes the final voltage of a neutral pH Al-air cell lower than the one for an alkaline electrolyte. The cell potential would be, in the best-case scenario of 1.2 to 1.5 V. Additionally, ionic conductivity is lower for this electrolyte and air cathodes will perform at lower voltage and current values than the ones for alkaline solutions.

Another important point for the saline electrolyte is the native aluminium oxide layer in aluminium metal. When in contact with oxygen, fresh aluminium forms spontaneously an oxide layer of 2 to 3 nm thick all over the surface. This native Al oxide layer protects aluminium from further corrosion [1,163]. The latter makes Al one of the most used metal because its stainless behaviour, but in an electrochemical system, this oxide layer must be removed before getting access to active fresh aluminium. In alkaline systems, the highly corrosive environment makes this oxide get dissolved, while in neutral pH it remains. And so, the potential of the electrode is shifted to more positive values.

This makes the potential of the cell suffer from a delayed action: at the beginning of a discharge the anode potential will be a mix between the metallic Al and the Al oxide potential, mostly dominated by the oxide, so more positive value; while when the oxide is being dissolved because of the applied current, more metallic Al is exposed and the voltage is shifted to more negative. This means than a saline Al-air cell would present an increasing voltage during a discharge, until the whole aluminium oxide film is being removed.

1.5.4. State of the art of Al-air battery.

1.5.4.1. History.

The aluminium as electrode material was firstly described in a cell by Hulot in the 1850s [164], as cathode material against zinc, while the first cell using aluminium as anode material was the Buff cell in the 1857 coupled with a carbon cathode [165]. Later in the 1950 aluminium was employed as anode in Leclanche type dry cell. In the following years several primary aluminium systems have been proposed such as Al-MnO2, Al-AgO, Al-H2O2, Al-S, Al-FeCN, Al-NiOOH, but due to the protective oxide layer a decrease of the electrode potential happens, resulting in a much lower working voltage in respect to the theoretical one.

The aluminium-oxygen system was first demonstrated in the early 1960s by Zaromb and Trevethan et al. [166,167], who found that the addition of zinc oxide or certain organic

inhibitors, to the electrolyte significantly decreased the corrosion of amalgamated Al anodes in 10 M sodium or potassium hydroxide solutions.

These early efforts, however, failed to use the aluminium anode in any commercial battery products. The latter was because of the explained aluminium oxide native layer, which shifts the potential of the anode to values even more cathodic than Zn. This oxide layer can be removed by several strategies, as aluminium amalgamation or highly alkaline solution, however, any gain in anode working potential is accompanied of accelerated corrosion and poor shelf life. These difficulties have long delayed the development of a satisfactory aluminium cell, even if considerable effort has been made to develop Al alloy anodes and electrolyte additives for aluminium batteries with aqueous electrolytes.

1.5.4.2. Aluminium anodes.

Aluminium reacts rapidly and irreversibly with oxygen to form a strongly-adhering oxide film, which largely determines the electrochemical behaviour of aluminium in aqueous electrolytes. Modifications of the formed oxide layer has been extensively explored by means of alloying specific elements to the Al matrix.

Several strategies have been focused with these specific metallic additions: moderating the thickness of the native oxide layer, reducing the rate of hydrogen evolution or controlling the Al dissolution morphology.

It is reported that alloying elements in the aluminium anode can modify the native Al oxide layer, to become Al anode more active. Elements like Hg, Pb, Ga, Sn, Zn, Mg, etc. have been identified to induce activation when alloyed with aluminium or present as additives in a sodium chloride, potassium hydroxide or sodium hydroxide electrolyte [168–171].

In the 1990s due to the big efforts made in aluminium anodes for energy storage, patents started to be filed [171–176]. Companies like Alupower, subsidiary of Alcan, invested big amount of resources for the commercial production of aluminium alloys for energy storage and generation. Their patents were based in ternary or quaternary alloys starting from a high purity aluminium matrix. Metals like Sn, Ga, In, Mg, Mn, etc. were

added to the pure aluminium matrix in patented proportions for developing commercial alloys under the name of AB50, AB50V, EB50V, etc.

These compositions were based in previous studies carried out by several researchers: Hunter et al. [177] investigated Al-Sn binary alloys of varied compositions of Sn, achieving OCP values of -1.45 V *vs* SHE in 4 M NaOH. Rao et al. presented a 8 M KOH electrolyte based Al-air battery, using Al-Sn-Mg alloys, able to achieve 435 $Wh \cdot kg^{-1}$ (whole system weight) [178]. Shen et al. used an Al-Mg-Sn-Ga alloy in a multi-cathode system based of cobalt oxide catalyst with a 2 M sodium chloride electrolyte [179]. This system performed more than 1000 $Wh \cdot kg^{-1}$ energy density values in low current rate discharges.

Rudd and Gibbons presented an Al-air battery using KOH electrolyte pumped by an electronic control system, which used Al-In-Mn-Mg alloy as anode [180]. This device was able to deliver 3.9 $kWh \cdot kg^{-1}$.

Most recent works like the one presented by Zhuk et al. used Al-In alloys for semi fuel cell Al-air batteries, and collected the generated hydrogen for its use in fuel cell that could be connected to the battery to enhance the power density [181,182]. In the last year, a company called Phinergy presented an Al-air battery stack fuelled car, able to travel for 3000 km, just be refuelling distilled water every 300 km [183]. The employed alloy is not being revealed, while the cathode is Ag based. Their calculations based in an anode cost of 1.1 $€ \cdot kg^{-1}$, show an incredibly low energy generation cost of just 30 $€ \cdot kWh^{-1}$, an order of magnitude less than other technologies like Li-ion.

Contrary to the addition of some specific alloying elements, the presence of certain impurities such as iron and copper in the aluminium can markedly affect the electrochemical behaviour. For example, the corrosion rate is found to be particularly sensitive to the concentration of iron in the metal [184,185]. And so, Super-purity metal (at least 99.999 % purity) has been used to prepare anodes, but from an economic point of view, the Al matrix should be decreased to high-purity smeltergrade metal (99.8 %) to achieve cost-effectivity [186,187]. Another approach, which is presented in the

current work, is the use of commercial alloys, much more extended and cheap, which could result in low-cost batteries, even if the final performance would be not so notable.

As Nisancioglu announced this corrosion of aluminium alloys that contain intermetallic phases is essentially a microgalvanic process between the intermetallic particles and the matrix alloy [184]. So, other approaches must be followed to prevent not super-pure aluminium from corrosion, as electrolyte formulations (support electrolyte + additives).

1.5.4.3. Electrolyte formulations.

The major efforts to date of developing aluminium-air batteries have been focused in two electrolyte types: alkaline and saline.

→ Saline electrolytes:

Despic et al. were the first who explored Al-air batteries with saline electrolyte. A concentration of 12 % of sodium chloride solution, near to the maximum conductivity, was tested [171]. The conductivity of salt water was, however, lower than that of an alkaline electrolyte. To minimize the power loss due to internal resistance, a narrow anode– cathode gap is required. The anodic dissolution of aluminium in saline solutions results initially in an aluminium hydroxide gelatinous precipitate that impedes the well-functioning of the anode and binds water to increases in the water requirement.

Additives such as sodium phosphate, sulfate, fluoride and bicarbonate to sodium chloride solutions have been investigated to increase the compactness of aluminium hydroxide and therefore reduce the water requirements [147]. These additives serve as coagulants to precipitate the reaction product. NaF is being found to be the more effective additive to obtain a crystalline precipitate.

Another way is to separate continuously the formed gel and the electrolyte by an external process to the battery and continuously pumping the “clean” electrolyte to the cell. Additionally, the formed gel can be dried and reformed to obtain new fresh aluminium, as Zaromb patented [188].

→ Alkaline electrolytes:

The development of the Al-air battery with alkaline electrolytes is attributed to Zaromb and Trevethan et al. in the early 1960s [166,167]. The studies of this researchers demonstrated the technical feasibility of alkaline Al-air batteries. Thereafter, most of the studied electrolytes for this technology are strongly alkaline.

The alkaline electrolyte permits an optimal performance for the air cathode, which is decreased in saline electrolyte, and a low-level of aluminium polarisation under normal operation. KOH solution does not allow the retreatment of alumina via the industrial Hall–Heroult process, because potassium ions can damage the cathode of electrolysis cell. Consequently, NaOH was suggested by Doche et al [161].

Most of the efforts have been focused in the addition of inhibitor of hydrogen evolution, or complexing agents to the electrolyte. Among a long list of investigated additives, oxides of gallium, indium, calcium and zinc as well as stannates and citrates were found to be effective in inhibiting corrosion and/or enhancing electrode efficiencies [162,189].

1.5.4.4. Non-water based electrolytes.

Important efforts have been also made in secondary aluminium based batteries due to the high theoretical conditions of Al. Some of the most relevant results are presented below, but are not going to be extensively treated because they are out of the scope of this work, which is focused in primary batteries.

Chloroaluminate melts, such as the binary NaCl-$AlCl_3$ or the ternary KCl-NaCl-$AlCl_3$, have been widely studied for aluminium electrodeposition since the 1970s, and them were considered as possible electrolytes for the development of secondary Al batteries [190]. These systems with a general formula of MCl-$AlCl_3$ (where M^+ can be a monovalent cation like Li^+, Na^+ or K^+, or an organic cation like pyrrolidinium or imidazolium) can be synthesised in basic, neutral or acid, when the MCl/$AlCl_3$ mole ratio is, respectively, higher, equal or lower than one. In acid melts the dominant species is $Al_2Cl_7^-$; in the neutral melt the only anionic species is $AlCl_4^-$ while in basic melts $AlCl_4^-$, and Cl^- species

coexists [191]. In basic and neutral melts the electrodeposition of Al is defined as follows:

$$\rightarrow \ AlCl_4^- + 3e^- \ \rightarrow Al + 4Cl^- \qquad \textit{eq. 1.5.4.4.1}$$

In acid melt however, the reaction is defined as follows:

$$\rightarrow \ 4Al_2Cl_7^- + 3e^- \ \rightarrow Al + 7AlCl_4^- \qquad \textit{eq. 1.5.4.4.2}$$

This acid melt is being considered as the most suitable electrolyte for Al platting and stripping [192].

Among all the chloroaluminate melts, the most promising one are the room temperature liquids. These electrolytes, also known as ionic liquids, present an eutectic point that permits its melt at temperature lower than 100 ºC, being possible to synthesise melts at room temperature.

Imidazolium and pyrrolidinium organic cations have been the most explored ones, being the 1-butyl-3-methylimidazolium (BMIM) or 1-ethyl-3-methylimidazolium (EMIM) the ones that presented the state-of-the-art best results for Al platting and stripping [193,194].

Reed and co-workers presented a battery comprised of an Al anode and a vanadium oxide cathode, with an acid $AlCl_3$:EMIMCl melt as electrolyte [195], achieving charge-discharge cycles, but important issues were found due to the corrosive nature of the electrolyte. Wang et al. continued this work, for achieving cyclable capacities of 165 $mAh \cdot g^{-1}$ for 100 cycles.

Gifford and Palmisano proved the intercalation of Al in pyrolytic graphite, and tested an Al-PG battery for several cycles, with a discharge voltage plateau of 1.5 V [196]. Later, Sun et al., and Lin et al. [197,198] presented a Al-PG based battery with $AlCl_3$:EMIMCl acid melt electrolyte able to perform for more than 3000 cycles, in very stable plateaus of 2.2 V for discharge and 2.5 V for charge. The specific capacity however is low, in the order of 60 to 80 $mAh \cdot g^{-1}$.

A European government funded project, called ALION, is being carried out with the aim of developing a successful Al-ion battery for large scale energy storage. Albufera Energy Storage S.L. the company which financed the project in the framework of this thesis, and to which I currently work for, is involved in this European project.

1.6. References.

[1] D. Linden, T.B. Reddy, eds., Handbook of batteries, 3rd ed, McGraw-Hill, New York, 2002.

[2] S. Manzetti, F. Mariasiu, Electric vehicle battery technologies: From present state to future systems, Renewable and Sustainable Energy Reviews. 51 (2015) 1004–1012. doi:10.1016/j.rser.2015.07.010.

[3] K. Vignarooban, R. Kushagra, A. Elango, P. Badami, B.-E. Mellander, X. Xu, T.G. Tucker, C. Nam, A.M. Kannan, Current trends and future challenges of electrolytes for sodium-ion batteries, International Journal of Hydrogen Energy. 41 (2016) 2829–2846. doi:10.1016/j.ijhydene.2015.12.090.

[4] D. Golodnitsky, E. Strauss, E. Peled, S. Greenbaum, Review—On Order and Disorder in Polymer Electrolytes, Journal of The Electrochemical Society. 162 (2015) A2551–A2566. doi:10.1149/2.0161514jes.

[5] M. Piccolino, Luigi Galvani's path to animal electricity, Comptes Rendus Biologies. 329 (2006) 303–318. doi:10.1016/j.crvi.2006.03.002.

[6] S. Trasatti, 1799-1999: Alessandro Volta's "Electric Pile"., Journal of Electroanalytical Chemistry. 460 (1999) 1–4. doi:10.1016/S0022-0728(98)00302-7.

[7] P. Kurzweil, HISTORY | Electrochemistry, in: Encyclopedia of Electrochemical Power Sources, Elsevier, 2009: pp. 533–554. doi:10.1016/B978-044452745-5.00007-1.

[8] J.N. Spencer, G.M. Bodner, L.H. Rickard, Chemistry: structure and dynamics, 5th ed, Wiley, Hoboken, N.J, 2012.

[9] R. Dell, D.A.J. Rand, Understanding batteries, Royal Society of Chemistry, Cambridge, 2001.

[10] S.S. Misra, Advances in VRLA battery technology for telecommunications, Journal of Power Sources. 168 (2007) 40–48. doi:10.1016/j.jpowsour.2006.11.005.

[11] J. Larcin, W.C. Maskell, F.L. Tye, Leclanche cell investigations. Part II: Zinc potential as a tool for studying intermittent discharge, Electrochimica Acta. 44 (1998) 191–199. doi:10.1016/S0013-4686(98)00172-8.

[12] J.-Y. Huot, CHEMISTRY, ELECTROCHEMISTRY, AND ELECTROCHEMICAL APPLICATIONS | Zinc, in: Encyclopedia of Electrochemical Power Sources, Elsevier, 2009: pp. 883–892. doi:10.1016/B978-044452745-5.00061-7.

[13] B. Szczefniak, M. Cyrankowska, A. Nowacki, Corrosion kinetics of battery zinc alloys in electrolyte solutions, Journal of Power Sources. 75 (1998) 130–138. doi:10.1016/S0378-7753(98)00108-6.

[14] H. Karami, M.F. Mousavi, M. Shamsipur, A new design for dry polyaniline rechargeable batteries, Journal of Power Sources. 117 (2003) 255–259. doi:10.1016/S0378-7753(03)00168-X.

[15] M.C. Wu, T.S. Zhao, H.R. Jiang, L. Wei, Z.H. Zhang, Facile preparation of high-performance MnO 2 /KB air cathode for Zn-air batteries, Electrochimica Acta. 222 (2016) 1438–1444. doi:10.1016/j.electacta.2016.11.122.

[16] C.N. Chervin, J.W. Long, N.L. Brandell, J.M. Wallace, N.W. Kucko, D.R. Rolison, Redesigning air cathodes for metal-air batteries using MnOx-functionalized carbon nanofoam architectures, Journal of Power Sources. 207 (2012) 191–198. doi:10.1016/j.jpowsour.2012.01.146.

[17] Z. Huang, G. Du, Nickel-based batteries for medium- and large-scale energy storage, in: Advances in Batteries for Medium and Large-Scale Energy Storage, Elsevier, 2015: pp. 73–90. doi:10.1016/B978-1-78242-013-2.00004-2.

[18] J.-Y. Huot, M. Malservisi, High-rate capability of zinc anodes in alkaline primary cells, Journal of Power Sources. 96 (2001) 133–139. doi:10.1016/S0378-7753(01)00496-7.

[19] D. Saxman, World market for industrial batteries, in: Industrial Applications of Batteries, Elsevier, 2007: pp. 737–766. doi:10.1016/B978-044452160-6/50016-4.
[20] J.J. Lander, Sealed Silver-Zinc Batteries; Presented as Preprint 64-749 at the Third Biennial Aerospace Power Systems Conference, Philadelphia, Pa., September 1-4, 1964., in: Progress in Astronautics and Rocketry, Elsevier, 1966: pp. 1101–1110. doi:10.1016/B978-1-4832-3056-6.50053-0.
[21] H. Arai, M. Hayashi, PRIMARY BATTERIES - AQUEOUS SYSTEMS | Zinc-Air, in: Encyclopedia of Electrochemical Power Sources, Elsevier, 2009: pp. 55–61. doi:10.1016/B978-044452745-5.00101-5.
[22] N. Furukawa, Development and commercialization of nickel-metal hydride secondary batteries, Journal of Power Sources. 51 (1994) 45–59. doi:10.1016/0378-7753(94)01928-2.
[23] K. Nishio, PRIMARY BATTERIES – NONAQUEOUS SYSTEMS | Lithium Primary: Overview, in: Reference Module in Chemistry, Molecular Sciences and Chemical Engineering, Elsevier, 2014. doi:10.1016/B978-0-12-409547-2.10938-2.
[24] J.O. Besenhard, H.P. Fritz, Cathodic reduction of graphite in organic solutions of alkali and NR4+ salts, Journal of Electroanalytical Chemistry and Interfacial Electrochemistry. 53 (1974) 329–333. doi:10.1016/S0022-0728(74)80146-4.
[25] J.O. Besenhard, The electrochemical preparation and properties of ionic alkali metal-and NR4-graphite intercalation compounds in organic electrolytes, Carbon. 14 (1976) 111–115. doi:10.1016/0008-6223(76)90119-6.
[26] J.O. Besenhard, R. Schöllhorn, The discharge reaction mechanism of the MoO3 electrode in organic electrolytes, Journal of Power Sources. 1 (1976) 267–276. doi:10.1016/0378-7753(76)81004-X.
[27] R. Schöllhorn, R. Kuhlmann, J.O. Besenhard, Topotactic redox reactions and ion exchange of layered MoO3 bronzes, Materials Research Bulletin. 11 (1976) 83–90. doi:10.1016/0025-5408(76)90218-X.
[28] M. Hu, X. Pang, Z. Zhou, Recent progress in high-voltage lithium ion batteries, Journal of Power Sources. 237 (2013) 229–242. doi:10.1016/j.jpowsour.2013.03.024.
[29] K. Degirmenci, M.H. Breitner, Consumer purchase intentions for electric vehicles: Is green more important than price and range?, Transportation Research Part D: Transport and Environment. 51 (2017) 250–260. doi:10.1016/j.trd.2017.01.001.
[30] B. Junquera, B. Moreno, R. Álvarez, Analyzing consumer attitudes towards electric vehicle purchasing intentions in Spain: Technological limitations and vehicle confidence, Technological Forecasting and Social Change. 109 (2016) 6–14. doi:10.1016/j.techfore.2016.05.006.
[31] R. Bayindir, I. Colak, G. Fulli, K. Demirtas, Smart grid technologies and applications, Renewable and Sustainable Energy Reviews. 66 (2016) 499–516. doi:10.1016/j.rser.2016.08.002.
[32] H. Farhangi, Smart Grid, in: Reference Module in Earth Systems and Environmental Sciences, Elsevier, 2017. doi:10.1016/B978-0-12-409548-9.10135-6.
[33] M. Faheem, V. Cagri Gungor, Capacity and spectrum-aware communication framework for wireless sensor network-based smart grid applications, Computer Standards & Interfaces. 53 (2017) 48–58. doi:10.1016/j.csi.2017.03.003.
[34] F.H. Malik, M. Lehtonen, A review: Agents in smart grids, Electric Power Systems Research. 131 (2016) 71–79. doi:10.1016/j.epsr.2015.10.004.
[35] M. Eremia, L. Toma, M. Sanduleac, The Smart City Concept in the 21st Century, Procedia Engineering. 181 (2017) 12–19. doi:10.1016/j.proeng.2017.02.357.
[36] A. Ahuja, Integration of nature and technology for smart cities, 2016. http://public.eblib.com/choice/publicfullrecord.aspx?p=4454225 (accessed June 24, 2017).

[37] S. Passerini, B.B. Owens, F. Coustier, Lithium-ion batteries for hearing aid applications: I. Design and performance, Journal of Power Sources. 89 (2000) 29–39. doi:10.1016/S0378-7753(00)00378-5.
[38] D. García-Gusano, D. Garraín, J. Dufour, Prospective life cycle assessment of the Spanish electricity production, Renewable and Sustainable Energy Reviews. 75 (2017) 21–34. doi:10.1016/j.rser.2016.10.045.
[39] G. Zubi, J.L. Bernal-Agustín, A.B. Fandos Marín, Wind energy (30%) in the Spanish power mix—technically feasible and economically reasonable, Energy Policy. 37 (2009) 3221–3226. doi:10.1016/j.enpol.2009.04.012.
[40] M.-J. Li, W. Zhao, X. Chen, W.-Q. Tao, Economic analysis of a new class of vanadium redox-flow battery for medium- and large-scale energy storage in commercial applications with renewable energy, Applied Thermal Engineering. 114 (2017) 802–814. doi:10.1016/j.applthermaleng.2016.11.156.
[41] M.S. Hossain, N.A. Madlool, N.A. Rahim, J. Selvaraj, A.K. Pandey, A.F. Khan, Role of smart grid in renewable energy: An overview, Renewable and Sustainable Energy Reviews. 60 (2016) 1168–1184. doi:10.1016/j.rser.2015.09.098.
[42] S. Ould Amrouche, D. Rekioua, T. Rekioua, S. Bacha, Overview of energy storage in renewable energy systems, International Journal of Hydrogen Energy. 41 (2016) 20914–20927. doi:10.1016/j.ijhydene.2016.06.243.
[43] A. Parasuraman, T.M. Lim, C. Menictas, M. Skyllas-Kazacos, Review of material research and development for vanadium redox flow battery applications, Electrochimica Acta. 101 (2013) 27–40. doi:10.1016/j.electacta.2012.09.067.
[44] G. Tomazic, M. Skyllas-Kazacos, Redox Flow Batteries, in: Electrochemical Energy Storage for Renewable Sources and Grid Balancing, Elsevier, 2015: pp. 309–336. doi:10.1016/B978-0-444-62616-5.00017-6.
[45] D. Bresser, E. Paillard, S. Passerini, Lithium-ion batteries (LIBs) for medium- and large-scale energy storage:, in: Advances in Batteries for Medium and Large-Scale Energy Storage, Elsevier, 2015: pp. 125–211. doi:10.1016/B978-1-78242-013-2.00006-6.
[46] D.G. Enos, Lead-acid batteries for medium- and large-scale energy storage, in: Advances in Batteries for Medium and Large-Scale Energy Storage, Elsevier, 2015: pp. 57–71. doi:10.1016/B978-1-78242-013-2.00003-0.
[47] M. Broussely, G. Pistoia, eds., Industrial applications of batteries: from cars to aerospace and energy storage, Elsevier, Amsterdam ; Boston, 2007.
[48] S. Dhameja, Electric vehicle battery systems, Newnes, Boston, 2001.
[49] M.M. Thackeray, M.F. Mansuetto, D.W. Dees, D.R. Vissers, The thermal stability of lithium-manganese-oxide spinel phases, Materials Research Bulletin. 31 (1996) 133–140. doi:10.1016/0025-5408(95)00190-5.
[50] M. Yoshio, H. Noguchi, SECONDARY BATTERIES - LITHIUM RECHARGEABLE SYSTEMS - LITHIUM-ION | Positive Electrode: Manganese Oxides, in: Encyclopedia of Electrochemical Power Sources, Elsevier, 2009: pp. 307–317. doi:10.1016/B978-044452745-5.00200-8.
[51] A.K. Padhi, Phospho-olivines as Positive-Electrode Materials for Rechargeable Lithium Batteries, Journal of The Electrochemical Society. 144 (1997) 1188. doi:10.1149/1.1837571.
[52] S. Chauque, F.Y. Oliva, A. Visintin, D. Barraco, E.P.M. Leiva, O.R. C?mara, Lithium titanate as anode material for lithium ion batteries: Synthesis, post-treatment and its electrochemical response, Journal of Electroanalytical Chemistry. 799 (2017) 142–155. doi:10.1016/j.jelechem.2017.05.052.
[53] G. Gutmann, APPLICATIONS - TRANSPORTATION | Electric Vehicle: Batteries, in: Reference Module in Chemistry, Molecular Sciences and Chemical Engineering, Elsevier, 2013. doi:10.1016/B978-0-12-409547-2.01118-5.

[54] D.A.J. Rand, P.T. Moseley, Lead-acid battery fundamentals, in: Lead-Acid Batteries for Future Automobiles, Elsevier, 2017: pp. 97–132. doi:10.1016/B978-0-444-63700-0.00003-9.
[55] P. Bernard, M. Lippert, Nickel-Cadmium and Nickel-Metal Hydride Battery Energy Storage, in: Electrochemical Energy Storage for Renewable Sources and Grid Balancing, Elsevier, 2015: pp. 223–251. doi:10.1016/B978-0-444-62616-5.00014-0.
[56] Y. Morioka, State-of-the-art of alkaline rechargeable batteries, Journal of Power Sources. 100 (2001) 107–116. doi:10.1016/S0378-7753(01)00888-6.
[57] E.J. Cairns, Batteries, Overview, in: Encyclopedia of Energy, Elsevier, 2004: pp. 117–126. doi:10.1016/B0-12-176480-X/00109-1.
[58] K. Kordesch, W. Taucher-Mautner, HISTORY | Primary Batteries, in: Encyclopedia of Electrochemical Power Sources, Elsevier, 2009: pp. 555–564. doi:10.1016/B978-044452745-5.00003-4.
[59] T. Takamura, PRIMARY BATTERIES - AQUEOUS SYSTEMS | Alkaline Manganese-Zinc, in: Encyclopedia of Electrochemical Power Sources, Elsevier, 2009: pp. 28–42. doi:10.1016/B978-044452745-5.00098-8.
[60] M.A. Rahman, X. Wang, C. Wen, High Energy Density Metal-Air Batteries: A Review, Journal of the Electrochemical Society. 160 (2013) A1759–A1771. doi:10.1149/2.062310jes.
[61] G.E. Gilligan, D. Qu, Zinc-air and other types of metal-air batteries, in: Advances in Batteries for Medium and Large-Scale Energy Storage, Elsevier, 2015: pp. 441–461. doi:10.1016/B978-1-78242-013-2.00012-1.
[62] J.-S. Lee, S. Tai Kim, R. Cao, N.-S. Choi, M. Liu, K.T. Lee, J. Cho, Metal-Air Batteries with High Energy Density: Li-Air versus Zn-Air, Advanced Energy Materials. 1 (2011) 34–50. doi:10.1002/aenm.201000010.
[63] Y. Manane, R. Yazami, Accurate state of charge assessment of lithium-manganese dioxide primary batteries, Journal of Power Sources. 359 (2017) 422–426. doi:10.1016/j.jpowsour.2017.05.065.
[64] D. Lisbona, T. Snee, A review of hazards associated with primary lithium and lithium-ion batteries, Process Safety and Environmental Protection. 89 (2011) 434–442. doi:10.1016/j.psep.2011.06.022.
[65] T.R. Crompton, Lithium-thyonil chloride primary batteries - Battery reference book, 3rd ed, Newnes, Oxford, England ; Boston, 2000.
[66] T.I. Băjenescu, New aspects of the reliability of lithium thyonil chloride cells, Microelectronics Reliability. 32 (1992) 1651–1653. doi:10.1016/0026-2714(92)90469-2.
[67] B. Scrosati, J. Hassoun, Lithium batteries: current technologies and future trends, in: Functional Materials for Sustainable Energy Applications, Elsevier, 2012: p. 573–600e. doi:10.1533/9780857096371.4.573.
[68] H. Arai, Metal Storage/Metal Air (Zn, Fe, Al, Mg), in: Electrochemical Energy Storage for Renewable Sources and Grid Balancing, Elsevier, 2015: pp. 337–344. doi:10.1016/B978-0-444-62616-5.00018-8.
[69] M. Pino, D. Herranz, J. Chacón, E. Fatás, P. Ocón, Carbon treated commercial aluminium alloys as anodes for aluminium-air batteries in sodium chloride electrolyte, Journal of Power Sources. 326 (2016) 296–302. doi:10.1016/j.jpowsour.2016.06.118.
[70] X. Zhang, X.-G. Wang, Z. Xie, Z. Zhou, Recent progress in rechargeable alkali metal–air batteries, Green Energy & Environment. 1 (2016) 4–17. doi:10.1016/j.gee.2016.04.004.
[71] D. Gelman, B. Shvartsev, Y. Ein-Eli, Challenges and Prospect of Non-aqueous Non-alkali (NANA) Metal–Air Batteries, Topics in Current Chemistry. 374 (2016). doi:10.1007/s41061-016-0080-9.
[72] F. Cheng, J. Chen, Metal–air batteries: from oxygen reduction electrochemistry to cathode catalysts, Chemical Society Reviews. 41 (2012) 2172. doi:10.1039/c1cs15228a.

[73] G. Cohn, D. Starosvetsky, R. Hagiwara, D.D. Macdonald, Y. Ein-Eli, Silicon-air batteries, Electrochemistry Communications. 11 (2009) 1916–1918. doi:10.1016/j.elecom.2009.08.015.
[74] G. Cohn, Y. Ein-Eli, Study and development of non-aqueous silicon-air battery, Journal of Power Sources. 195 (2010) 4963–4970. doi:10.1016/j.jpowsour.2010.02.070.
[75] A.F. Sammells, Secondary Calcium Solid Electrolyte High Temperature Battery, Journal of The Electrochemical Society. 133 (1986) 235. doi:10.1149/1.2108533.
[76] H. Yin, D. Tang, X. Mao, W. Xiao, D. Wang, Electrolytic calcium hexaboride for high capacity anode of aqueous primary batteries, J. Mater. Chem. A. 3 (2015) 15184–15189. doi:10.1039/C5TA03728J.
[77] G. Girishkumar, B. McCloskey, A.C. Luntz, S. Swanson, W. Wilcke, Lithium−Air Battery: Promise and Challenges, The Journal of Physical Chemistry Letters. 1 (2010) 2193–2203. doi:10.1021/jz1005384.
[78] J.P. Zheng, R.Y. Liang, M. Hendrickson, E.J. Plichta, Theoretical Energy Density of Li-Air Batteries, Journal of The Electrochemical Society. 155 (2008) A432. doi:10.1149/1.2901961.
[79] J.B. Goodenough, P. Singh, Review—Solid Electrolytes in Rechargeable Electrochemical Cells, Journal of The Electrochemical Society. 162 (2015) A2387–A2392. doi:10.1149/2.0021514jes.
[80] M. Tatsumisago, A. Hayashi, Development of Glass-Based Solid Electrolytes for Lithium-Ion Batteries, in: T. Osaka, Z. Ogumi (Eds.), Nanoscale Technology for Advanced Lithium Batteries, Springer New York, New York, NY, 2014: pp. 63–80. doi:10.1007/978-1-4614-8675-6_7.
[81] B. Kumar, J. Kumar, R. Leese, J.P. Fellner, S.J. Rodrigues, K.M. Abraham, A Solid-State, Rechargeable, Long Cycle Life Lithium?Air Battery, Journal of The Electrochemical Society. 157 (2010) A50. doi:10.1149/1.3256129.
[82] K. Xu, Nonaqueous Liquid Electrolytes for Lithium-Based Rechargeable Batteries, Chemical Reviews. 104 (2004) 4303–4418. doi:10.1021/cr030203g.
[83] K.M. Abraham, A Polymer Electrolyte-Based Rechargeable Lithium/Oxygen Battery, Journal of The Electrochemical Society. 143 (1996) 1. doi:10.1149/1.1836378.
[84] Y. Sun, Lithium ion conducting membranes for lithium-air batteries, Nano Energy. 2 (2013) 801–816. doi:10.1016/j.nanoen.2013.02.003.
[85] W. Xu, J. Xiao, D. Wang, J. Zhang, J.-G. Zhang, Effects of Nonaqueous Electrolytes on the Performance of Lithium/Air Batteries, Journal of The Electrochemical Society. 157 (2010) A219. doi:10.1149/1.3269928.
[86] M.D. Radin, D.J. Siegel, Non-aqueous Metal-Oxygen Batteries: Past, Present, and Future, in: Z. Zhang, S.S. Zhang (Eds.), Rechargeable Batteries, Springer International Publishing, Cham, 2015: pp. 511–539. doi:10.1007/978-3-319-15458-9_18.
[87] N.B. Aetukuri, B.D. McCloskey, J.M. García, L.E. Krupp, V. Viswanathan, A.C. Luntz, Solvating additives drive solution-mediated electrochemistry and enhance toroid growth in non-aqueous Li-O2 batteries, Nature Chemistry. 7 (2014) 50–56. doi:10.1038/nchem.2132.
[88] K.U. Schwenke, M. Metzger, T. Restle, M. Piana, H.A. Gasteiger, The Influence of Water and Protons on Li2O2 Crystal Growth in Aprotic Li-O2 Cells, Journal of the Electrochemical Society. 162 (2015) A573–A584. doi:10.1149/2.0201504jes.
[89] K.G. Gallagher, S. Goebel, T. Greszler, M. Mathias, W. Oelerich, D. Eroglu, V. Srinivasan, Quantifying the promise of lithium-air batteries for electric vehicles, Energy & Environmental Science. 7 (2014) 1555. doi:10.1039/c3ee43870h.
[90] J. Adams, M. Karulkar, Bipolar plate cell design for a lithium air battery, Journal of Power Sources. 199 (2012) 247–255. doi:10.1016/j.jpowsour.2011.10.041.

[91] B. Sun, X. Huang, S. Chen, P. Munroe, G. Wang, Porous Graphene Nanoarchitectures: An Efficient Catalyst for Low Charge-Overpotential, Long Life, and High Capacity Lithium-Oxygen Batteries, Nano Letters. 14 (2014) 3145–3152. doi:10.1021/nl500397y.

[92] Y. Shao, F. Ding, J. Xiao, J. Zhang, W. Xu, S. Park, J.-G. Zhang, Y. Wang, J. Liu, Making Li-Air Batteries Rechargeable: Material Challenges, Advanced Functional Materials. 23 (2013) 987–1004. doi:10.1002/adfm.201200688.

[93] J. Wang, Y. Li, X. Sun, Challenges and opportunities of nanostructured materials for aprotic rechargeable lithium-air batteries, Nano Energy. 2 (2013) 443–467. doi:10.1016/j.nanoen.2012.11.014.

[94] F. Li, H. Kitaura, H. Zhou, The pursuit of rechargeable solid-state Li–air batteries, Energy & Environmental Science. 6 (2013) 2302. doi:10.1039/c3ee40702k.

[95] Z. Lu, A. Schechter, M. Moshkovich, D. Aurbach, On the electrochemical behavior of magnesium electrodes in polar aprotic electrolyte solutions, Journal of Electroanalytical Chemistry. 466 (1999) 203–217. doi:10.1016/S0022-0728(99)00146-1.

[96] P. Saha, M.K. Datta, O.I. Velikokhatnyi, A. Manivannan, D. Alman, P.N. Kumta, Rechargeable magnesium battery: Current status and key challenges for the future, Progress in Materials Science. 66 (2014) 1–86. doi:10.1016/j.pmatsci.2014.04.001.

[97] H. Kim, G. Jeong, Y.-U. Kim, J.-H. Kim, C.-M. Park, H.-J. Sohn, Metallic anodes for next generation secondary batteries, Chemical Society Reviews. 42 (2013) 9011. doi:10.1039/c3cs60177c.

[98] D. Aurbach, I. Weissman, Y. Gofer, E. Levi, Nonaqueous magnesium electrochemistry and its application in secondary batteries, The Chemical Record. 3 (2003) 61–73. doi:10.1002/tcr.10051.

[99] T. Zhang, Z. Tao, J. Chen, Magnesium–air batteries: from principle to application, Mater. Horiz. 1 (2014) 196–206. doi:10.1039/C3MH00059A.

[100] T.D. Gregory, Nonaqueous Electrochemistry of Magnesium, Journal of The Electrochemical Society. 137 (1990) 775. doi:10.1149/1.2086553.

[101] R. Mohtadi, M. Matsui, T.S. Arthur, S.-J. Hwang, Magnesium Borohydride: From Hydrogen Storage to Magnesium Battery, Angewandte Chemie International Edition. 51 (2012) 9780–9783. doi:10.1002/anie.201204913.

[102] T.S. Arthur, N. Singh, M. Matsui, Electrodeposited Bi, Sb and Bi1-xSbx alloys as anodes for Mg-ion batteries, Electrochemistry Communications. 16 (2012) 103–106. doi:10.1016/j.elecom.2011.12.010.

[103] N. Singh, T.S. Arthur, C. Ling, M. Matsui, F. Mizuno, A high energy-density tin anode for rechargeable magnesium-ion batteries, Chem. Commun. 49 (2013) 149–151. doi:10.1039/C2CC34673G.

[104] Y. Shao, M. Gu, X. Li, Z. Nie, P. Zuo, G. Li, T. Liu, J. Xiao, Y. Cheng, C. Wang, J.-G. Zhang, J. Liu, Highly Reversible Mg Insertion in Nanostructured Bi for Mg Ion Batteries, Nano Letters. 14 (2014) 255–260. doi:10.1021/nl403874y.

[105] L. Carlsson, Bifunctional Air Electrode for Metal-Air Batteries, Journal of The Electrochemical Society. 127 (1980) 525. doi:10.1149/1.2129705.

[106] V. Barsukov, F. Beck, eds., New Promising Electrochemical Systems for Rechargeable Batteries, Springer Netherlands, Dordrecht, 1996. doi:10.1007/978-94-009-1643-2.

[107] S.R. Narayanan, G.K.S. Prakash, A. Manohar, B. Yang, S. Malkhandi, A. Kindler, Materials challenges and technical approaches for realizing inexpensive and robust iron-air batteries for large-scale energy storage, Solid State Ionics. 216 (2012) 105–109. doi:10.1016/j.ssi.2011.12.002.

[108] B.T. Hang, M. Eashira, I. Watanabe, S. Okada, J.-I. Yamaki, S.-H. Yoon, I. Mochida, The effect of carbon species on the properties of Fe/C composite for metal-air battery anode, Journal of Power Sources. 143 (2005) 256–264. doi:10.1016/j.jpowsour.2004.11.044.

[109] G.P. Kalaignan, V.S. Muralidharan, K.I. Vasu, Triangular potential sweep voltammetric study of porous iron electrodes in alkali solutions, Journal of Applied Electrochemistry. 17 (1987) 1083–1092. doi:10.1007/BF01024374.
[110] R.D. McKerracher, C. Ponce de Leon, R.G.A. Wills, A.A. Shah, F.C. Walsh, A Review of the Iron-Air Secondary Battery for Energy Storage, ChemPlusChem. 80 (2015) 323–335. doi:10.1002/cplu.201402238.
[111] A.K. Manohar, S. Malkhandi, B. Yang, C. Yang, G.K. Surya Prakash, S.R. Narayanan, A High-Performance Rechargeable Iron Electrode for Large-Scale Battery-Based Energy Storage, Journal of the Electrochemical Society. 159 (2012) A1209–A1214. doi:10.1149/2.034208jes.
[112] A.K. Manohar, C. Yang, S. Malkhandi, G.K.S. Prakash, S.R. Narayanan, Enhancing the Performance of the Rechargeable Iron Electrode in Alkaline Batteries with Bismuth Oxide and Iron Sulfide Additives, Journal of the Electrochemical Society. 160 (2013) A2078–A2084. doi:10.1149/2.066311jes.
[113] B.T. Hang, D.H. Thang, N.T. Nga, P.T.L. Minh, E. Kobayashi, Nanoparticle Fe2O3-Loaded Carbon Nanofibers as Iron-Air Battery Anodes, Journal of the Electrochemical Society. 160 (2013) A1442–A1445. doi:10.1149/2.066309jes.
[114] A. Ito, L. Zhao, S. Okada, J. Yamaki, Synthesis of nano-Fe3O4-loaded tubular carbon nanofibers and their application as negative electrodes for Fe/air batteries, Journal of Power Sources. 196 (2011) 8154–8159. doi:10.1016/j.jpowsour.2011.05.043.
[115] L. Lin, R. E. Durkot, P. B. Harris, US Patent nº 6284410, n.d.
[116] H. Shimomura, M. Shinoda, S. Fuchino, T. Odahara, A. Oyama, US Patent nº 6746509, n.d.
[117] X.G. Zhang, Fibrous zinc anodes for high power batteries, Journal of Power Sources. 163 (2006) 591–597. doi:10.1016/j.jpowsour.2006.09.034.
[118] J.-F. Drillet, M. Adam, S. Barg, A. Herter, D. Koch, V. Schmidt, M. Wilhelm, Development of a Novel Zinc/Air Fuel Cell with a Zn Foam Anode, a PVA/KOH Membrane and a MnO, in: 2010: pp. 13–24. doi:10.1149/1.3507923.
[119] Y. Li, H. Dai, Recent advances in zinc–air batteries, Chem. Soc. Rev. 43 (2014) 5257–5275. doi:10.1039/C4CS00015C.
[120] Y.-D. Cho, G.T.-K. Fey, Surface treatment of zinc anodes to improve discharge capacity and suppress hydrogen gas evolution, Journal of Power Sources. 184 (2008) 610–616. doi:10.1016/j.jpowsour.2008.04.081.
[121] K. Wang, P. Pei, Z. Ma, H. Chen, H. Xu, D. Chen, X. Wang, Dendrite growth in the recharging process of zinc-air batteries, J. Mater. Chem. A. 3 (2015) 22648–22655. doi:10.1039/C5TA06366C.
[122] J. Vatsalarani, D.C. Trivedi, K. Ragavendran, P.C. Warrier, Effect of Polyaniline Coating on “Shape Change” Phenomenon of Porous Zinc Electrode, Journal of The Electrochemical Society. 152 (2005) A1974. doi:10.1149/1.2008992.
[123] C.-C. Yang, W.-C. Chien, P.-W. Chen, C.-Y. Wu, Synthesis and characterization of nano-sized calcium zincate powder and its application to Ni–Zn batteries, Journal of Applied Electrochemistry. 39 (2009) 39–44. doi:10.1007/s10800-008-9637-9.
[124] J. Cheng, Z. Zhang, Y. Zhao, W. Yu, H. Hou, Effects of additives on performance of zinc electrode, Transactions of Nonferrous Metals Society of China. 24 (2014) 3551–3555. doi:10.1016/S1003-6326(14)63500-7.
[125] J. McBreen, E. Gannon, Bismuth oxide as an additive in pasted zinc electrodes, Journal of Power Sources. 15 (1985) 169–177. doi:10.1016/0378-7753(85)80070-7.
[126] J. McBreen, E. Gannon, The electrochemistry of metal oxide additives in pasted zinc electrodes, Electrochimica Acta. 26 (1981) 1439–1446. doi:10.1016/0013-4686(81)90015-3.
[127] Y. Ein-Eli, M. Auinat, D. Starosvetsky, Electrochemical and surface studies of zinc in alkaline solutions containing organic corrosion inhibitors, Journal of Power Sources. 114 (2003) 330–337. doi:10.1016/S0378-7753(02)00598-0.

[128] K. Kinoshita, Electrochemical oxygen technology, Wiley, New York, 1992.
[129] E.S. Davydova, I.N. Atamanyuk, A.S. Ilyukhin, E.I. Shkolnikov, A.Z. Zhuk, Nitrogen-doped carbonaceous catalysts for gas-diffusion cathodes for alkaline aluminum-air batteries, Journal of Power Sources. 306 (2016) 329–336. doi:10.1016/j.jpowsour.2015.11.112.
[130] Y. Yuan, B. Zhao, Y. Jeon, S. Zhong, S. Zhou, S. Kim, Iron phthalocyanine supported on amino-functionalized multi-walled carbon nanotube as an alternative cathodic oxygen catalyst in microbial fuel cells, Bioresource Technology. 102 (2011) 5849–5854. doi:10.1016/j.biortech.2011.02.115.
[131] C. Zu, L. Li, L. Qie, A. Manthiram, Expandable-graphite-derived graphene for next-generation battery chemistries, Journal of Power Sources. 284 (2015) 60–67. doi:10.1016/j.jpowsour.2015.03.009.
[132] Y. Li, K. Huang, J.D. MacGregor, Y. Xing, The Role of PTFE in Cathode Transition Layer in Aqueous Electrolyte Li-Air Battery, Electrochimica Acta. 191 (2016) 996–1000. doi:10.1016/j.electacta.2016.01.143.
[133] S. Cheng, J. Wu, Air-cathode preparation with activated carbon as catalyst, PTFE as binder and nickel foam as current collector for microbial fuel cells, Bioelectrochemistry. 92 (2013) 22–26. doi:10.1016/j.bioelechem.2013.03.001.
[134] E. Yeager, Dioxygen electrocatalysis: mechanisms in relation to catalyst structure, Journal of Molecular Catalysis. 38 (1986) 5–25. doi:10.1016/0304-5102(86)87045-6.
[135] R. Ndzebet, Manganese oxide based electrode for alkaline electrochemical system and method of its production, U.S. Patent 6 780 347, 2002.
[136] C.-Y. Wu, P.-W. Wu, P. Lin, Y.-Y. Li, Y.-M. Lin, Silver-Carbon Nanocapsule Electrocatalyst for Oxygen Reduction Reaction, Journal of The Electrochemical Society. 154 (2007) B1059. doi:10.1149/1.2767421.
[137] H. Meng, P.K. Shen, Novel Pt-free catalyst for oxygen electroreduction, Electrochemistry Communications. 8 (2006) 588–594. doi:10.1016/j.elecom.2006.01.020.
[138] E. Curelop, S. Lu, S. McDevitt, J. Sunstrom, Cathodes for metal air electrochemical cells, U.S. Patent 6 632 557, 1999.
[139] J. Goldstein, N. Naimer, E. Khasin, A. Brokman, Electrodes for metal/air batteries and fuel cells and bipolar metal/air batteries incorporating the same, U.S. Patent 5 190 833, n.d.
[140] Z. Zhong, Lanthanum nickel compound/metal mixture as a third electrode in a metal-air battery, U.S. Patent 6 383 675, n.d.
[141] S.R. Ovshinsky, C. Fierro, B. Reichman, W. Mays, J. Strebe, M.A. Fetcenko, A. Zallen, T. Hicks, Catalyst for fuel cell oxygen electrodes, U.S. Patent 7 097 933, n.d.
[142] N. Miura, H. Horiuchi, Y. Shimizu, N. Yamazoe, Gas diffusion electrodes for oxygen reduction loaded with transition metal nitrides., NIPPON KAGAKU KAISHI. (1987) 617–622. doi:10.1246/nikkashi.1987.617.
[143] W.J. King, A.C.C. Tseung, The reduction of oxygen on nickel-cobalt oxides, Electrochimica Acta. 19 (1974) 485–491. doi:10.1016/0013-4686(74)87029-5.
[144] T. Hyodo, M. Hayashi, S. Mitsutake, N. Miura, N. Yamazoe, Oxygen Reduction Activities of Praseodymium Manganites in Alkaline Solution, Journal of the Ceramic Society of Japan. 105 (1997) 412–417. doi:10.2109/jcersj.105.412.
[145] E.S. Buzzet, Metal/air cells and improved air electrodes for use therein, U.S. Patent 3 977 901, n.d.
[146] Y. Shimizu, Bi-Functional Oxygen Electrode Using Large Surface Area La[1-x]Ca[x]CoO[3] for Rechargeable Metal-Air Battery, Journal of The Electrochemical Society. 137 (1990) 3430. doi:10.1149/1.2086234.
[147] D.R. Egan, C. Ponce de León, R.J.K. Wood, R.L. Jones, K.R. Stokes, F.C. Walsh, Developments in electrode materials and electrolytes for aluminium–air batteries, Journal of Power Sources. 236 (2013) 293–310. doi:10.1016/j.jpowsour.2013.01.141.

[148] M. Pino, J. Chacón, E. Fatás, P. Ocón, Performance of commercial aluminium alloys as anodes in gelled electrolyte aluminium-air batteries, Journal of Power Sources. 299 (2015) 195–201. doi:10.1016/j.jpowsour.2015.08.088.
[149] Wöhler, F., "Ueber das Aluminium". Annalen der Physik und Chemie., 1827.
[150] Charles Martin Hall, Process of Reducing Aluminium from its Fluoride Salts by Electrolysis, US patent 400664, n.d.
[151] F. Habashi, A short history of hydrometallurgy, Hydrometallurgy. 79 (2005) 15–22. doi:10.1016/j.hydromet.2004.01.008.
[152] D.H. Wallace, Market control in the aluminum industry, Arno Press, New York, 1977.
[153] M. Pino, C. Cuadrado, J. Chacón, P. Rodríguez, E. Fatás, P. Ocón, The electrochemical characteristics of commercial aluminium alloy electrodes for Al/air batteries, Journal of Applied Electrochemistry. 44 (2014) 1371–1380. doi:10.1007/s10800-014-0751-6.
[154] S. Shamsudin, M. Lajis, Z.W. Zhong, Evolutionary in Solid State Recycling Techniques of Aluminium: A review, Procedia CIRP. 40 (2016) 256–261. doi:10.1016/j.procir.2016.01.117.
[155] N. Ding, F. Gao, Z. Wang, X. Gong, Z. Nie, Environment impact analysis of primary aluminum and recycled aluminum, Procedia Engineering. 27 (2012) 465–474. doi:10.1016/j.proeng.2011.12.475.
[156] T. Doksanovic, I. Dseba, D. Markulak, Variability of structural aluminium alloys mechanical properties, Structural Safety. 67 (2017) 11–26. doi:10.1016/j.strusafe.2017.03.004.
[157] I. Polmear, D. StJohn, J.-F. Nie, M. Qian, Wrought Aluminium Alloys, in: Light Alloys, Elsevier, 2017: pp. 157–263. doi:10.1016/B978-0-08-099431-4.00004-X.
[158] K.K. Sankaran, R.S. Mishra, Metallurgy and Design of Alloys with Hierarchical Microstructures., 2017.
[159] J.R. King, The aluminium industry, Woodhead Publishing, Cambridge, 2001. http://site.ebrary.com/id/10832970 (accessed June 25, 2017).
[160] A.V. Mikhaylovskaya, A.G. Mochugovskiy, A.D. Kotov, O.A. Yakovtseva, M.V. Gorshenkov, V.K. Portnoy, Superplasticity of clad aluminium alloy, Journal of Materials Processing Technology. 243 (2017) 355–364. doi:10.1016/j.jmatprotec.2016.12.025.
[161] M.L. Doche, F. Novel-Cattin, R. Durand, J.J. Rameau, Characterization of different grades of aluminum anodes for aluminum/air batteries, Journal of Power Sources. 65 (1997) 197–205. doi:10.1016/S0378-7753(97)02473-7.
[162] K. Xhanari, M. Finsgar, Organic corrosion inhibitors for aluminum and its alloys in chloride and alkaline solutions: A review, Arabian Journal of Chemistry. (2016). doi:10.1016/j.arabjc.2016.08.009.
[163] V.F. Henley, Anodic oxidation of aluminium and its alloys, 1st ed, Pergamon Press, Oxford ; New York, 1982.
[164] Joseph W. Richards, Aluminium. Its History, Occurrence, Properties, Metallurgy and Applications, Including Its Alloys, H.C. Baird, 1887.
[165] Q. Li, N.J. Bjerrum, Aluminum as anode for energy storage and conversion: a review, Journal of Power Sources. 110 (2002) 1–10. doi:10.1016/S0378-7753(01)01014-X.
[166] S. Zaromb, The Use and Behavior of Aluminum Anodes in Alkaline Primary Batteries, Journal of The Electrochemical Society. 109 (1962) 1125. doi:10.1149/1.2425257.
[167] L. Bockstie, D. Trevethan, S. Zaromb, Control of Al Corrosion in Caustic Solutions, Journal of The Electrochemical Society. 110 (1963) 267. doi:10.1149/1.2425727.
[168] J.T. Reding, J.J. Newport, The influence of alloying elements on Aluminum anodes in sea water, Mater Prot. 5 (1966) 15–18.
[169] M. Jingling, W. Jiuba, Z. Hongxi, L. Quanan, Electrochemical performances of Al–0.5Mg–0.1Sn–0.02In alloy in different solutions for Al–air battery, Journal of Power Sources. 293 (2015) 592–598. doi:10.1016/j.jpowsour.2015.05.113.

[170] M. Srinivas, S.K. Adapaka, L. Neelakantan, Solubility effects of Sn and Ga on the microstructure and corrosion behavior of Al-Mg-Sn-Ga alloy anodes, Journal of Alloys and Compounds. 683 (2016) 647–653. doi:10.1016/j.jallcom.2016.05.090.
[171] Dragutin M. Drazic, Aleksandar R. Despic, Budimir B. Jovanovic, Electrochemically active aluminum alloy and composite, US 4288500 A, n.d.
[172] John Anthony Hunter, Aluminium batteries, EP 0326338 A2, n.d.
[173] John Anthony Hunter, Aluminium batteries, EP 0326338 A3, n.d.
[174] Gary P. Tarcy, Robert M. Mazgaj, Aluminum alloy and associated anode, US 4808498 A, n.d.
[175] M.J. Niksa, D.J. Wheeler, ALUMINUM-OXYGEN BATTERIES FOR SPACE APPLICATIONS, (1987).
[176] Wojciech Halliop, Paul William Jeffrey, Frank Neale Smith, Aluminium anode alloy, EP 0209402 A1, n.d.
[177] J. Hunter, G. Scamans, J. Sykes, Chemistry of the Aluminum Permanganate Battery, Power Sources, The 17th International Power Sources Symposium. 13 (1991) 193–211.
[178] B.M.L. Rao, R. Cook, W. Kobasz, G.D. Deuchars, Aluminum-air batteries for military applications, in: IEEE, 1992: pp. 34–37. doi:10.1109/IPSS.1992.282061.
[179] P.K. Shen, A.C.C. Tseung, C. Kuo, Development of an aluminium/sea water battery for sub-sea applications, Journal of Power Sources. 47 (1994) 119–127. doi:10.1016/0378-7753(94)80055-3.
[180] E.J. Rudd, D.W. Gibbons, High Energy Density aluminum/oxygen cell, Journal of Power Sources. 47 (1994) 329–340. doi:10.1016/0378-7753(94)87012-8.
[181] G.N. Ambaryan, M.S. Vlaskin, A.O. Dudoladov, E.A. Meshkov, A.Z. Zhuk, E.I. Shkolnikov, Hydrogen generation by oxidation of coarse aluminum in low content alkali aqueous solution under intensive mixing, International Journal of Hydrogen Energy. 41 (2016) 17216–17224. doi:10.1016/j.ijhydene.2016.08.005.
[182] A.V. Ilyukhina, B.V. Kleymenov, A.Z. Zhuk, Development and study of aluminum-air electrochemical generator and its main components, Journal of Power Sources. 342 (2017) 741–749. doi:10.1016/j.jpowsour.2016.12.105.
[183] Avraham Arbel, Jonathan R. Goldstein, Metal-air fuel cells and methods of removing spent fuel therefrom, 9660313, n.d.
[184] Nisancioglu, K, Corrosion of aluminium alloys, Proceedings of ICAA3. 3 (1992) 239–259.
[185] Q. Zhao, M. Slagsvold, B. Holmedal, Comparison of the influence of Si and Fe in 99.999% purity aluminum and in commercial-purity aluminum, Scripta Materialia. 67 (2012) 217–220. doi:10.1016/j.scriptamat.2012.04.023.
[186] Y.-J. Cho, I.-J. Park, H.-J. Lee, J.-G. Kim, Aluminum anode for aluminum-air battery - Part I: Influence of aluminum purity, Journal of Power Sources. 277 (2015) 370–378. doi:10.1016/j.jpowsour.2014.12.026.
[187] I.-J. Park, S.-R. Choi, J.-G. Kim, Aluminum anode for aluminum-air battery – Part II: Influence of In addition on the electrochemical characteristics of Al-Zn alloy in alkaline solution, Journal of Power Sources. 357 (2017) 47–55. doi:10.1016/j.jpowsour.2017.04.097.
[188] Solomon Zaromb, Gas-depolarized cell with aluminum anode, US 3513031 A, n.d.
[189] M. Mokhtar, M.Z.M. Talib, E.H. Majlan, S.M. Tasirin, W.M.F.W. Ramli, W.R.W. Daud, J. Sahari, Recent developments in materials for aluminum–air batteries: A review, Journal of Industrial and Engineering Chemistry. 32 (2015) 1–20. doi:10.1016/j.jiec.2015.08.004.
[190] J. Braunstein, G. Mamantov, G.P. Smith, Advances in molten salt chemistry. Volume 3, 1975. http://dx.doi.org/10.1007/978-1-4615-8270-0 (accessed June 25, 2017).
[191] K. Grjotheim, C. Krohn, M. Malinovsky, eds., Aluminium electrolysis: fundamentals of the Hall-Héroult process, 2. ed., [improved and enlarged], Aluminium-Verlag, Düsseldorf, 1982.

[192] G.L. Holleck, The Reduction of Chlorine on Carbon in AlCl[sub 3]-KCl-NaCl Melts, Journal of The Electrochemical Society. 119 (1972) 1158. doi:10.1149/1.2404432.
[193] P.R. Gifford, A Substituted Imidazolium Chloroaluminate Molten Salt Possessing an Increased Electrochemical Window, Journal of The Electrochemical Society. 134 (1987) 610. doi:10.1149/1.2100516.
[194] J.S. Wilkes, J.A. Levisky, R.A. Wilson, C.L. Hussey, Dialkylimidazolium chloroaluminate melts: a new class of room-temperature ionic liquids for electrochemistry, spectroscopy and synthesis, Inorganic Chemistry. 21 (1982) 1263–1264. doi:10.1021/ic00133a078.
[195] L.D. Reed, E. Menke, The Roles of V2O5 and Stainless Steel in Rechargeable Al-Ion Batteries, Journal of the Electrochemical Society. 160 (2013) A915–A917. doi:10.1149/2.114306jes.
[196] P.R. Gifford, An Aluminum/Chlorine Rechargeable Cell Employing a Room Temperature Molten Salt Electrolyte, Journal of The Electrochemical Society. 135 (1988) 650. doi:10.1149/1.2095685.
[197] M.-C. Lin, M. Gong, B. Lu, Y. Wu, D.-Y. Wang, M. Guan, M. Angell, C. Chen, J. Yang, B.-J. Hwang, H. Dai, An ultrafast rechargeable aluminium-ion battery, Nature. 520 (2015) 324–328. doi:10.1038/nature14340.
[198] H. Sun, W. Wang, Z. Yu, Y. Yuan, S. Wang, S. Jiao, A new aluminium-ion battery with high voltage, high safety and low cost, Chem. Commun. 51 (2015) 11892–11895. doi:10.1039/C5CC00542F.

OBJECTIVES

2. Research objectives

The aim of this thesis was to develop aluminium-air battery systems by using commercial aluminium alloys as anodes. During the development of this general objective, the following specific goals were established:

→ To characterise the behaviour of different series commercial aluminium alloys in alkaline and neutral pH electrolytes.

→ To explore the processes happening during battery discharge for the different commercial Al alloys compositions.

→ To formulate alkaline pH electrolytes for high-performance Al-air batteries.

- To study the processes taking place in the Al anode.
- To explore new approaches for facing Al self-corrosion.
- To build a >1 V working voltage 10 Ah capacity Al-air battery able to discharge at 1 A (C/10 rate) current.

→ To formulate neutral pH electrolytes for high-performance Al-air batteries.

- To study the processes taking place in the Al anode.
- To explore new pathways for enhancing Al anode performance.

EXPERIMENTAL

3. Experimental

3.1. Materials: electrodes and cell casing.

3.1.1. Commercial aluminium alloy anodes.

For the use of commercial aluminium alloys as anodes, samples of 3 to 9 cm^2 were cut from a 1 to 2 mm thick (depending on the alloy composition) commercial sheet. Pure aluminium Cladded alloy presented a protective film adhered to the surface for protecting pure Al from ambient oxidation. All the Cladded alloys were cut in the required dimensions without removing the film, and when the cell was completely assembled this protection was removed.

For the uncladded alloys however, a polishing process was carried out with emery paper from grade 200 to 800 progressively. Once the native Al oxide layer was removed, samples were cleaned in water and acetone to remove possible organic remains.

The complete composition of the whole tested alloys is presented in Table 3.1.1.1

All the alloys are well-known manufacturing and construction materials because of their good balance between hardiness and lightness [1]. Al2024 is a typical aircraft fuselage material, Al7475 is used in applications where corrosion is a limiting factor, such as airplane air collision zones, and the Cladded version of both is used in some specific applications where the properties of each are needed and extra corrosion protection is required. Al6061 presents good mechanical properties (lower hardiness than the previous ones), as well as good corrosion resistance, and so, it is a general-purpose aluminium used in bicycles, trains, trucks, vessels, etc. Al7075 presents lower strength than the previous alloys, but higher corrosion resistance as well as moderate price. That is why this alloy, also known as Zicral, is used in general purpose manufacturing were stainless properties are required for an adjusted cost: cutlery, thermos, cookware, etc.

Table 3.1.1.1: composition of the tested commercial aluminium alloys. Source [1]

Numeric denomination	Symbolic denomination	Si	Fe	Cu	Mn	Mg	Cr	Zn	Ti	Others
EN AW-2024	**Al2024**	0.5	0.5	3.8 4.9	0.3 0.9	1.2 1.8	0.1	0.25	0.15	--
EN AW-7475	**Al7475**	0.1	0.12	1.2 1.9	0.06	1.9 2.6	0.18 0.25	5.2 6.2	0.06	--
EN AW-6061	**Al6061**	0.4 0.8	0.7	0.15 0.4	0.15	0.8 1.2	0.04 0.35	0.25	0.15	--
EN AW-7075	**Al7075**	0.4	0.5	1.2 2	0.3	2.1 2.9	0.18 0.28	5.1 6.1	0.2	Zr: 0.08 -0.2
EN AW-3002	**Al3002 (can)**	0.3	0.7	0.25	1 1.5	0.8 1.3	--	0.25	--	--
EN AW-1085	**Al1085**	0.1	0.16	0.03	0.02	0.02	--	0.03	0.01	Ga + V: 0.01
EN AW-2024 CLAD	**Al2024Clad**	0.5	0.5	3.8 4.9	0.3 0.9	1.2 1.8	0.1	0.25	0.15	3 µm thick Pure Al cladding
EN AW-7475 CALD	**Al7475Clad**	0.1	0.12	1.2 1.9	0.06	1.9 2.6	0.18 0.25	5.2 6.2	0.06	3 µm thick Pure Al cladding

Data in weight percentage.

Al3002 is the most used aluminium alloy worldwide, because its unbeatable corrosion resistant and strength to price ratio. This alloy is used in drink and food cans (mostly acid food, high sugar contents, etc.), but also in low cost manufacturing. Finally, Al1085 is commonly used in construction/decoration after polishing, which results in a bright and clear metal.

These alloys were chosen since they represent an inexpensive and an accessible input for industries, and so, the results obtained in batteries based in these alloys could suppose a cheap energy source for diverse applications.

3.1.2. Positive electrodes: NiOOH cathode and air-cathode.

In this work two positives electrodes were used to assembly Al based batteries. The first tests were carried out with a NiOOH electrode. This cathode is commercially available for Ni-Cd and Ni-MHx batteries, and it is in use since many years ago. It is constituted of

a metallic nickel mesh of foam, which acts as current collector, where a dispersion of $Ni(OH)_2$ with a binder (commonly carboxyl-methyl cellulose, CMC) is pasted. This paste results of black colour because of the $Ni(OH)_2$ powder. The electrode is then dried to remove the water solvent, and calendered for obtaining a well compacted electrode [2].

Then, an activation must be done at a current of 100 $mA \cdot cm^{-2}$ in a highly alkaline solution (4 M KOH). In this activation $Ni(OH)_2$ powder gets oxidised to NiO, which results of light green colour. At the end of the activation a completely charged electrode ready to use is obtained, composed of a mix between $Ni(OH)_2$ and NiO, and so it is called NiOOH electrode. This colour change of the electrode when charged and discharged resulted very indicative to know the state of charge of the NiOOH cathode, so when the colour of an electrode was not as green as it was supposed to be, an overcharge was performed to ensure the maximum capacity. The dimensions of the cathodes were 5 x 5 cm and 0.5 cm thickness, for a total active area of 25 cm^{-2}.

The other used electrode, and the main one of this work, was the air cathode. It was a commercial cathode from *Electric Fuel Ltd.* Company from Israel, called *E4A*. As the producers indicated it was composed of a Ni mesh were a hydrophobic non-woven carbon cloth was pressed in one side and in the other a powder mix of MnO_2 (catalyst) + carbon powder (conductive additive) + binder (fluorated compound, like PTFE or similar). Then, a PTFE thin film was situated in the hydrophobic side of the electrode and the set was hot pressed in a rolling press [3]. Additionally, a cellulose separator film could be pressed in the catalytic face, to avoid short circuiting between anode and cathode in case of contact. Electrodes from 4 cm^2 to 9 cm^2 were cut, and the electric contacts were made of copper by pressing the Ni mesh of the electrode to a copper pin.

3.1.3. Electrochemical characterisation assembly.

For the electrochemical characterisation of the commercial aluminium alloys in alkaline and neutral pH electrolytes a three-electrode half-cell was used. The counter electrode was a graphite bar, the working electrode was the aluminium sample, and the reference

electrode variated as function of the electrolyte pH, for neutral was a Ag/AgCl (KCl saturated) electrode and for alkaline was a SHE (standard hydrogen electrode). The results obtained in alkaline were then transformed to Ag/AgCl reference for an easier comparison with results obtained in neutral media. This half-cell was connected to a watertight pipe which ended in a water filled burette. Because of the water surface tension, water contained in the burette did not drip until an internal pressure in the system pushed it. This internal pressure was generated because of the evolution of hydrogen gas in the anode, so there was a direct correlation between the dripped water volume and the generated hydrogen volume in room conditions (25 ºC and 1 atm). These measurements were carried out during galvanostatic polarisations to explore how current affected the hydrogen evolution.

3.1.4. Aluminium-air cell casings.

For the battery tests with the air cathode, new cell casing designs were ideated to allow one side of the electrode to be in direct contact with the air (oxygen) and the contrary side directly with the electrolyte. To allow this situation the cathodes were situated between two frames with silicone O-rings that once fastened by screws get completely watertight. First cell designs were manually assembled from methacrylate parts cut from a sheet. These casings resulted interesting from the point of view that allowed to see what was happening inside the battery, because of the transparent nature of methacrylate. But they resulted in a very high weight and, due to the high alkalinity of the electrolyte, the joints get damaged. In the case of gelled electrolyte batteries, the casing was much more simple, and it was used just to hold the electrodes, due to the self-standing capability of the polymer electrolyte.

The second-generation battery casings were made in a 3D printing machine. The selected plastic was ABS (Acrylonitrile butadiene styrene), an alkaline and acid compatible material, with good strength and lightweight. The designs were modelled in a modelling software called Solid Works©, then computationally sliced, and printed layer by layer in the 3D printer. This method allowed a very fast response to the faults observed during the tests, and so a new improved cell casing could be printed in the

same day. This technique permits the use of cheap plastics, in a very fast and valid way, so, for lots of experiments the cell assemblies could be designed and printed in the same without having to order expensive and difficult to find test arrays.

3.2. Electrolyte formulations and carbon treatment.

3.2.1. Reagents.

The used reagents during this work are listed below. Every reactant was from a leader chemical company (Panreac, Sigma Aldrich and Merck), and all of them were at least >99% pure and anhydrous.

For the alkaline electrolyte systems: KOH, ZnO, $ZnCl_2$, MBA (N,N'-methylene-bisacrylamide), AA (acrylic acid), $K_2S_2O_8$, NaOH, $Na_3C_6H_5O_7$ (sodium citrate), $CaCl_2$ and NaCl were used.

For the neutral pH electrolyte system: NaCl, PvDF (Polyvinylidene fluoride), NMP (N-Methyl-2-pyrrolidone), Carbon Black (CB, Cabot Corp., USA), Graphene (reduced graphene oxide, rGO, NanoInnova, Spain) and Pyrolytic Graphite (PG, Lurederra T.C., Spain) were used.

3.2.2. Gelled alkaline electrolyte synthesis.

The alkaline gel electrolyte was synthetized by casting a mixture of KOH solution, with or without additives, a gel agent (AA + MBA) and a polymerization initiator as described by Y. Zuo et al. [4]. KOH (10 g) and ZnO (0.35 g) or $ZnCl_2$ (0.25 g) were dissolved in distilled water (16 ml). ZnO and $ZnCl_2$ additives were added as inhibitors of the aluminium self-corrosion in alkaline solutions [5]. A cross-linker, MBA (0.25 g), was dissolved in AA (liquid, 1.58 ml). The alkaline solution was added to the gel agent to obtain a clear dissolution with white granular precipitates, and subsequently were removed through filtration, to obtain a viscous liquid collected in a Petri plate. Afterward, the polymerisation was started by adding an initiator, $K_2S_2O_4$ dissolution (2 ml, 32%wt in

water). After 10 minutes, a 3 mm thick elastic, transparent gel was obtained. All processing was performed at room temperature.

3.2.3. Carbon treatment for anodes.

A paste was prepared by mixing by weight:

- 2 parts of the carbonaceous material (CB, rGO or PG)
- 1 part of binder (PvDF)
- 7 parts of solvent (NMP)

The mix resulted in a medium-viscous paste, which was homogeneously dispensed over the alloy anode surface. For higher area treatments, a spray ink could be obtained by increasing the amount of solvent. Once the paste/ink was extended, the NMP was evaporated in an oven at 120ºC for 12h. Finally, the treatment resulted in a homogeneous thin black coverage all over the aluminium plate.

The influence of the binder percentage was also studied by varying the ratio between carbon and binder (2:1, 4:1 and 9:1).

3.3. Electrochemical characterisation.

For the electrochemical characterisation of the anodes, as well as for the discharges of the batteries, different electrochemical measurements were carried out. The equipment used for this tests was a Galvanostat-Potentiostat 12-channel Arbin Instruments BT2143 workstation at room temperature (25ºC). Once assembled the cell for every test, a period of at least 5 minutes was felt at OCP, until a constant voltage value was obtained.

All measurements were repeated at least three times to ensure reproducibility.

3.3.1. Potentiodynamic polarisation curves: Tafel Plots.

Potentiodynamic polarisation curve is an electrochemical measuring mode for obtaining information on the corrosion rate, pitting susceptibility, passivity, as well as the cathodic behaviour of an electrochemical system [6]. It consists in the application of a potential scan between two values at a scan rate, normally expressed in $mV \cdot s^{-1}$, to explore the current response to this polarisation. When the scan goes from values near to the OCP of the sample to more anodic values, anodic polarisation, information about the metal oxidation, passivation and corrosion can be obtained. While, when the scan moves to more electronegative values, cathodic polarisation, information about metal deposition (when thermodynamically possible, not for aluminium), or oxygen evolution can be obtained.

When the date acquired from a potentiodynamic polarisation curve is graphed as function of the current logarithm, Tafel Plots are obtained. This Tafel Plots gave rapid and easy information about the behaviour of a metal as anode. From this plots Tafel equation can be applied to know the overpotential value related to the rate of an electrochemical reaction. The equation is named after Swiss chemist Julius Tafel.

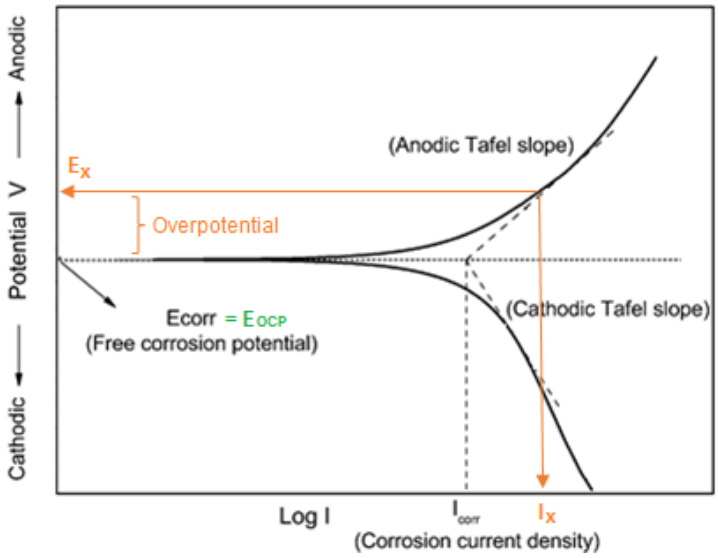

Figure 3.3.1.1: Tafel plot example, anodic and cathodic slopes, corrosion potential and current, and Voltage/overpotential related to a current density.

As can be seen, the intersection between the tangents of the anodic and cathodic slopes indicates the E_{CORR}, corrosion potential, which corresponds to the OCP of the sample in the electrolyte, as well as the corrosion current, I_{CORR}. Additionally, the anodic slopes represent how impeded is the oxidation reaction, indicating for a current value the voltage response, as well as the overpotential. This information results very useful in batteries, due to the high information related to the behaviour of the electrodes in the electrolyte. The potential difference between the E_{CORR} of two electrodes would be the OCP of a battery comprised of these two electrodes with the same electrolyte [7].

In this work potentiodynamic polarisation between -700 mV to +700 mV from the OCP of the samples were carried out at a scan rate of 1 $mV \cdot s^{-1}$, to graph the Tafel plot of the commercial aluminium alloys *vs* the positive electrodes.

Additionally to the Tafel Plots, anodic potentiodynamic polarisations were carried out to compare the current response of Al alloys treated with carbon, at a scan rate of 1$mV \cdot s^{-1}$.

3.3.2. Galvanostatic polarisation curves.

Galvanostatic polarisation curve is an electrochemical measuring mode for electrochemical analysis or for the determination of the kinetics and mechanism of electrode reactions based on the control of the current flowing through the system. The control apparatus used is called a galvanostat. Contrary to potentiostatic polarizations where the potential between reference electrode and the working electrode is maintained constant to see the evolution of the current density, in Galvanostatic polarisations the current value between working electrode and counter electrode is fixed, to see how voltage between reference and working electrodes variates with time [6].

These galvanostatic curves were used for the characterisation of aluminium alloys in KOH as well as in NaCl. Constant currents between 20 to 100 $mA \cdot cm^{-2}$ were applied for test times of 30 minutes, and the potential was registered. The latter gave interesting information about the response of a possible Al anode in terms of voltage to discharges

at different currents. During these experiments the evolution of hydrogen was measured as explained in the point 3.1.3. Additionally, the weight of the working electrodes was registered before and after the tests to know the Al mass consumption during the test.

3.3.3. Galvanostatic battery discharge.

The galvanostatic battery discharge is the more common technique for battery testing. It consists in the application of a constant current (sometimes refer to specific currents, $mA \cdot cm^{-2}$) and to register the cell potential, until a cut-off potential is reached [7]. This cut-off potential is normally fixed regarding to the requirements of the final application of the battery (below what potential is going to result unsuccessful).

The obtained discharging time until the cut of potential is reached, multiplied by the applied constant current gives as result the capacity of the cell, see eq. 3.3.3.1.

$$\rightarrow \quad Q = I \times t \qquad \textit{eq. 3.3.3.1}$$

Where Q is the capacity of the cell (normally expressed in mAh or Ah); I is the discharging constant current (normally in mA or A); and t is the discharging time until the cut-off is reached (expressed in hours) [8].

When a study of a concrete electrode is being performed, another interesting variable is specific capacity, expressed in $mAh \cdot g^{-1}$, which refers to the capacity obtained during the discharge as function of the electrode weight. So, the equation should be:

$$\rightarrow \quad Q_{SPE} = {I \times t}/{m} \qquad \textit{eq. 3.3.3.2}$$

Where Q_{SPE} is the specific capacity (expressed in $mAh \cdot g^{-1}$ or $Ah \cdot kg^{-1}$), I and t represent current and time, and m refers to the electrode, in this case Al, mass (expressed in g or kg).

Capacity is often expressed as C instead of Q, which is more related to the charge.

3.3.4. Multireference galvanostatic battery discharge.

This technique consisted in a galvanostatic battery discharge, in the same way than presented before, with the particularity that the working potentials of each electrode were being registered additionally to the cell potential [8]. This technique allowed to know the response against constant current of not only the battery, but also of the anode and the cathode. The behaviour of the commercial cathode as well as the commercial aluminium alloy anode were registered by this technique in liquid electrolytes, while in the gel electrolyte was not possible. The used references were Ag/AgCl for neutral pH and SHE for alkaline solutions. It just was necessary to register the cell voltage and the potential of one single electrode against a reference. And then, following equation 3.3.4.1, it was possible to calculate the resting one:

$$\rightarrow \; E_{CELL} = E_{Cathode} - E_{Anode} \qquad \textit{eq. 3.3.4.1}$$

3.3.5. Dynamic galvanostatic battery discharge.

Dynamic galvanostatic battery discharge consisted in a succession of galvanostatic battery discharges with an increasing discharge current. A specific constant current was fixed in every step as well as a step time. A 10 minutes galvanostatic discharge was performed and subsequently a higher current galvanostatic discharge started for another 10 minutes, and so. The experiment ended when a cut-off potential was reached, in the same way than simple galvanostatic battery discharges. Current increases of 0.5, 2.5 and 5 $mA \cdot cm^{-2}$ were programmed until a maximum current of 83.33 $mA \cdot cm^{-2}$ (equal to 500 mA), which was the current limit of the galvanostat-potenciostat. Once reached this current the discharge was just limited by the cut-off potential and not by the time.

In this case the capacity, as well as the specific capacity, reached for the experiments was calculated as follows:

$$\rightarrow \; Q_{TOTAL} = \sum Q_{STEP} = \sum I_{STEP} \times t_{STEP} \qquad \textit{eq. 3.3.5.1}$$

3.4. Physical-chemical characterisation.

Some of the aluminium alloy anodes were analysed by SEM-EDX for a better understanding of the processes taking place in aluminium surface. a Hitachi S-300 scanning electron microscope (SEM) and an energy-dispersive X-ray spectroscopy (EDX) system equipped with an INCAx-sight (Oxford Instruments) were used.

3.4.1. Scanning Electron Microscopy (SEM).

A scanning electron microscope (SEM) is a type of electron microscope that produces images of a sample by scanning the surface with a focused beam of electrons. The electrons interact with atoms in the sample, producing various signals that contain information about the sample's surface topography and composition. The electron beam is scanned in a raster scan pattern, and the beam's position is combined with the detected signal to produce an image. SEM can achieve resolution better than 1 nanometer. Specimens can be observed in high vacuum in conventional SEM, or in low vacuum or wet conditions in variable pressure or environmental SEM, and at a wide range of cryogenic or elevated temperatures with specialised instruments [9].

The most common SEM mode is detection of secondary electrons emitted by atoms excited by the electron beam. The number of secondary electrons that can be detected depends, among other things, on specimen topography. By scanning the sample and collecting the secondary electrons that are emitted using a special detector, an image displaying the topography of the surface is created.

The signals used by a scanning electron microscope to produce an image result from interactions of the electron beam with atoms at various depths within the sample. Various types of signals are produced including secondary electrons (SE), reflected or back-scattered electrons (BSE), characteristic X-rays and light (cathode-luminescence, CL), absorbed current (specimen current) and transmitted electrons. Secondary electron detectors are standard equipment in all SEMs, but it is rare that a single machine would have detectors for all other possible signals.

In secondary electron imaging, or SEI, the secondary electrons are emitted from very close to the specimen surface. Consequently, SEM can produce very high-resolution images of a sample surface, revealing details less than 1 nm in size.

Due to the very narrow electron beam, SEM micrographs have a large depth of field yielding a characteristic three-dimensional appearance useful for understanding the surface structure of a sample.

3.4.2. Energy dispersive X-ray detection (EDX).

Energy-dispersive X-ray spectroscopy (EDS, EDX, EDXS or XEDS) is an analytical technique used for the elemental analysis or chemical characterisation of a sample. It relies on an interaction of some source of X-ray excitation and a sample. Its characterisation capabilities are due to the fundamental principle that each element has a unique atomic structure allowing a unique set of peaks on its electromagnetic emission spectrum (which is the main principle of spectroscopy) [10].

To stimulate the emission of characteristic X-rays from a specimen, a high-energy beam of charged particles such as electrons or protons, or a beam of X-rays, is focused into the sample being studied. At rest, an atom within the sample contains ground state (or unexcited) electrons in discrete energy levels or electron shells bound to the nucleus. The incident beam may excite an electron in an inner shell, ejecting it from the shell while creating an electron hole where the electron was. Then, an electron from an outer higher-energy shell fills the hole, and the difference in energy between the higher-energy shell and the lower energy shell may be released in the form of an X-ray. The number and energy of the X-rays emitted from a specimen can be measured by an energy-dispersive spectrometer. As the energies of the X-rays are characteristic of the difference in energy between the two shells and of the atomic structure of the emitting element, EDX allows the elemental composition of the specimen to be measured.

EDX can be used to determine which chemical elements are present in a sample, and can be used to estimate their relative abundance.

3.5. References

[1] I. Polmear, D. StJohn, J.-F. Nie, M. Qian, Wrought Aluminium Alloys, in: Light Alloys, Elsevier, 2017: pp. 157–263. doi:10.1016/B978-0-08-099431-4.00004-X.

[2] N. Furukawa, Development and commercialization of nickel-metal hydride secondary batteries, Journal of Power Sources. 51 (1994) 45–59. doi:10.1016/0378-7753(94)01928-2.

[3] J. Goldstein, N. Naimer, E. Khasin, A. Brokman, Electrodes for metal/air batteries and fuel cells and bipolar metal/air batteries incorporating the same, U.S. Patent 5 190 833, n.d.

[4] Z. Zhang, C. Zuo, Z. Liu, Y. Yu, Y. Zuo, Y. Song, All-solid-state Al-air batteries with polymer alkaline gel electrolyte, J. Power Sources 251 (2014) 470-475.

[5] J. Cheng, Z. Zhang, Y. Zhao, W. Yu, H. Hou, Effects of additives on performance of zinc electrode, Transactions of Nonferrous Metals Society of China. 24 (2014) 3551–3555. doi:10.1016/S1003-6326(14)63500-7.

[6] D. Pletcher, F.C. Walsh, Industrial Electrochemistry, Springer Netherlands : Imprint : Springer, Dordrecht, 1993. http://public.eblib.com/choice/publicfullrecord.aspx?p=3069403 (accessed June 25, 2017).

[7] A.B. Bocarsly, Electrochemical Techniques, Introduction, in: E.N. Kaufmann (Ed.), Characterization of Materials, John Wiley & Sons, Inc., Hoboken, NJ, USA, 2012. doi:10.1002/0471266965.com049.pub2.

[8] E. Talaie, P. Bonnick, X. Sun, Q. Pang, X. Liang, L.F. Nazar, Methods and Protocols for Electrochemical Energy Storage Materials Research, Chemistry of Materials. 29 (2017) 90–105. doi:10.1021/acs.chemmater.6b02726.

[9] D. Stokes, Principles and Practice of Variable Pressure Environmental Scanning Electron Microscopy (VP-ESEM), John Wiley & Sons, New York, NY, 2008. http://nbn-resolving.de/urn:nbn:de:101:1-201412097184 (accessed June 25, 2017).

[10] J. Goldstein, ed., Scanning electron microscopy and x-ray microanalysis, 3rd ed, Kluwer Academic/Plenum Publishers, New York, 2003.

RESULTS AND DISCUSSION

Results and discussion

As introduced, this work is focused in the use of commercial aluminium alloys as anodes for developing high performance aluminium-air primary batteries. In this sense, several aluminium compositions have been measured, as well as different electrolytes.

For a clear presentation of the achieved results, this work is divided in 2 chapters: the first chapter collets the results related to the use of alkaline pH electrolytes, where several electrolyte formulations for low and high power, as well as liquid and gelled electrolytes are presented; and the second chapter summarises the results obtained with a neutral pH electrolyte, where different strategies where used to prevent aluminium hydroxide accumulation in the anode.

4. Chapter 1: Aluminium-air batteries with alkaline pH electrolytes

As introduced before, aluminium in alkaline media suffers from corrosion, a process where aluminium is consumed and hydrogen gas is released (see equation 4.1). When a current is applied to aluminium in an alkaline environment, metallic Al reacts with surrounding hydroxyl ions to deliver electrons and give as product aluminium hydroxide (see equation 4.2). These two processes normally occur simultaneously.

$$\rightarrow \quad Al + 3H_2O + OH^- \rightarrow Al(OH)_4^- + H_2 \uparrow \qquad \textit{eq. 4.1}$$

$$\rightarrow \quad Al + 4OH^- \rightarrow Al(OH)_4^- + 3e^- \qquad \textit{eq.4.2}$$

Three different electrolyte formulations were measured, following different approaches to minimise the self-corrosion. Two of them based in KOH, one of low concentration and the other of high concentration and gelled, and an additional one based in NaOH.

The first measurements with alkaline electrolytes of this work consisted in the characterization of some of the before presented aluminium alloys by chronopotentiometry measurements in KOH. In these measurements, potential evolution, hydrogen generation and mass loss data were collected to have a comparison for their future use as anode in an alkaline electrolyte cell.

4.1. Potassium hydroxide electrolyte based commercial aluminium alloy-air battery.

4.1.1. Characterisation of commercial aluminium alloys in potassium hydroxide electrolyte.

For choosing successful candidates as anodes for alkaline pH based batteries, potentiodynamic polarisation technique was used to represent the Tafel plots. This curve was carried out from anodic to cathodic side at a ±700mV range from OCP, at a scan rate of 1 $mV \cdot s^{-1}$. Several commercial aluminium alloys were measured, as well as two possible cathodes for alkaline pH batteries: air cathode (MnO_2 based) and NiOOH cathode from Ni-Cd batteries.

For the first electrochemical characterization of commercial aluminium alloys in alkaline electrolyte, 4M KOH electrolyte was selected due to the extended use of this formulation in Al-air, metal-air and alkaline based batteries [1,2].

As shown in figure 4.1.1.1, commercial aluminium alloys presented similar corrosion potentials between -1.65 to -1.30 V. These corrosion potentials (E_{CORR}) are the result of the different processes taking place in the surface of the aluminium, as native aluminium oxide layer dissolution, Al oxidation, hydrogen evolution and aluminium hydroxide generation. Because of the latter, in real conditions Al´s E_{CORR} will never be as high as the theoretical -2.4 V in alkaline (*vs* SHE, -2.6 V vs Ag/AgCl). The measured cathodes were a NIOOH cathode from Ni-Cd battery and an air cathode based in MnO_2 as the catalyst.

With the objective in mind of developing the higher voltage value battery, Al2024Clad, Al2024 and Al7475 were selected as most promising candidates for further characterization in alkaline based electrolyte.

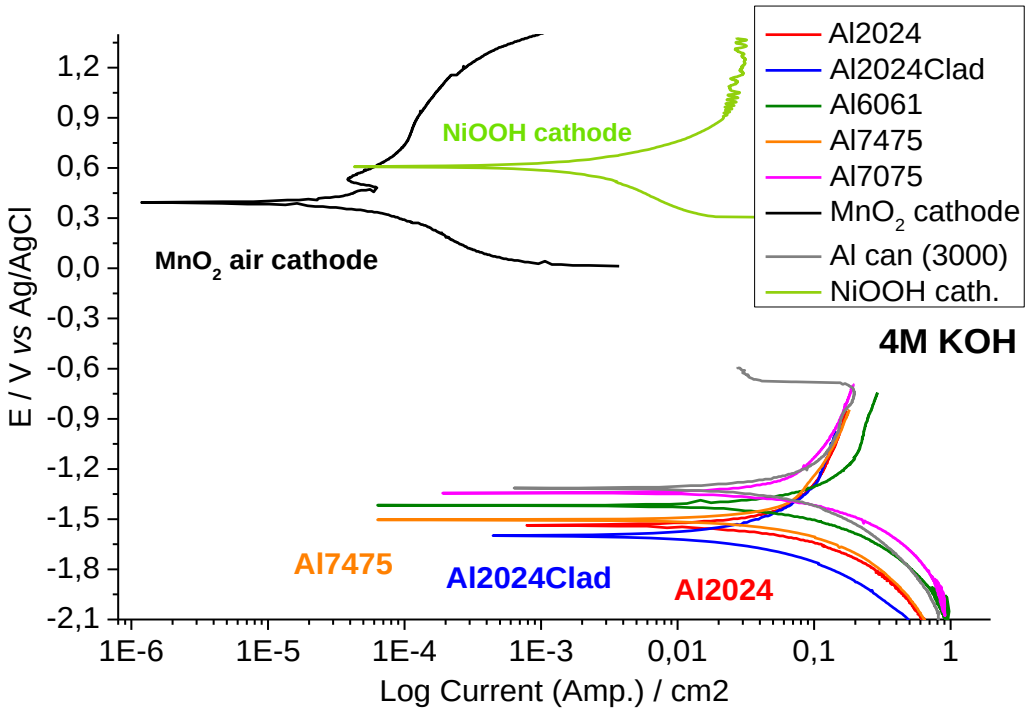

Fig. 4.1.1.1: Tafel plots of commercial aluminium alloys and cathodes for alkaline pH based batteries.

The characterization of commercial aluminium alloys was carried out in the assembly showed in the figure 4.1.1.2. This mounting permitted the electrochemical tests for the aluminium electrode, while the generated hydrogen was registered. The system was watertight, so the water stored in the measuring pipe was just displaced by the pressure of the generated hydrogen.

However, this system was difficult to assembly and the internal pressure of the hydrogen was not being considering, so the results are going to be analysed more from a qualitative point of view than from a quantitative form. In fact, subsequent measurements corroborated the tendencies presented below, so this characterization test was approved.

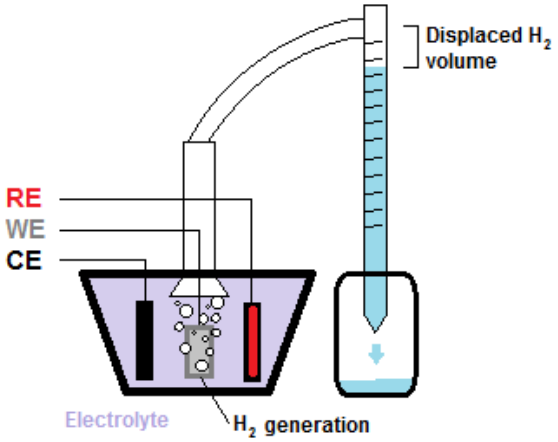

Fig. 4.1.1.2: Schematic diagram of electrochemical characterization assembly.

Aluminium electrode weight was also registered before and after the electrochemical test for controlling the aluminium mass lost. So, the working electrode was a commercial aluminium alloy sample of 1 cm^2, the counter electrode a much higher surface area graphite electrode and the reference was a NHE electrode. The results obtained were converted to Ag/AgCl reference, for future comparison with neutral pH electrolyte in the subsequent chapter. Measurements of 0 to 100 $mA \cdot cm^{-2}$ were carried out in room temperature.

The tested alloys were Al2024, Al7475 and Al2024Clad, (see composition in point 3. Experimental). First test was carried out at OCP (open circuit potential), just by simple immersion of the samples in 4M KOH electrolyte. Figure 4.1.1.3 shows the hydrogen evolution registered during 30 minutes OCP.

As explained before, due to the self-corrosion reaction of Al in alkaline media, part of the aluminium mass is consumed to produce H_2. This test showed that Al7475 and Al2024 suffered from corrosion in a similar way, while Al2024Clad (cladded with a pure aluminium film) resisted better, what results in a lower volume of evolved H_2. The trend of the tree alloys was completely linear, indicating that the corrosion stays constant in time.

This result is not surprising, since it is well-known that the purity of aluminium is a key parameter in self-corrosion, being the purest Al the more resistant. The latter was reported by several groups in the 70s and 80s, and additionally, was one of the main

issues of the non-expansion of Al based commercial energy storage, due to the high price of pure Al.

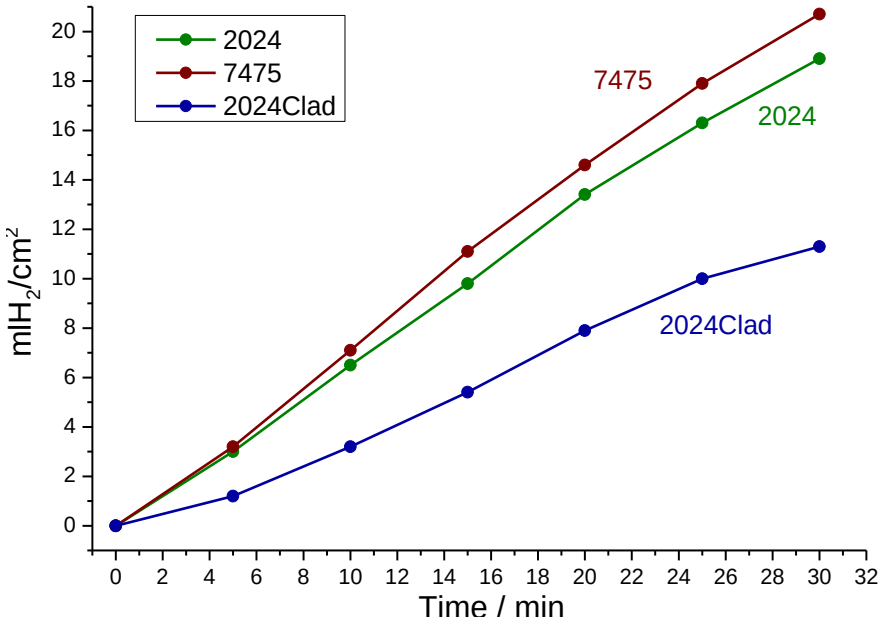

Fig. 4.1.1.3: Hydrogen evolution at OCP of different commercial aluminium alloys.

4.1.1.1. Hydrogen evolution at different current polarisations.

After the hydrogen evolution in OCP, chronopotentiometry measurements were carried out with all the alloys to explore their activity as anodes for batteries. Hydrogen evolution was registered again, and it is presented below alloy by alloy.

→ <u>Al2024:</u>

Figure 4.1.1.1.1 shows the hydrogen evolution of Al2024 alloy in 4M KOH in chronopotentiometries of 20 to 80 mA·cm^{-2}. The mass loss is also added next to each curve. The hydrogen evolution was found not to change too much between different applied currents, and if we look at the evolved volume compared to OCP measurement, the amount resulted in all cases lower (20 ml evolved at 30 minutes in OCP *vs* 15 ml for the higher current value). Even by simple observation it was easy to note that the amount of bubbles surrounding the aluminium anode was lower when a current was applied. The latter indicates a competitive process between aluminium oxidation (without gas evolution) and aluminium self-corrosion (with gas evolution), which is not

governed by the current density, just by the requesting of electrons. This phenomenon is detailed in succeeding points of this work.

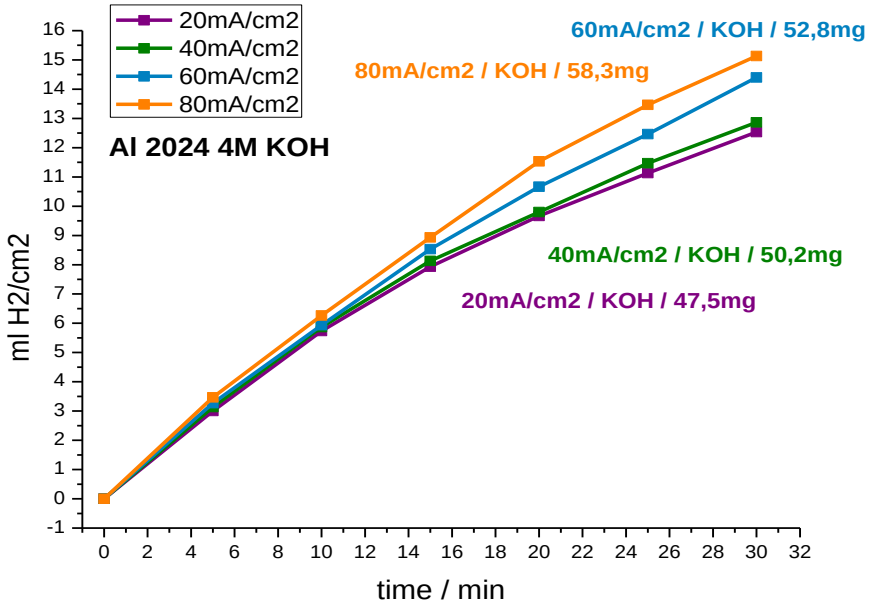

Fig. 4.1.1.1.1: Hydrogen evolution at 20 to 80 mA·cm^{-2} of Al2024 in 4M KOH.

In this case, the hydrogen evolution increased at higher current values, even if this increase was not so pronounced, just a 20% more from 20 to 80 mA·cm^{-2}.

→ Al7475:

Figure 4.1.1.1.2 shows the hydrogen evolution of Al7475 alloy in 4M KOH in chronopotentiometries of 20 to 80 mA·cm^{-2}. The behaviour of this alloy was similar to the Al2024: the H_2 evolution was lower during chronopotentiometry than in OCP; for the different current densities, the H_2 evolution did not change too much; but, in this case at higher current values the consumption of aluminium as well as the volume of H_2 generated, were lower than in low range currents.

This result is aligned with the phenomenon of the competition between reactions, but in the case of Al7475 alloys the current seems to pay a key role in the displacement of self-corrosion in favour of aluminium oxidation. As commented before, this effect is treated more in detail in subsequent points of this work.

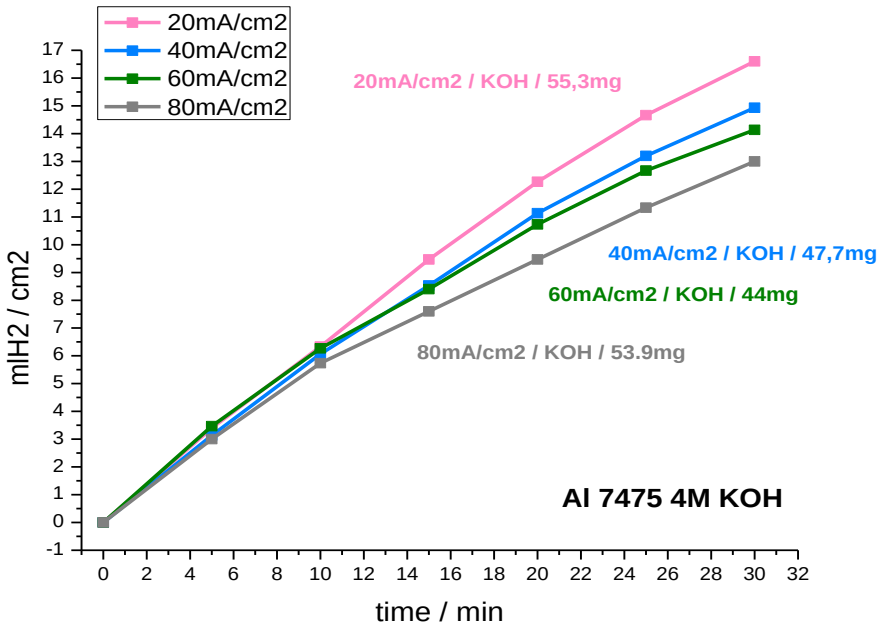

Fig. 4.1.1.1.2: Hydrogen evolution at 20 to 80 mA·cm^{-2} of Al7475 in 4M KOH.

→ Al2024Clad:

Figure 4.1.1.1.3 shows the hydrogen evolution of Al2024Clad alloy in 4M KOH in chronopotentiometries of 20 to 100 mA·cm^{-2}.

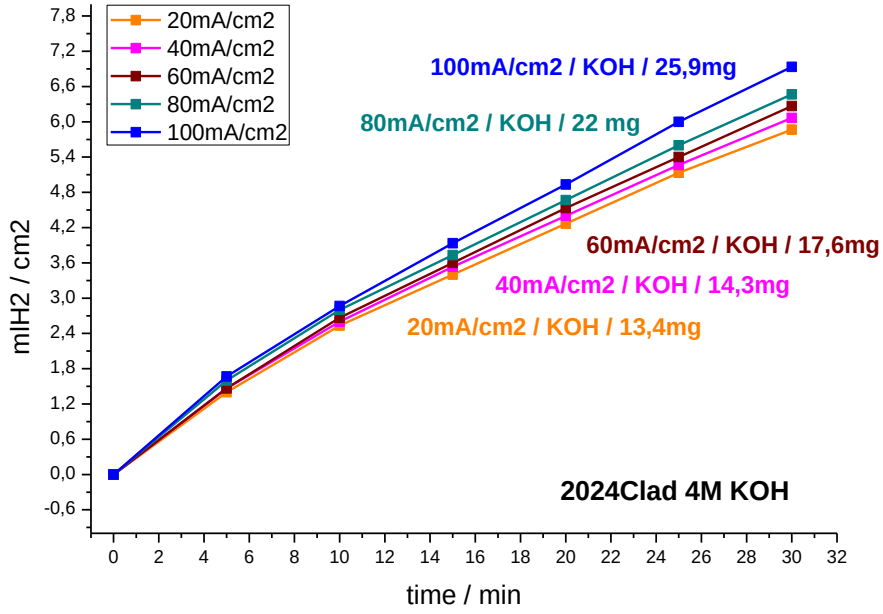

Fig. 4.1.1.1.3: Hydrogen evolution at 20 to 100 mA·cm^{-2} of Al2024Clad in 4M KOH.

The influence of the current density continued being low, in addition to lower generation of H_2 when a current was applied compared to OCP measurements. In this case the consumption of aluminium resulted to be very low, as well as the total evolved gas volume, just 25.9 mg of Al and 7 ml H_2, sustaining the better resistance against self-corrosion of pure aluminium.

The latter is also notable in terms of efficiency, doubling the amount of aluminium consumed from 20 to 100 $mA \cdot cm^{-2}$, while just producing 15% more hydrogen (from 6 to 7.2 ml).

4.1.1.2. Mass loss at different current polarisations.

The consumption of aluminium is showed next, see figure 4.1.1.2.1, in comparison with the evolved H_2 for a better understanding of the phenomenon commented before.

For Al2024 evolution of hydrogen decreased once polarised but increased progressively with the gain of current density. The mass loss associated to this processes increased from OCP to higher current values, indicating a combinate process between aluminium corrosion and oxidation.

For Al7475 evolution of hydrogen decreased constantly with the gain of current, being the lower H_2 liberation at the higher current density. Unlike with Al2024, mass loss decreased with the gain of current density, indicating a competitive process, where the consumption of Al was dominated by the amount of demanded current.

The latter indicated that the Al2024 alloys suffers less from corrosion in low current rates, presenting less aluminium consumption and H_2 evolution, while Al7475 presents better working conditions in high current rates.

In the case of pure aluminium (Al2024Clad), the corrosion rate was notably lower, and remained constant when polarised independent to the value of current density. The consumption of aluminium increased with the current gain, but compared to previous alloys the total amount was notably lower, indicating a “cleaner” process and therefore higher efficiency.

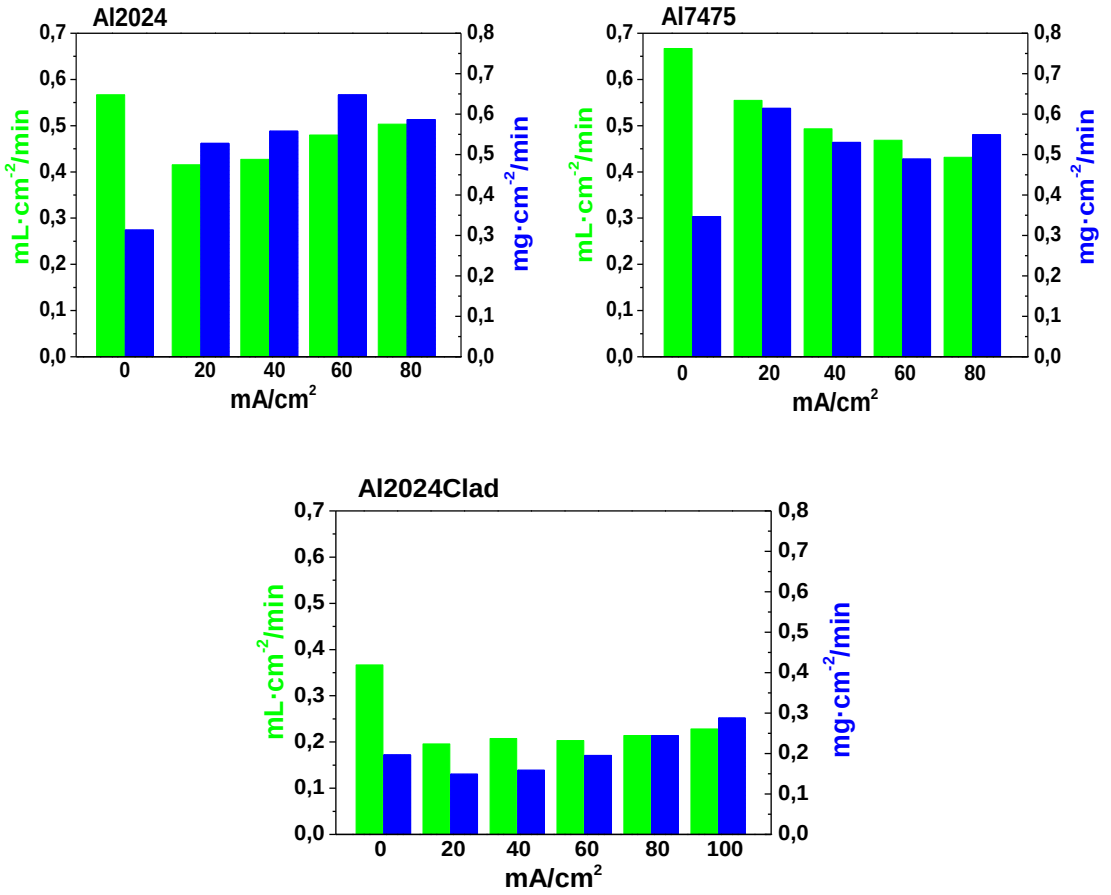

Fig. 4.1.1.2.1: Hydrogen evolution and mass loss of different Al alloys at 0 to 100 mA·cm^{-2} in 4M KOH.

4.1.1.3. Potential evolution at different current polarisations.

Another important parameter for the use of an aluminium alloy as anode is the response of the potential when a current is applied. This potential evolution shows which could be the voltage of a cell when certain alloy was coupled to a cathode.

→ Al2024:

Figure 4.1.1.3.1 shows the potential evolution of Al2024 alloy in 4M KOH in chronopotentiometries of 20 to 80 mA·cm^{-2}. The OCP of this alloys was -1.52 ±0.040 V, which remained constant in time during the OCP hydrogen evolution measurements. Overpotential increased with the raise of current, achieving a flat potential evolution of around -1.320 V when 20 mA·cm^{-2} were applied, while this value turned to -1.120 V

when the current was 80 mA·cm^{-2}. The latter comes in line with the data presented before, so this alloy could work better at low current rates than at higher rates.

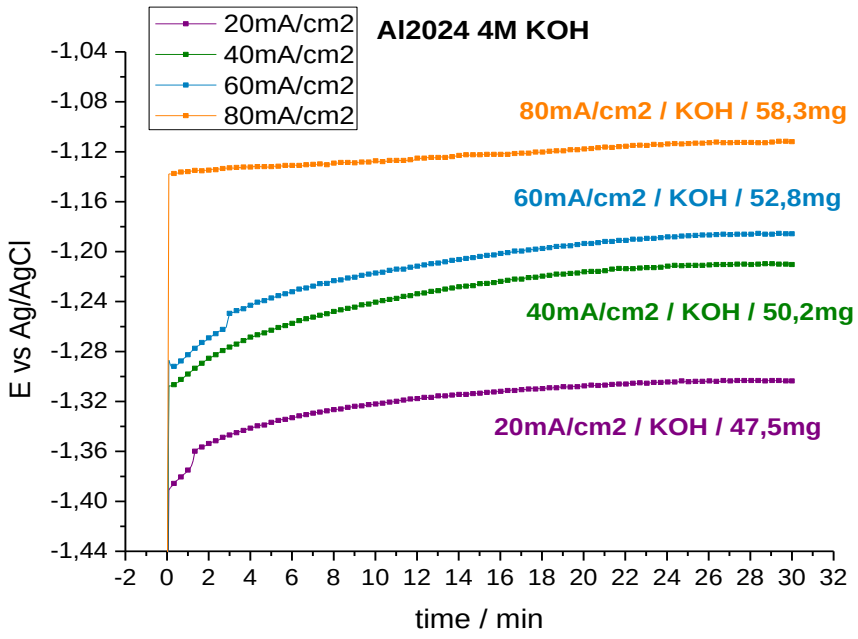

Fig. 4.1.1.3.1: Potential evolution of Al2024 alloy at 20 to 80 mA·cm^{-2} in 4M KOH.

→ Al7475:

Figure 4.1.1.3.2 shows the potential evolution of Al7475 alloy in 4M KOH in chronopotentiometries of 20 to 80 mA·cm^{-2}. The OCP of this alloys was -1.460 ±0.010 V, which remained constant in time during the OCP hydrogen evolution measurements. In this case overpotential was lower than for Al2024, even at high current values. The plateau potential at 80 mA·cm^{-2} was of about -1.200 V, 260 mV from the OCP. The latter is agreeing with the better behaviour of this alloy at high current rates, compared to Al2024. Even at low current rate of 20 mA·cm^{-2}, the response of the potential is of similar value for Al7475 (-1.340 V) vs Al2024 (-1.320 V), but as presented before, the evolution of H_2 as well as the mass loss due to self-corrosion were more significant for this first.

For this alloy an initial decay in the potential is overserved at the higher current rate. This could be due to a surface process at the beginning of the oxidation related with the presence of Zn in the alloy. This process is explained more in detail later.

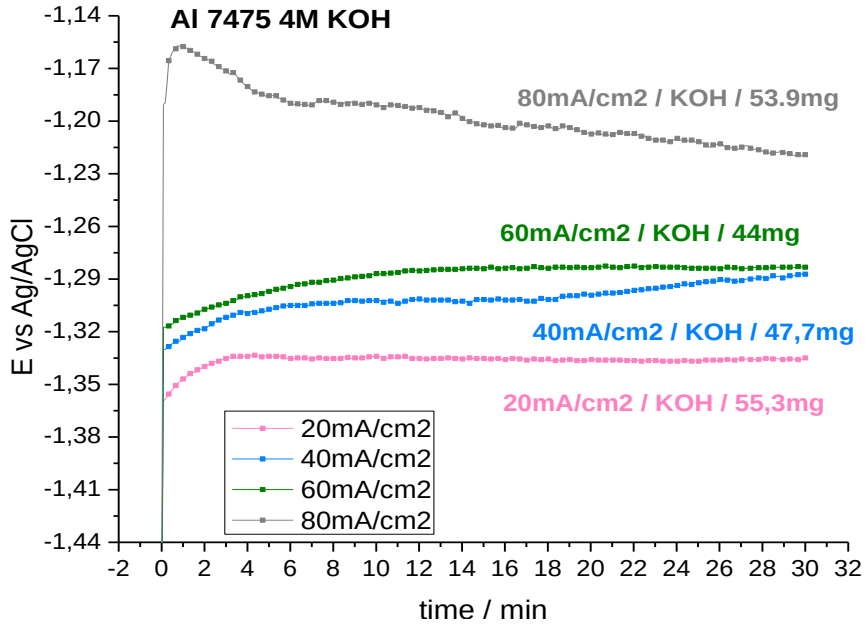

Fig. 4.1.1.3.2: Potential evolution of Al7475 alloy at 20 to 80 mA·cm^{-2} in 4M KOH.

→ Al2024Clad:

Figure 4.1.1.3.3 shows the potential evolution of Al2024Clad alloy in 4M KOH in chronopotentiometries of 20 to 100 mA·cm^{-2}. The OCP of this alloys was -1.610 ±0.030 V, the higher of the measured alloys, which remained constant in time during the OCP.

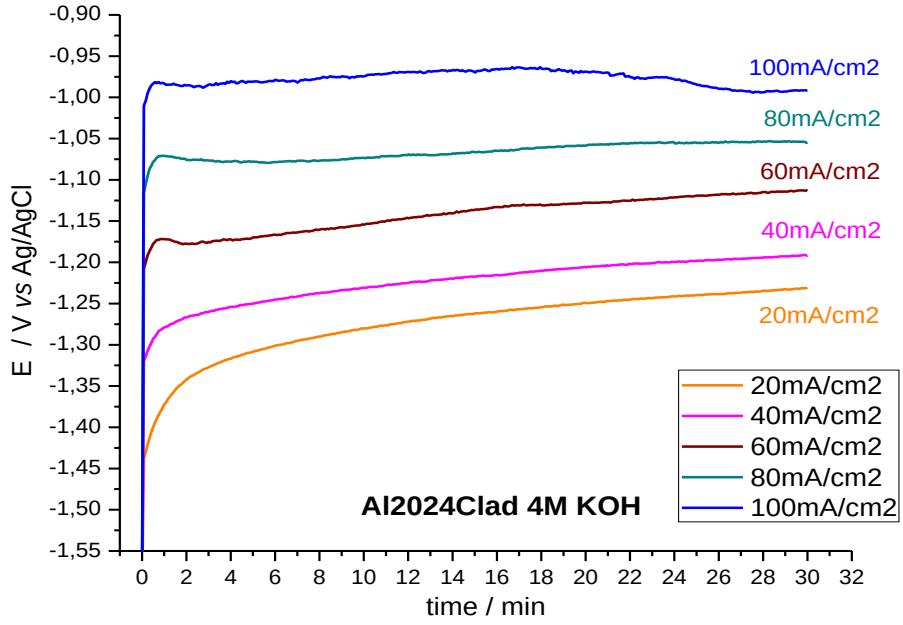

Fig. 4.1.1.3.3: Potential evolution of Al2024Clad alloy at 20 to 80 mA·cm^{-2} in 4M KOH.

Even of the high OCP, once a current was applied, Al2024Clad, pure Al covered, suffered significant overpotentials, being the voltage plateau at 20 $mA \cdot cm^{-2}$ of -1.230 V, lower than the ones for the other two alloys. This value decayed even more at 100 $mA \cdot cm^{-2}$, reaching values above -1 V (overpotential of more than 0.6 V). The latter makes pure aluminium impractical as anode for medium to high power alkaline based batteries.

So, if we look at the behaviour of these three alloys, corrosion resistance increases as follows: Al7475<Al2024<Al2024Clad, being the last one the alloy with less aluminium mass consumption as well as less hydrogen generation; OCP electronegativity increases as follows: Al7475<Al2024<Al2024Clad, being the Al2024Clad the more electronegative alloy, with not so much difference against the other two; and the successful response of the oxidation potential against applied current increases as follows: Al2024Clad<Al2024<Al7475, this means that the Al7475 suffered lower overpotentials when current was increased, while Al2024 performed better in low current range. Due to these results, and with the objective of assembling a low power first alkaline battery, Al2024 was selected as anode for Al-NiOOH cell tests. Even if the overpotentials of this alloy were not as good as the ones for Al7475 or the resistance to corrosion not as successful as the one for Al 2024Clad, Al2024 presented the best compromise between oxidation behaviour and self-corrosion protection. Additionally, Al2024 is one of the most extended aluminium alloys so, the price is very low and it is very easy to find supply.

4.1.2. Potassium hydroxide electrolyte based commercial aluminium alloy-NIOOH battery performance.

After characterising the aluminium alloys by galvanostatic measurements, a redox couple was selected to form a primary battery. Thus, an Al2024-NiOOH battery was first assembled. The idea of using a NiOOH cathode came from the knowledge of our group in Ni-Cd batteries, topic in which important research had been made some years ago. This cathode consisted in a 25 cm^2 Ni foam where nickel hydroxide powder was pasted. This $Ni(OH)_2$, black colour powder, was then oxidised by applying a charging current in a

highly alkaline solution (4M KOH) to obtain a light green electrode composed of a major part of NiO and some rests of $Ni(OH)_2$. So, this electrode could be used as cathode obtaining in a reversible way a black nickel hydroxide electrode again when reduced. As commented before, the area of these electrodes was very high compared to the area of aluminium anodes (25 cm^2 *vs* 5 cm^2), just not to limit the capacity of the anodes and to have the chance to study them as anodes.

So, for the first tests an easy assembly was prepared composed of a 5 cm^2 Al2024 anode and a 25 cm^2 NiOOH cathode immersed in a 4M KOH electrolyte. The volume of electrolyte was in this case completely oversized not to limit the reaction behaviour.

A low discharge current density of 0.8 $mA \cdot cm^{-2}$ was selected for tests owing to other publications in this topic. The first studies resulted in the loss of the whole Al anode after a discharge of 14 h because of the high self-corrosion rate in this highly alkaline solution. Therefore, the study was focused in understanding the effect of the KOH concentration on the increase or decrease in the cell´s capacity. KOH concentrations between 0.2 and 4 M were evaluated at a low constant current density of 0.80 $mA \cdot cm^{-2}$, see figure 4.1.2.1.

After every test the cathodes were overcharged separately to ensure the same conditions at the beginning of every new test.

As can be seen, the capacity of the cell as well as the cell potential, are directly related to the concentration of KOH in the electrolyte. 0.2 M KOH solution was found to be the better working electrolyte for this battery. This is no surprising since the applied current was very low, so at higher KOH concentration the amount of aluminium lost because of self-corrosion was very notable. The obtained specific capacity for 0.2 M KOH solution was 87.2 $Ah \cdot kg^{-1}$ with a flat potential plateau between 1.6 and 1.5 V.

The self-corrosion resulted an important issue at this point of the work because of the liberation of hydrogen during the discharge, and the impossibility to exploit the whole aluminium mass for energy generation. So, it was decided to continue the study of this battery by fixing the concentration of KOH electrolyte in 0.2 M, with the aim to obtain the higher capacities and lower corrosion rates.

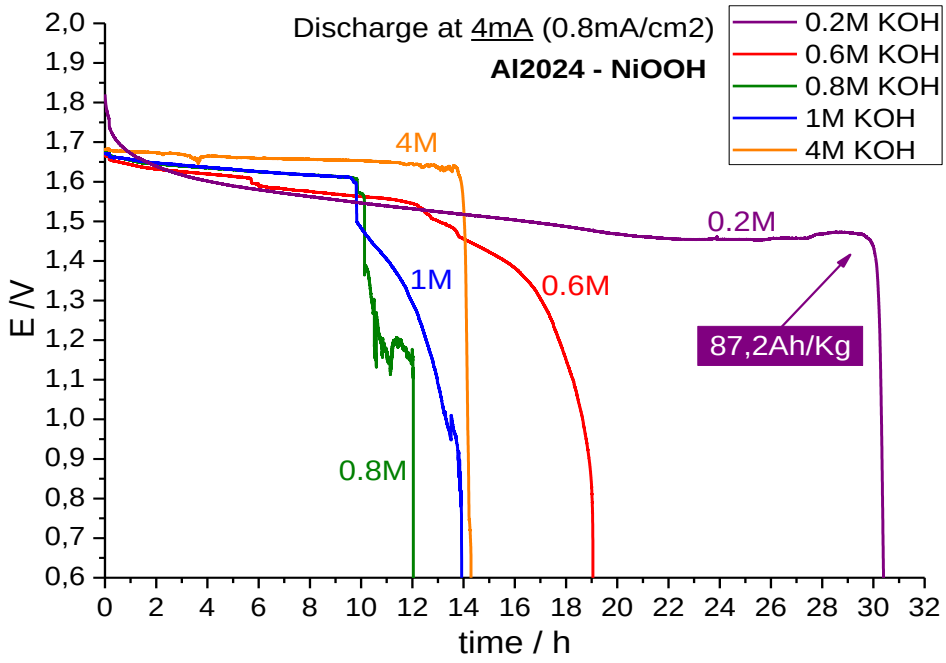

Fig. 4.1.2.1: Al2024-NiOOH battery discharges at 0.8 mA·cm^{-2} with different KOH electrolyte concentrations.

Figure 4.1.2.2 shows the discharges of 0.2 M KOH electrolyte based Al2024-NiOOH batteries in different current rates from 2 to 20 mA·cm^{-2}. The battery at 10 mA (2 mA·cm^{-2}) presented a quite flat potential evolution of 1.6 to 1.5 volts during 16.5 hours, for a specific capacity of 126 Ah·kg^{-1}. At 20 mA (4 mA·cm^{-2}) the discharge potential evolution was not so "clean", performing an initial plateau of 5 hours close to the previous discharge but then, some instabilities were registered. This test was repeated at least for three times, and the obtained potential behaviour was flattest (more like the other represented ones), but this curve is being represented to explain a process happening in some of the experiments that impeded a constant discharge behaviour. Even of the obtained potential evolution, the specific capacity was the same (±5%) for the different experiments carried out in the same conditions. At higher specific currents of 10 and 20 mA·cm^{-2} (50 and 100 mA for the total area) the overpotentials were much more notable, in agreement with the results exposed in the point 4.1.1 Characterization of commercial aluminium alloys in alkaline pH electrolyte.

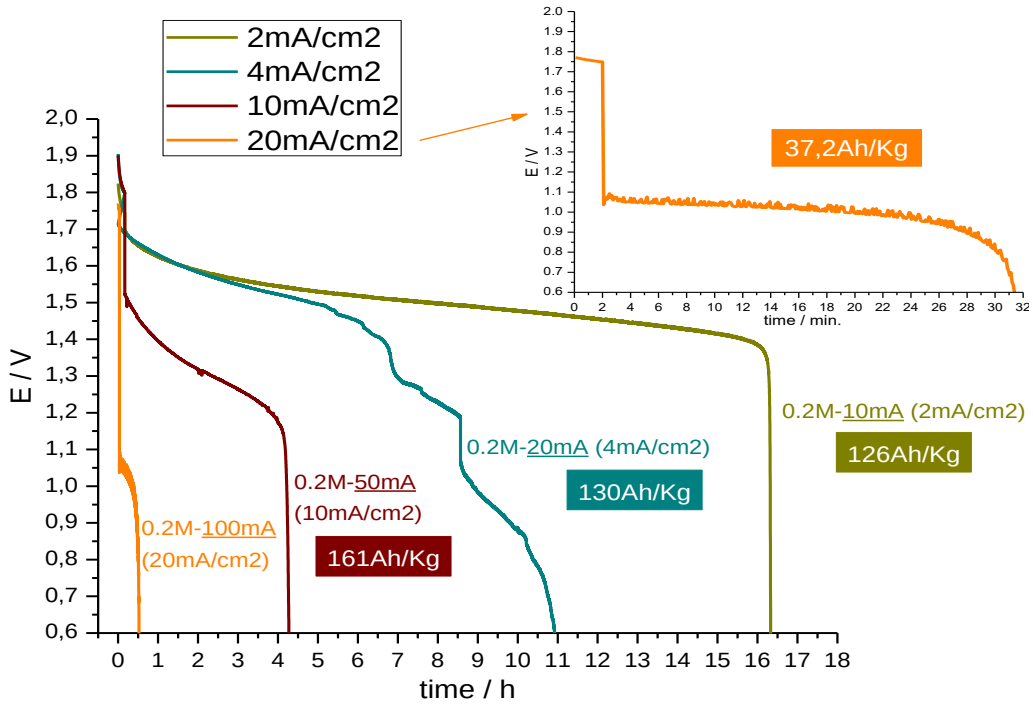

Fig. 4.1.2.2: Al2024-NiOOH battery discharges at different current rates with 0.2 M KOH electrolyte (at the right top discharge detail at 20 mA·cm^{-2}).

However, the obtained specific capacity for 10 mA·cm^{-2} was the higher with a value of 161 Ah·kg^{-1} and a useful potential from 1.5 to 1.2 volts, like that of alkaline batteries. The latter makes sense with the theory of competition between the kinetic discharge drain and the self-corrosion, being the obtained capacity higher when discharge current were higher. So, current increments could displace aluminium self-corrosion in favour of aluminium oxidation.

In the case of the higher current tested, the capacity decayed significantly, as well as the cell potential, possibly because of the impossibility of surrounding hydroxyl ions to face the high demand. And consequently, the hydroxyl ion depletion in the surface of aluminium made the cell die prematurely.

As commented before, the discharge curve at 10 mA·cm^{2} with the non-constant potential evolution suffered a process that is described next. This process was registered in most of the experiments but, in some cases affected to the discharge behaviour, while in others did not interfere the evolution potential.

The aluminium hydroxide formed during the discharge of the battery and by self-corrosion, results completely soluble in acidic media, and completely insoluble in alkaline media, while partially soluble in neutral pH. So, in 0.2 M KOH electrolyte, during the discharge of the battery, crust like aluminium hydroxide layers were accumulated in the surface of the aluminium anode, and when them grew till certain weight, get detached and precipitated in the bottom of the cell.

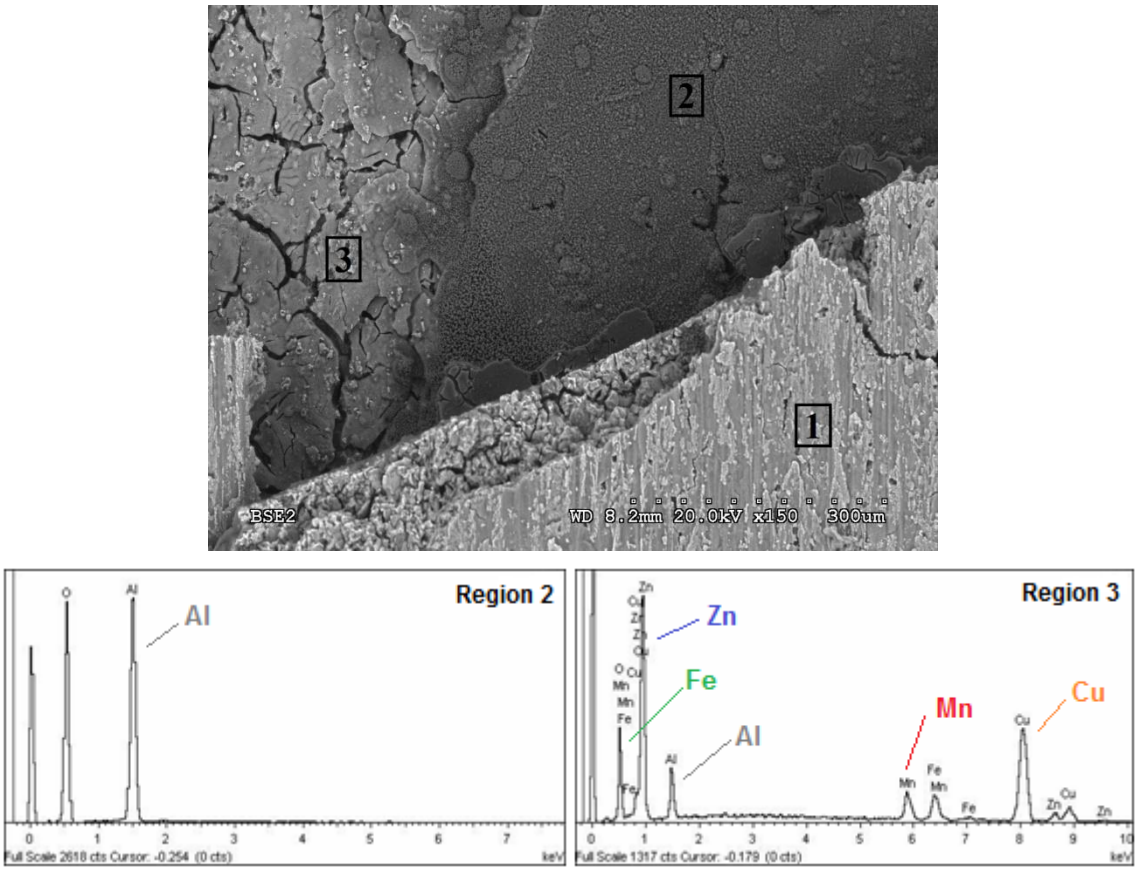

Fig. 4.1.2.3: SEM/EDX captures of Al2024-NiOOH battery anode after discharge of 2 mA·cm^{-2} with 0.2 M KOH electrolyte.

Figure 4.1.2.3 shows a scanning electron microscopy (SEM) capture of a post mortem Al2024-NiOOH battery anode analysis. This battery was discharged at 2 mA·cm^{-2} in 0.2 M KOH electrolyte for 10 hours to prevent the complete dissolution of aluminium. Additionally, two Energy-dispersive X-ray spectroscopy (EDX) captures are presented.

The SEM capture shows three differentiated regions: region numbered 1, presents the region of the alloy that was not immersed in electrolyte, and there is no significant wear in this area. The small points of corrosion that are present in this region are because of

the electrolyte being entrained by the evolved H_2. In the second region, numbered 2, a homogeneous mottled area is shown. The composition of this area was mostly aluminate, see Figure 4.1.2.3 EDX region 2. Thus, this area was likely the most active area of the anode, where oxidation and self-corrosion of fresh aluminium was taking place. When the anode was taken out from the battery, it was cleaned with distilled water to prevent further corrosion from the KOH, and consequently the exposed fresh aluminium due to the environmental oxygen get oxidised to aluminate.

In the last region, numbered 3, a quartered like region is shown, where the principal components registered by EDX were the trace metals of the alloy (Cu, Zn, Mn, Fe, etc) in addition to the aluminium. This composition could indicate the precipitation of the alloying metals to the surface while the Al oxidation was taking place, producing an enrichment of those trace metals in some anode areas, mixed together with the aluminium hydroxide reaction product. While the battery was discharging, these crust like trace metal-rich films were emerging and breaking away from the anode to precipitate in the bottom of the battery container.

This process took place continuously during the discharge of the batteries, giving as result a black precipitation layer in the bottom of cells once the discharge was finished. But in some cases, the alloying metal + aluminium hydroxide layer was not detached from the anode surface so easily, giving rise to the formation of a big crust all over the anode that impeded hydroxyl ion diffusion to the fresh aluminium, as well as reaction products migration to the electrolyte. Additionally, this crust created concavities where the generated hydrogen due to self-corrosion get detained, forming big size bubbles that occupied some percentage of the active area of the negative electrode.

And thus, the requested current was distributed in lower active area, resulting in variations in the potential of the cell during the discharge, as previously shown in Figure 4.1.2.2.

To prevent this situation two approaches were explored: first, with the objective of reducing the self-corrosion a study of the pH was realised by decreasing the concentration of KOH below 0.2 M; and second, the use of additives in the electrolyte to prevent self-corrosion, as well as aluminium hydroxide accumulation, was explored.

Concentrations below 0.2 M KOH were measured trying to prevent aluminium self-corrosion. 0.2 M KOH solution presented a pH of 13.3, so pH of 13 (0.1 M), 12,6 (0.05 M) and 12 (0.01 M) were measured in the same battery assembly Al2024-NiOOH at a current discharge of 2 mA·cm^{-2}.

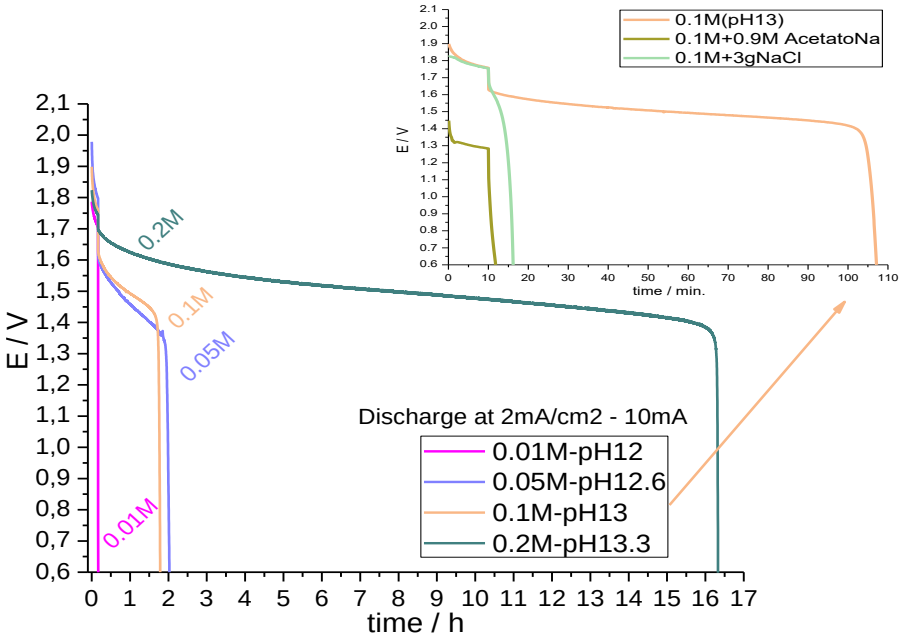

Fig. 4.1.2.4: Discharges of Al2024-NiOOH batteries with different pH electrolytes at 2 mA·cm^{-2}.

As shown in Figure 4.1.2.4, when the concentration of KOH was decreased below 0.2 M, the results were not satisfactory, achieving just an eighth part of discharging time in the case of pH 13 and 12.6, while the discharge not even started at pH 12. The latter was attributed to the lower conductivity of hydroxyl ions of the electrolyte. But, even of these non-satisfactory results in the electrochemical behaviour, hydrogen generation was drastically reduced. So, some extra tries were carried out with 0.1 M KOH solution (pH 13), by adding to the electrolyte an extra salt to enhance ionic conductivity. In this sense, addition of sodium acetamide and sodium chloride were tried with even more poor results, see right top part of Figure 4.1.2.4.

Thereby, 0.2 M KOH concentration was reaffirmed as the better choice for further measurements. And some additive in the electrolyte was tried with the aim of reducing the effect of self-corrosion of the alkaline media.

The selected additive was zinc oxide, a well-known anticorrosive [3,4], used in alkaline and Zn-air batteries together with ZnCl (which is explored later). ZnO is a white fine

powder, insoluble in alkaline electrolyte but which gets dispersed for long time giving as result a whitish solution. The amount used was 1 part for every 30 parts of KOH by weight, owing to bibliography [5].

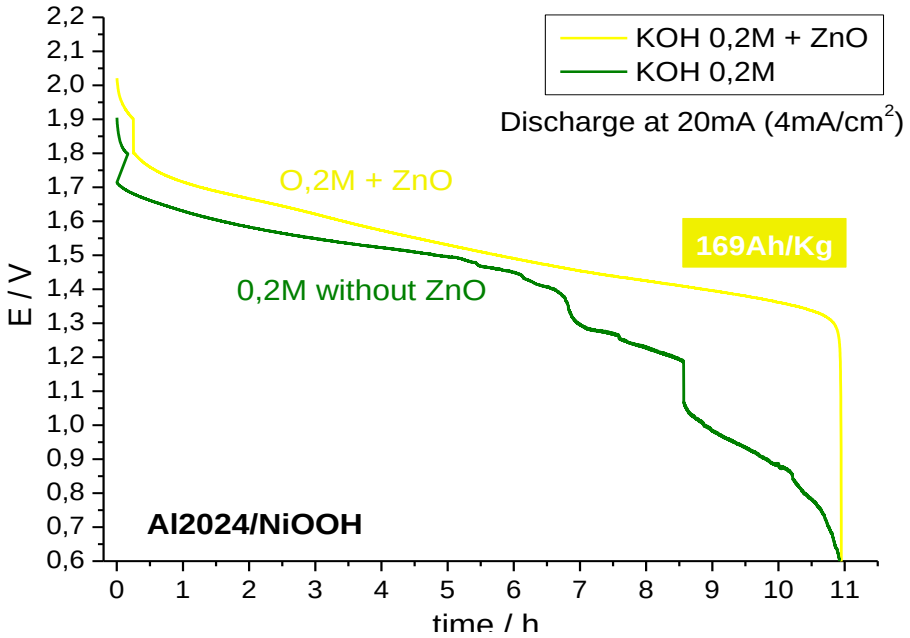

Fig. 4.1.2.5: Discharges of Al2024-NiOOH batteries with 0.2 M KOH electrolyte with and without ZnO additive at 4 mA·cm^{-2}.

Figure 4.1.2.5 shows the discharge behaviour of the Al2024-NiOOH battery with 0.2 M KOH electrolyte with and without ZnO additive at 4mA·cm^{-2}. The discharge without additive suffered the process explained before: a crust of aluminium hydroxide rich in major alloying elements grew up around the Al anode, accumulating hydrogen bubbles that impeded the contact with the electrolyte, and so, the evolution of the cell potential was not flat and stable. When ZnO additive was present in the electrolyte, this effect was significantly reduced, first by lowering the self-corrosion of Al, and so the hydrogen evolution, and second by suppressing the anchor points of the aluminium hydroxide crust, allowing an easy precipitation of the reaction product.

The obtained capacity was the same when ZnO additive was used but, the cell potential was in all cases flatter and slightly higher. The latter indicates that the self-corrosion reaction (-0.89 V *vs* SHE) was being displaced in favour of the aluminium oxidation reaction (-1.66 V *vs* SHE).

Just to ensure the good functioning of the aluminium anode and to have a greater knowledge of how the NiOOH cathode was working, a discharge in the best conditions was repeated while the potentials of each electrode were being registered, see Figure 4.1.2.6.

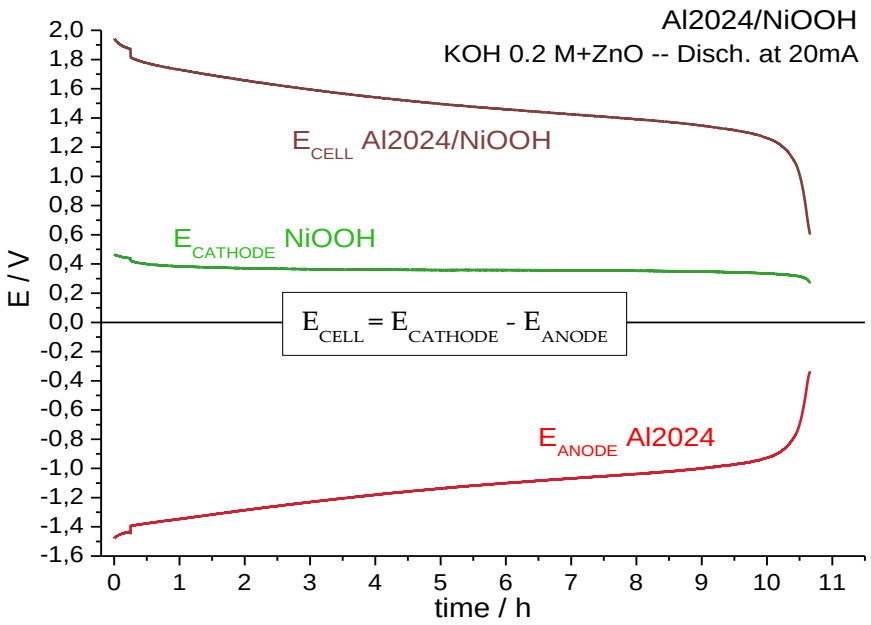

Fig. 4.1.2.6: Breakdown of electrode potentials in a discharge of Al2024-NiOOH battery with 0.2 M KOH + ZnO electrolyte at 4 mA·cm^{-2}.

As can be seen, the behaviour of the cathode during the discharge was incredibly flat, in a value of about 0.350 V. So, the Al2024 alloy anode was the principal responsible of the cell potential evolution. Additionally, this measurement permitted us to ensure that the cathode was not limiting the capacity of the cell, as it was assumed from the beginning of the work, being the aluminium anode the limiting factor in the achieved discharging time. Another important point of this test was the ratification of the high reproducibility of this battery, achieving the same discharging time (10.6 *vs* 11h) and E_{CELL} plateau (from 1.8 to 1.4 V) than in the previous discharges in the same conditions.

So, as final use of this Al2024-NiOOH battery a 6 series cell stack was assembled to try it as energy supply in an electric radio control vehicle. The characteristics of the original Ni-MHx battery of the car were 9.6 V and 750 mAh.

Fig. 4.1.2.7: Capture of 6 series Al2024-NiOOH cell stack and its mounting in radio control vehicle.

The used electrolyte was 0.2 M KOH + ZnO additive, and in this case the Al2024 aluminium alloy anodes were increased to 20 cm^2 for being able to supply 800 mA current peaks during the car boot and acceleration, 300 to 400 mA at constant velocity and additional 100 mA for steering motors. This use of the battery resulted quite funny and comforting because of the possibility to see how the experiments carried out in the laboratory could be used for real applications with satisfactory results. The car worked for at least 2 or 3 hours of intermittent driving, like the autonomy of the original Ni-MHx battery. The measured OCP of the cell was 10.4 V, which decayed to 8.2 V at the car boot (maximum discharge current) and to 9 -9.4 V at constant use of the car. A constant discharge of the whole cell was carried out at 200 mA, what equalled 10 $mA \cdot cm^{-2}$, and it was compared to the discharge of a unique vase of cell discharge at the same conditions.

As Shown in the Figure 4.1.2.8, the discharge of just one vase performed a flat plateau between 1.7 and 1.5 V for a total discharging time near to 3 hours. The OCP was 1.9 V. However, when 6 vases were connected in series the resulting OCP was 10.4 V, instead of the theoretical 6 x 1.9 = 11.4 V, and the discharge plateau was between 9.6 and 8.2 V, lower than the theoretical values if we look at the results of just one vase discharge. The discharging time was again notoriously lower, of just 1.25 hours.

This diminished performance is attributed to the high ohmic losses between the connections of the cells that were made of crocodile chips instead of welding or screwing. Even of this coarse constitution of the battery, the weight of every component

was measured and the percentage of them in the total weight of the 6 series cell battery is shown in Figure 4.1.2.9.

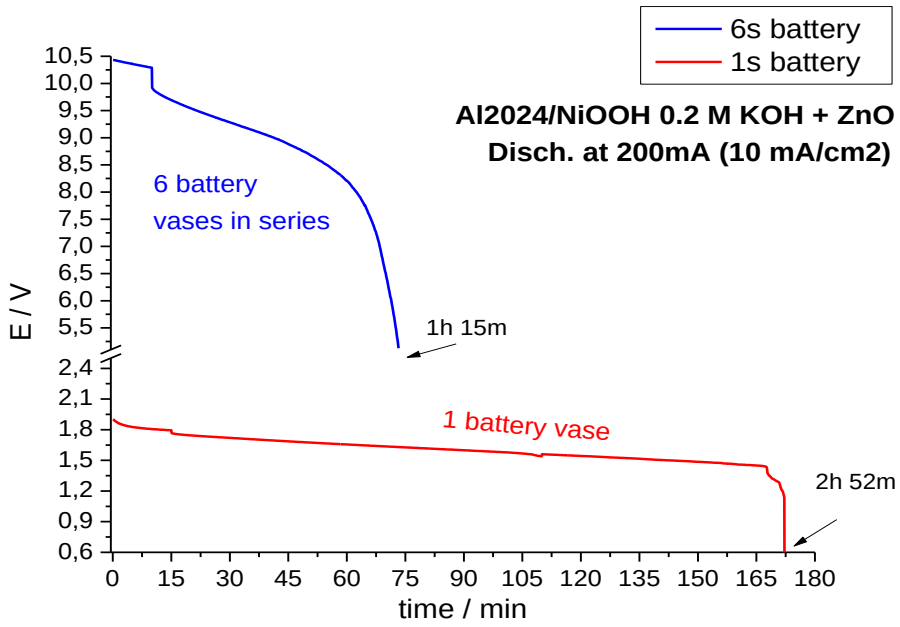

Fig. 4.1.2.8: Discharge of 6 series Al2024-NiOOH cell stack at 200 mA vs just 1 vase Al2024-NiOOH cell.

The electrode weight (anode + cathode) represented just a 22 % of the total battery weight, while the cell casing was a 27 % or the electrolyte a 46 %. This huge amount of electrolyte needed to be minimised for a real applicable system. The casing in this case was hand made with methacrylate sheets, but for an industrial application is very easy to build them of resistant and light plastics las polypropylene or polyethylene, which could reduce the weight up to represent just a 5 or 10 % of the total weight. The same happens with the electric connections that can be easily improved just with nowadays well-known technology.

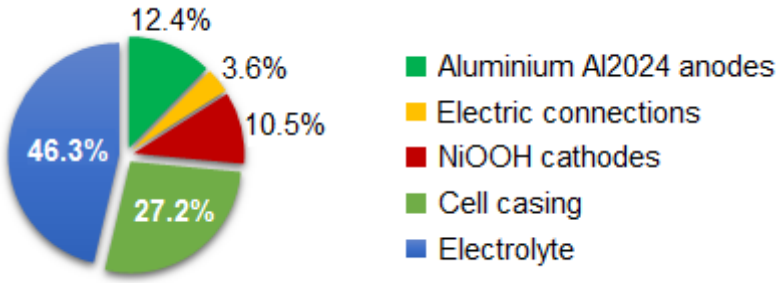

Fig. 4.1.2.9: Weight distribution of 6 series Al2024-NiOOH cell stack.

This system resulted very interesting for the understanding of the aluminium anode role in alkaline pH based electrolyte, and allowed us to fix some parameters related to the electrolyte formulation before moving to metal-air system.

4.1.3. Potassium hydroxide electrolyte based commercial aluminium alloy-air battery performance.

Once the test of the electrolyte was successfully carried out in the Al2024-NiOOH battery, the system was adapted to the use of an air cathode. A commercial available air cathode was selected from different options: *E4A cathode* from the company *Electric Fuel Ltd.* As the supplier described, this electrode was composed of a nickel mesh as current collector, where a mix of carbon powder with MnO_2 was pressed together with a hydrophobic carbon sheet. Finally, a Teflon layer was added to the "air" to prevent electrolyte leakage while enabling oxygen inlet.

A linear scan voltammetry was performed to the new air cathode in 0.2 M KOH with ZnO additive to explore the behaviour of this electrode in the system. A Tafel plot of the electrode is presented in Figure 4.1.3.1, in comparison with the NiOOH electrode used till this point of the work.

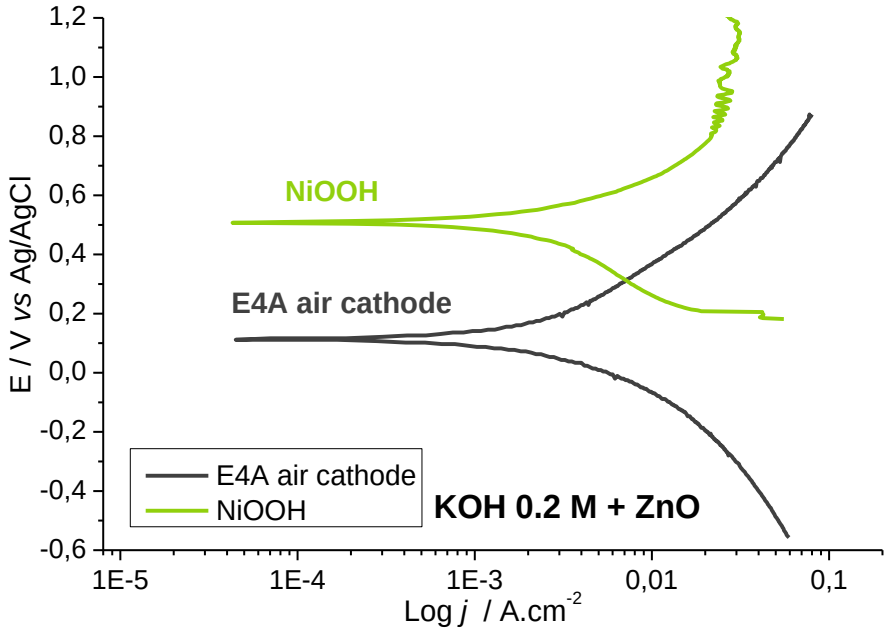

Fig. 4.1.3.1: Tafel plot of commercial E4A air cathode and NiOOH electrode.

The results of the Tafel plot for both electrodes indicated that the E_{OCP} for the new air electrode was 400 mV lower than the one for NiOOH electrode. This meant that any aluminium alloy tested till this point paired with this air electrode will deliver a 400 mV lower OCP that the same alloy paired to NiOOH. Additionally, the evolution of the Tafel slots for both was very similar till 10 $mA \cdot cm^{-2}$, but once reached this value, the air cathode tended to increase progressively the overpotential, while the NiOOH electrode tended to stabilise in the same voltage value.

So, a priori the air cathode compared to the NiOOH electrode was going to work worst, but an important reduction of the weight could be achieved with this electrode, as well as a longer discharge time without having the necessity to oversize the electrode.

A new cell was designed with the aim of using the air cathode as one of the main cell casing walls, to ensure a good oxygen flow in one face and electrolyte wettability in the other side. The air "window" as well as the area of air cathode in contact with electrolyte was 4 cm^2, and the anodes used this time were of 3 cm^2. Oversizing the positive electrode was the same strategy used with the NiOOH electrode: trying not to compromise the behaviour of the aluminium anode. But in this case capacity of the cell was never going to be affected by the cathode weight or area, because the main reactant was oxygen from the air (inexhaustible). However, the E_{CELL} was going to be significantly affected by the bad potential response of air cathode to high currents.

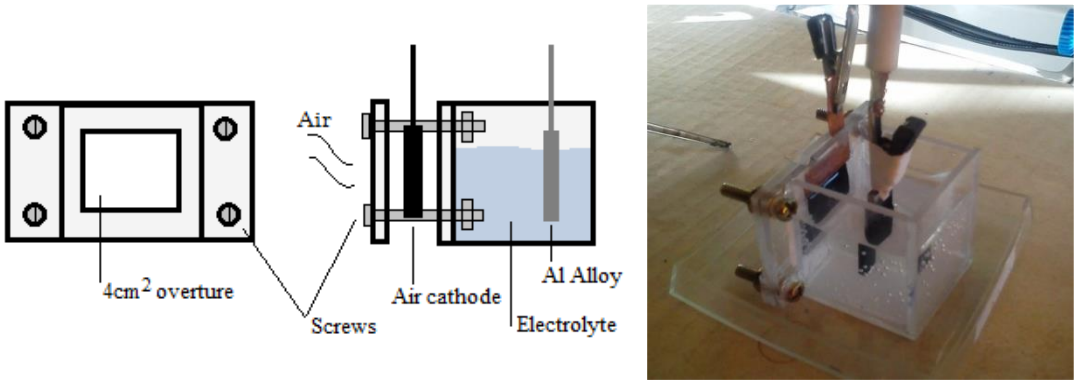

Fig. 4.1.3.2: Schematic diagram of air cathode cell design and capture of Al-air cell during discharge.

In this array tests with the Al2024 alloy as well as the Al2024Clad alloy were performed to compare their behaviour.

Figure 4.1.3.3 shows a comparison between the Al2024-air and Al2024Clad-air batteries at 0.8 and 1.6 $mA \cdot cm^{-2}$, as well as a galvanostatic study of the Al2024-air battery. The results showed that the Al2024 alloy as anode at 0.8 $mA \cdot cm^{-2}$ current had a larger discharge, up to 11 h, while Al2024Clad-air battery achieved a total discharge time of 9.5 h, which means a decrease of the specific capacity in 10.9 %. If we look at the E_{CELL} of both batteries, a higher E_{CELL} value, of 1.25 V during 300 minutes was performed by the Al2024Clad alloy. However, after this point was reached, the potential drop was faster than in the Al2024 alloy battery, which´s potential evolved in a more progressive way. The behaviour observed before the first 300 minutes for the cladded Al could be a result of the pure aluminium layer oxidation, and the subsequent Al oxidation could be from the alloy substrate that was below the cladding layer. At 1.6 $mA \cdot cm^{-2}$, the difference of the reached capacity between Al2024 and Al2024Clad alloys increased to 19.4 %, so the galvanostatic study was carried out just with Al2024 alloy. The cell potential in this case evolved similarly to the case of 0.8 $mA \cdot cm^{-2}$, being the potential of the Cladded alloy higher in the first 300 minutes, but after that, the Al2024Clad-air cell died. However, the potential of the Al2024-air cell presented a potential evolution with more pronounced scope, but reached higher discharging time.

The specific capacity of the Al2024-air battery raised with increases in the working current, and a capacity of 120 $Ah \cdot kg^{-1}$ was achieved at 6.4 and 12.8 $mA \cdot cm^{-2}$. That performance could be attributed to the influence of the discharge current value displacing the self-corrosion reaction at higher currents to better exploit the Al mass. The overpotentials were very accused at high currents, reaching 650 mV from OCP at 12.8 $mA \cdot cm^{-2}$. At discharges between 0.8 to 3.2 $mA \cdot cm^{-2}$, the overpotentials were not so pronounced and the medium cell potential was approximately 1 – 1.2 V.

So, a priori the use of commercial aluminium alloys as anodes in aluminium-air batteries with 0.2 M KOH was found interesting for low current range applications.

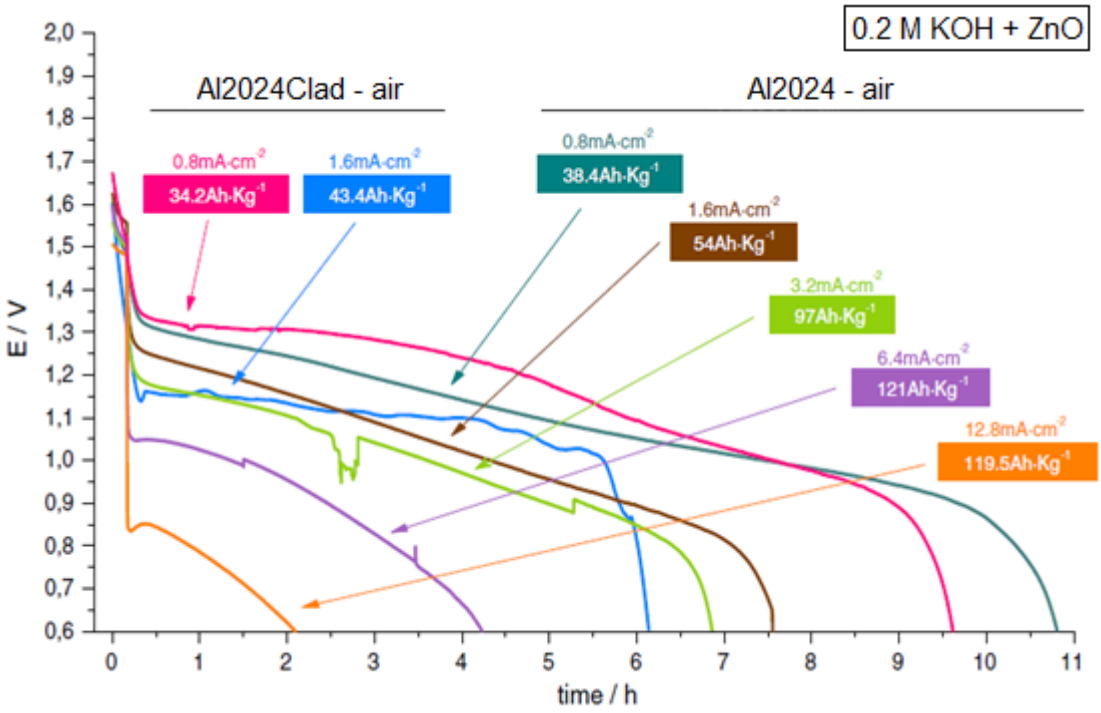

Fig. 4.1.3.3: Discharge of Al2024-air and Al2024Clad-air cells at 0.8 to 12.8 mA·cm^{-2} with 0.2 M + ZnO electrolyte.

In the same way that was measured with Al-NiOOH battery, a discharge of the Al-air battery was performed while the potentials of each electrode were being registered.

Figure 4.1.3.4 shows the electrode and full battery potentials of Al2024-air battery with 0.2 M KOH + ZnO electrolyte at 2 mA·cm^{-2} discharge. Contrary to what happened with NiOOH cathode, the E4A air cathode presented an important overpotential when discharging current was applied because of the low activity of MnO_2 catalyst for 4 electrons pathway oxygen reaction, while being active in the 2 electrons pathway. The latter makes the working potential of the air cathode notably lower, delivering a plateau of -0.200 V when 2 mA·cm^{-2} were applied to the battery (due to the oversizing of the air cathode *vs* the anode of 4:3, the resulting current for the positive electrode was even lower, 1.5 mA·cm^{-2}). So, in this case the air electrode was affecting in a notable way the performance of the battery, lowering the useful voltage of the cell to 0.8 to 1.2 volts.

Regarding to the anode behaviour, it was like that registered in the Al-NiOOH battery.

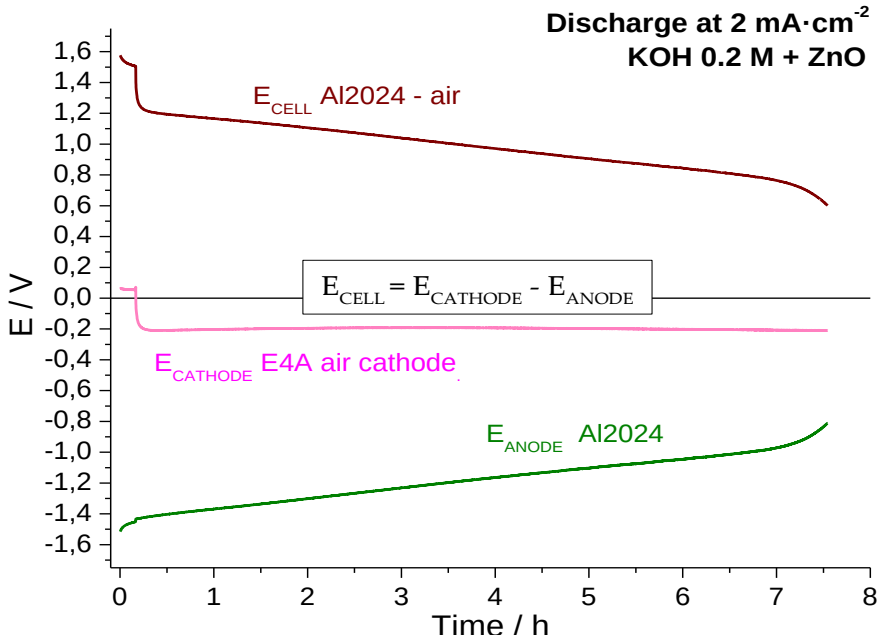

Fig. 4.1.3.4: Breakdown of electrode potentials in a discharge of Al2024-air battery with 0.2 M KOH + ZnO electrolyte at 2 mA·cm^{-2}.

So, with the objective of enhancing the performance of the commercial E4A air cathode, as well as reducing the total weight percentage comprised by the electrolyte in the system, a new electrolyte formulation was chosen. This electrolyte was also based in KOH but in higher concentration and in a gelled texture for an easier assembly of the cell as well as reduction in the amount of electrolyte needed.

4.2. Gelled potassium hydroxide electrolyte based commercial aluminium alloy-air dry battery.

A new electrolyte was chosen to be used for Al-air batteries. From recent bibliography [5], as well as from the knowledge of our research group in free standing electrolyte formulations, the jellification of a high concentration KOH electrolyte was found as a good approach for enhancing the air cathode performance, for easing the assembly of the cell, as well as for reducing the amount of the electrolyte. This gel was obtained by polymerization of acrylic acid in solution with KOH, giving as result a viscous, flexible and sticky electrolyte gel, which could be easily stuck to the electrodes without worrying of liquid leakage. This cells were called “dry” cells because of the absence of a liquid electrolyte.

4.2.1. Gelled potassium hydroxide electrolyte synthesis and Al-air dry cell assembly.

The alkaline gel electrolyte was synthesized by casting a mixture of KOH solution, with or without additives, a gel agent and a polymerization initiator as described by Y. Zuo et al. [5]. KOH (10 g) was dissolved in distilled water (16 ml). This solution was near to a 10 M concentration (once the gel was synthesised the effective molarity decayed to between 3 to 4 M as explained later). ZnO was used as anti-corrosive additive but some tries were also realised with $ZnCl_2$, which is reported to have inhibition activity for the aluminium self-corrosion in alkaline solutions [6]. N,N’-Methylenebis(acrylanide), MBA, was used as cross-linker. The MBA was dissolved in acrylic acid, AA, which is liquid. The alkaline solution was then added to the MBA+AA solution to obtain a clear dissolution with white granular precipitates. The latter was subsequently removed through filtration and a viscous liquid was collected in a Petri plate. Afterward, the polymerization of AA to PAA (poly acrylic acid) was carried out by addition of an oxidant agent, $K_2S_2O_4$ dissolution (32%wt). After 10 min, a 3 mm thick elastic, transparent gel was obtained. All processing was performed at room temperature.

Due to the lower diffusion facility for hydroxyl ions into the gel, the effective concentration was probed to be a 37% of the initial solution concentration, so the useful KOH concentration was near to 4 M (enough high to expect a good response of the air cathode).

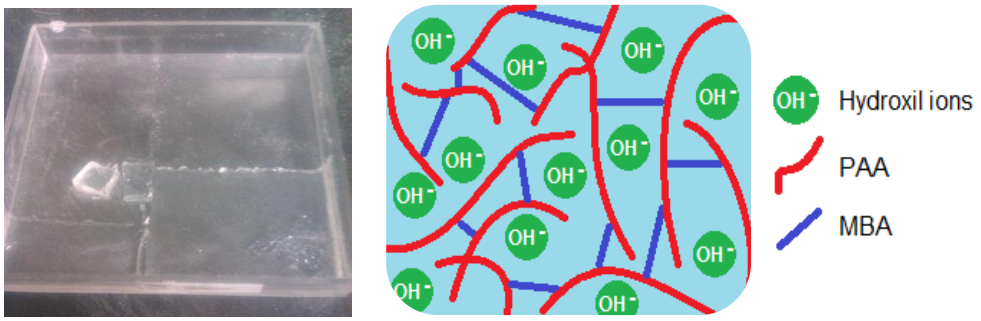

Fig. 4.2.1.1: Capture of the alkaline pH gel after polymerisation and schematic diagram of gel agents in the solution.

Due to the properties of this new gel electrolyte the assembly of the cell became easier, and so the cell casing was notably simplified. A schematic diagram of the cell structure is shown in Figure 4.2.1.2, as can be seen, it was decided to double the cathode by both faces of the aluminium anode, for a better use of the aluminium mass.

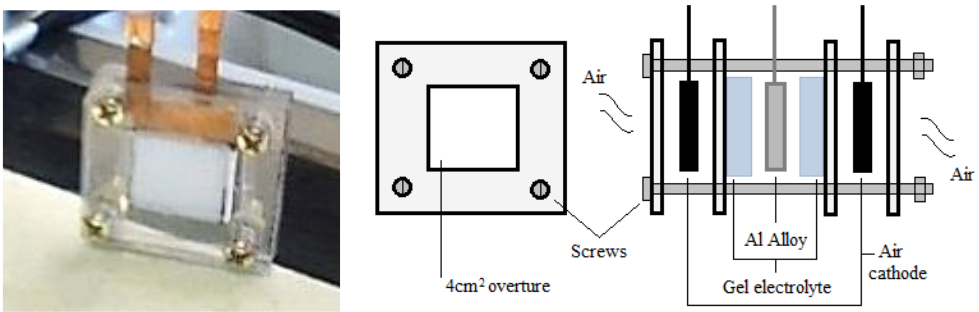

Fig. 4.2.1.2: Capture of the Al2024-air dry cell and schematic diagram of dry cell design.

The used methacrylate was thinner so the total weight of the casing was also lower. Additionally, the reservoirs for locating gel electrolyte were significantly smaller than the vases of the flooded cells, so the final device resulted lightweight and easy to handle in comparison with the previous flooded cells or the radio control vehicle battery. In this way, the total weight as well as the individual weight of the cell components were measured and compared to know the contribution of each. With this new jellification process, the weight of the electrolyte decayed to just a 4.07 % of the total *vs* a 46.3 % in the case of the flooded cell. Additionally, the anode and the cathode represented just a

3.64 % of the total, being the active part of the cell (electrodes + electrolyte) just a 7.7 %. On the other hand, the casing + electric connections + fastening screws represented more than the 90 % of the total weight of the system. The latter means that with a good engineering design, using the right materials, the total weight of the battery could be reduced drastically for really high energy devices with low weight and compact design.

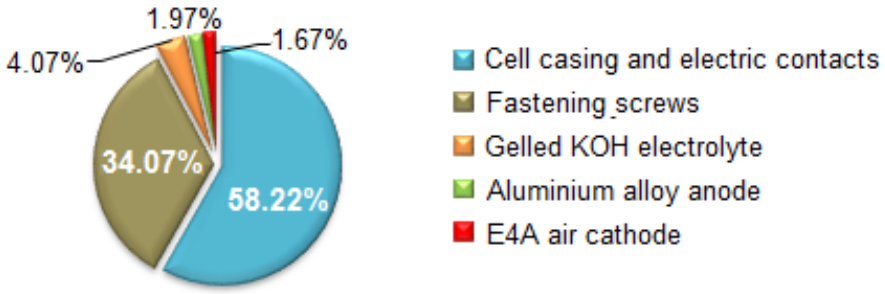

Fig. 4.2.1.3: Weight distribution of Al2024-air dry cell.

4.2.2. Gelled potassium hydroxide electrolyte based commercial aluminium alloy-air battery performance.

In the same way than with 0.2 M KOH electrolyte, first tries were carried out using the NiOOH cathode. And, when it was corroborated that the performance of the cells was similar to that with liquid electrolyte, air cathode was used as negative electrode.

Figure 4.2.2.1 shows the discharge behaviour of Al2024 and Al2024Clad alloys as anodes in Al-NiOOH and Al-air dry cells with gelled KOH + ZnO additive electrolyte.

The potential evolutions as well as the discharging times were equal for both redox pairs with the difference of 400 mV in favour of NiOOH cathode. This results was the same of the observed one in the Tafel curves. Al2024Clad as anode in both batteries performed a slightly higher voltage value plateau from 1.7 to 1.45 V for NiOOH pair and from 1.4 to 1.1 V for air cathode pair. In the case of Al2024 as anode the voltage plateau was slightly lower, but in both cases the discharging time was longer. These results agree with the discharge profiles obtained in the aluminium-air battery with 0.2 M KOH + ZnO liquid electrolyte, see Fig. 4.1.3.3.

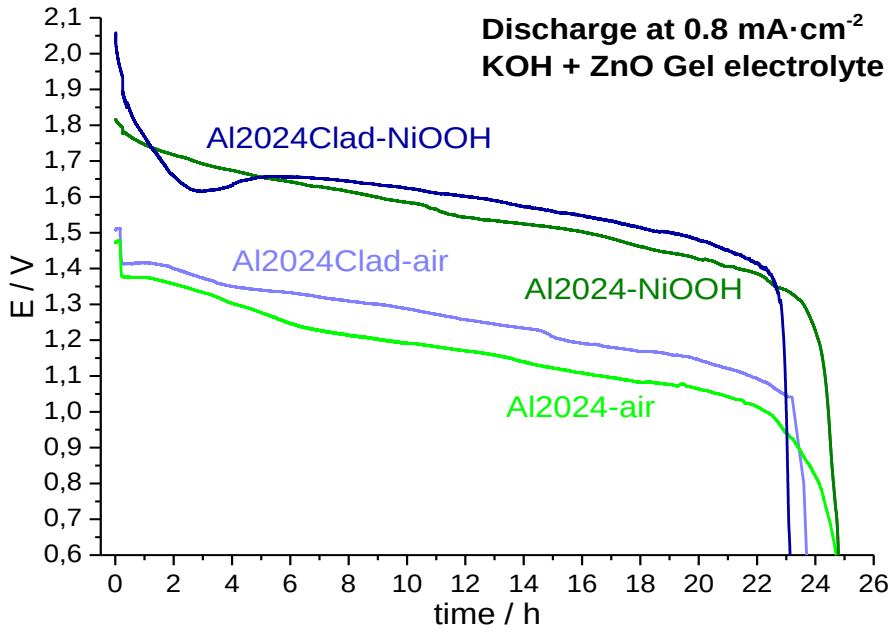

Fig. 4.2.2.1.: Discharge of Al2024-air and Al2024Clad-air vs Al2024Clad-NiOOH and Al2024-NiOOH cells with gelled KOH + ZnO electrolyte at 0.8 mA·cm^{-2}.

Because of the high overpotentials related to the bad voltage response of the air cathode to higher currents, it was decided to come back to the Al7475 alloy. The objective of the use of this alloy was to minimise the effect of the overpotential at higher current discharges in the anode to valance the losses in the cathode. As demonstrated in the first point of the KOH electrolyte study, see point 4.1.1. Characterization of commercial aluminium alloys in alkaline KOH electrolyte., the Al7475 performed the more electronegative potential plateau at medium to high discharging currents. Additionally, at this point of the research project, Al7475Clad alloy was obtained so, the same effect of the pure aluminium protection and higher potential in the first discharging period of the Al2024Clad was expected to be repeated for Al7475 alloy. Al1085 was also obtained and tested.

Due to the high number of alloys being tested in the next experiments, they are going to be represented in the graphic plots as follow for an easier identification of each: Al2024 as Al2U, Al2024Clad as Al2C, Al7475 as Al7U, Al7475Clad As Al7C and Al1085 as Al1U. The capital letter “C” refers to the cladding process, while the capital letter “U” refers to the uncladded nature of the alloy.

Figure 4.2.2.2 shows the evolution of the cell potential at 0.8 mA·cm^{-2} discharge for the Al-air batteries with gelled KOH + ZnO electrolyte using the alloys Al1U, Al2U, Al2C, Al7U and Al7C as anodes.

The voltage plateau of the cell depended on the alloy used; three different behaviours as a function of the alloying elements can be observed:

→ The longest discharging times and the flattest potential evolutions were achieved with the Al7475Clad alloy. A plateau of nearly 26 hours was reached with an E_{CELL} of 1.4 - 1.35 V, corresponding to a specific capacity of 256 mAh·g^{-1}. The same series unclad alloy, Al7475, gave a discharge of 22 h with a quite similar plateau.

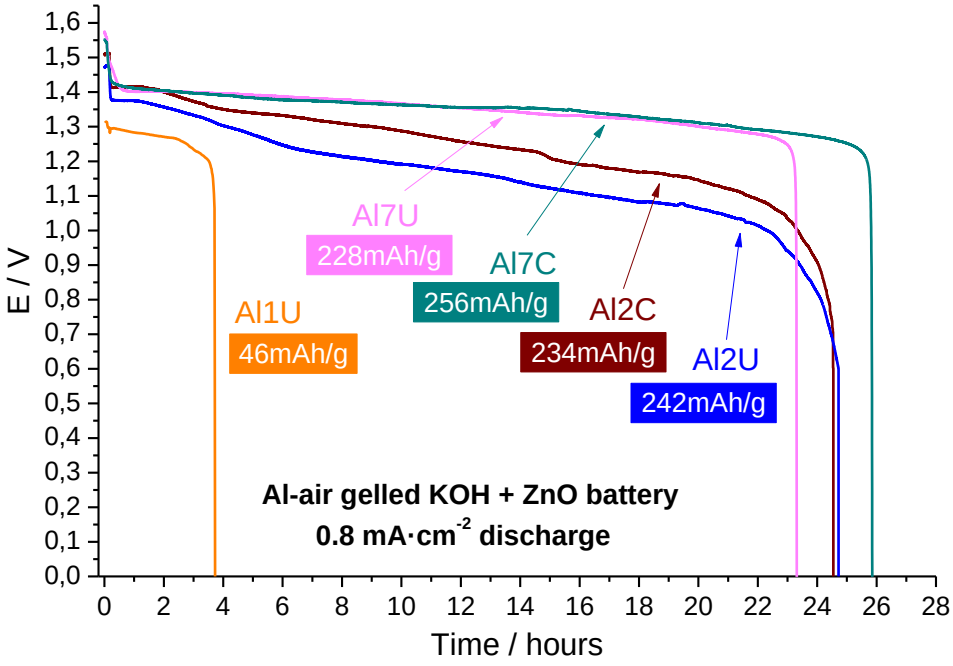

Fig. 4.2.2.2: Discharge of Al-air battery with gelled KOH + ZnO electrolyte at 0.8 mA·cm^{-2} with Al7U, Al7C, Al2U, Al2C and Al1U alloys as anodes.

The difference in relation to discharge times could be due to a first period where the pure aluminium cover (Al7C) is consumed in the oxidation process. This oxidation of pure Al at low current rates results in a cleaner process due to the absence of the impurity layer (alloying elements), as described Y.-J. Cho et al. [7-8]. Once the cladded pure aluminium was spent, the internal alloy began to oxidise.

Contrary to the flooded cell where the produced aluminium hydroxide could precipitate to que bottom of the cell, the gelled electrolyte did not allow this process. And so, the

absence of metallic impurities in the formed aluminium hydroxide during Cladded alloy oxidation could result an important advantage as demonstrated before.

→ The second tendency was that of was the Al2024 group. The most significant difference was the lower voltage during discharge compared to Al7475 group, with that of the Al2C being higher than that of the Al2U. Cooper is the dominant alloying element in Al2024 (4.5%), which´s standard potential is +0.340 V *vs* SHE. The latter drags the negative potential of Al to more electropositive values compared to pure Al, so the cell with Al2024Clad as anode, pure Al cladded, performed at a higher voltage value. This effect was not so notable for Al7475 alloys group, because the major alloying here was Zn which present also a high electronegative potential of -0.760 V vs SHE, closer to the Al oxidation potential, so the resulting mixed Alloy oxidation potential was more electronegative.

After 15 hours of discharge, a small change in the slope of the cell potential evolution can be observed for the Al2024Clad, which may be related to the total consumption of the pure Al cover. The discharge capacities for Al2024 and Al2024Clad, 242 and 226 $mAh \cdot g^{-1}$, respectively, were very close to the ones registered with Al7475Clad and Al7475. However, the specific energy was lower because of the different potential drop (1.35 V *vs.* 1.20-1.15 V).

→ The last differentiated performance was that of the Al1085 anode. The behaviour of Al1085 compared to the others alloys was highly different, achieving a low specific capacity of 48 $mAh \cdot g^{-1}$, five times lower than the one for Al7475Clad. This could be due to the relatively high content of Fe and Si compared to other alloying elements in the sample. It is reported that such metals as iron or silicon in aluminium can create intermetallic compounds in the Al alloy surface [9]. These compounds facilitate the corrosion of the aluminium, leading to higher evolution of H_2 and more points of pitting on the electrode surface. Therefore, the generation of aluminate via self-corrosion was higher, producing an early accumulation of $Al(OH)_3$ on the electrode surface. This process is called blackening [10] because of the black and porous aspect of the aluminate layer. The aluminium hydroxide results not soluble in alkaline media, as explained before, and therefore the death of the battery was directly related to the amount of aluminate accumulation between the gel electrolyte and the aluminium electrode that

could impede the diffusion of the OH^- ions to the anode. The $Al(OH)_3$ was generated not only by the self-corrosion but also by the oxidation of the aluminium anode. So, the more aluminium oxidation reaction displaces the self-corrosion reaction, the more energy could deliver the Al-air dry cell.

This phenomenon was common for all the alloys tested in this work with gelled KOH electrolyte. In all cases, at the end of the battery life the Al anode was not totally consumed; the accumulation of the aluminium hydroxide in the gel-anode interface was the reason for the death of the battery. Another problem was the H_2 evolution and the evacuation of this gas. The sticky texture of the gelled electrolyte resulted in close contact with the electrodes. Once the assembly of the cell was carried out, self-corrosion immediately started generating H_2. Some experiments ended early because of the generation of hydrogen bubbles in the electrode-gel interface. This hydrogen accumulation decreases the contact with the electrode and does so with the active area of the negative electrode, what produces an increase in the current density of the trial.

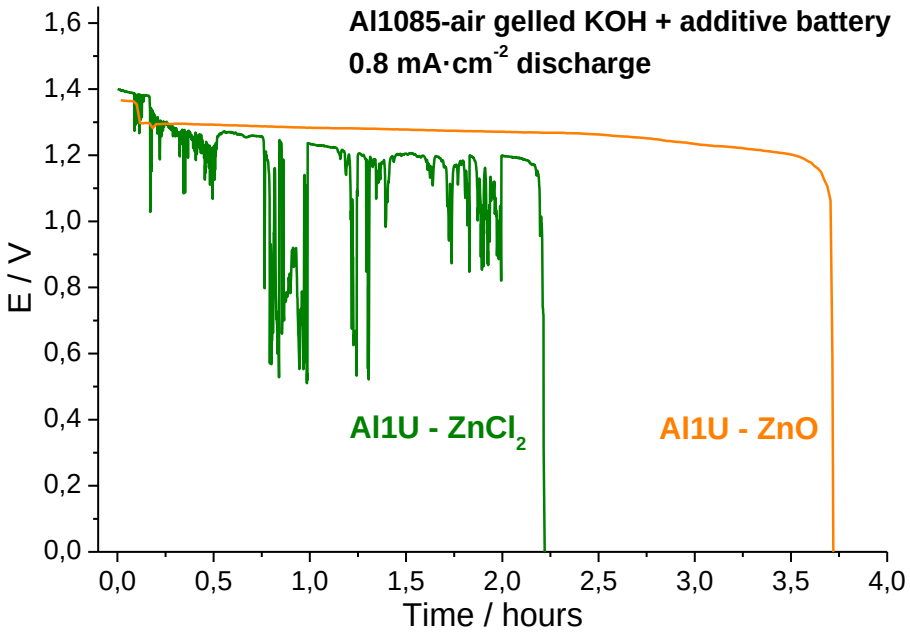

Fig. 4.2.2.3: Discharge of Al1085-air battery with gelled KOH + additive electrolyte at 0.8 mA·cm^{-2}, ZnO vs $ZnCl_2$.

This phenomenon was like the one observed in flooded cells, where the aluminium hydroxide + alloying metals crust created a barrier around Al negative electrode, giving

raise to malfunctioning of the cell due to the difficulty for hydroxyl ions to reach the electrode surface and for evolved hydrogen to be evacuated.

Due to the rapid generation of aluminate and hydrogen on the Al1085 anode, an alternative corrosion inhibitor additive to ZnO, $ZnCl_2$, was tested. As mentioned before, the gel synthesis procedure was the same. The evolution of the discharge at 0.8 mA·cm^{-2} compared to the previous test is shown in Figure 4.2.2.3. The $ZnCl_2$ was found to be a less effective inhibitor than ZnO. The instabilities observed during the discharge plateau are related to the H_2 evacuation from the gel-electrode interface, which was continuously evolving, in a much exaggerated way than with ZnO additive.

Once the electrolyte and the corrosion inhibitor contacted the Al anode, a galvanic couple was generated between Al and Zn. Zinc (-0.760 *vs* SHE) was more cathodic than Al (-1.660 V *vs* SHE). That induced galvanic corrosion, making the more electronegative metal tend to oxidise and the more electropositive tend to reduce. This galvanic couple acts like a "battery" inside the battery, being the Al the anode, The Zn (ZnO) the cathode and the KOH the electrolyte. So spontaneously Zn^{2+} gets reduced on the surface of the aluminium sheet. The process generated a protective layer of Zn, which protected the Al from corrosion and retarded the potential for H_2 generation. This effect took place using both Zn additives. The higher inhibition properties of the ZnO *vs* $ZnCl_2$ could be explained by the fact that the ZnO reacted to the zincate form in the highly alkaline solution to form the $Zn^{(0)}$ cover, as described by Wang et al. [11]:

$$\rightarrow ZnO + H_2O + 2OH^- \rightarrow Zn(OH)_4^{2-} \qquad \textit{eq. 4.2.2.1}$$

$$\rightarrow 3Zn(OH)_4^{2-} + 2Al \rightarrow 3Zn + 2Al(OH)_4^- + 4OH^- \qquad \textit{eq. 4.2.2.2}$$

This zincate results much more active precursor for Zn deposition than $ZnCl_2$.

This phenomenon was corroborated by SEM for the Al7475 alloy after a battery discharge of 0.8 mA·cm^2. The aluminium anode was first sonicated in distilled water to release the excess of aluminium hydroxide accumulated and then analysed. Figure 4.2.2.4 exhibits three differentiated sections:

→ The first one, indicated by number 1, was a light grey high aluminium hydroxide concentration region. Typical corrosion pitting points were distributed all over the area in different layers. This inhomogeneous consumption of the Al could be linked to the difficulty of maintaining full contact between the gelled electrolyte and the anode once the accumulation of aluminate started. Also, in this zone, a concentration of the alloying elements could be observed. As it has been reported for Al-NiOOH and Al-air flooded cells, the alloying elements, once the surrounding Al was consumed, were released into the electrolyte, and get concentrated in this crust like structure. These metals (Mg, Cu, Fe, etc.) also, get concentrated in several accumulations that because of the galvanic corrosion, were reduced on the surface of the anode, creating new defenceless points against self-corrosion, which enhanced the hydrogen generation as well as dropped down the potential of the cell.

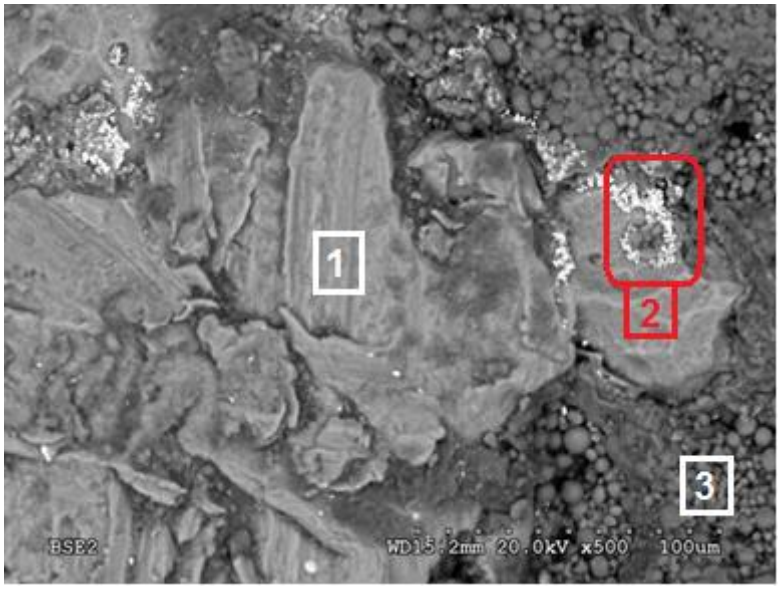

Fig. 4.2.2.4: SEM capture of Al7475 anode after discharge of Al7475-air battery with gelled KOH + ZnO electrolyte at 0.8 mA·cm^{-2}.

→ The second region, marked in red by 2, showed the deposition of Zn on the surface of the Al alloy anode. The bright white little points were metallic zinc deposits due to the galvanic couple with the Al. Most of this deposits were located in the metallic grain borders, where the corrosion, as well as hydrogen generation of Al was more active. This

location of the Zn deposits could explain the high corrosion inhibition of ZnO in alkaline solution.

→ The last region, indicated by 3, represented a high concentration of aluminate and zincate. Those hydroxides appeared as ball-type structures on the surface of the anode. This region seems to be the more active area were the previously described reaction is taking place, see eq. 4.2.2.2. In some places aluminate balls covered with metallic zinc could be seen, as well as zinc deposits hided by big amounts of aluminium hydroxide and oxide.

At this point of the project it was decided not to continue using the Al1085 due to the worst performance in the gelled electrolyte. Additionally, the inhibition properties of the $ZnCl_2$ were probed to be less effective than those of ZnO, so it was also discarded for future measurements.

The next area of interest was that of the alloy´s response to higher current densities to understand the performance of the battery. Figure 4.2.2.5 shows the evolution of the cell potential for Al7475, Al7475Clad, Al2024 and Al2024Clad at 1.6 mA·cm^{-2}.

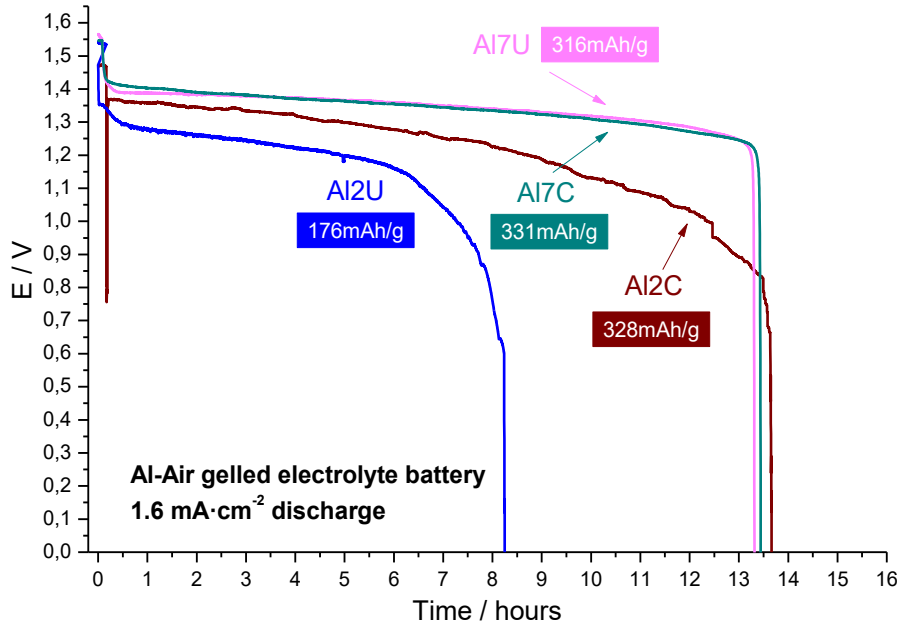

Fig. 4.2.2.5: Discharge of Al-air battery with gelled KOH + ZnO electrolyte at 1.6 mA·cm^{-2} with Al7U, Al7C, Al2U and Al2C alloys as anodes.

With higher currents, the influence of the alloying elements was higher, and therefore, the copper in the Al2U alloy limited the cell discharge more significantly because of the faster formation of the impurities layer on the surface of the specimen alloy. The protection against corrosion of the pure Al cladding process was more noticeable, as seen for the specific capacity of the Al2024Clad alloy which almost doubled that of Al2024: 328 *vs* 176 $mAh \cdot g^{-1}$. The potential plateau of the cell is also higher in the case of pure aluminium covered alloy because of the more electropositive metals in the Al2024.

The Al7475Clad and Al7475 performed a very similar discharge of more than 13 hours. Capacities of 320 - 330 $mAh \cdot g^{-1}$ were achieved. The alloying metals of the Al7475 series, mostly Zn and Mg, did not drag the potential of the cell to such cathodic values as the Cu did. In addition, Mg was quickly corroded to $Mg(OH)_2$, as Zn was to zincate, in such high alkaline media; therefore, the impurity layer was not as significant as it was in the Al2024 or Al1085 alloys. The latter could explain why the differences between Al7475 with and without pure aluminium cladding are not noticeable in low current rates.

Thus, the Al2024 alloy was also discarded for future measurements at higher values of discharge current. The alloying elements made it unsuitable as an anode for Al-air dry cells with gelled KOH electrolyte. Al2024Clad was decided to be still explored because the cladding process could become a cheap treatment for commercial aluminium alloys to be used as anodes, even if the matrix of the Al alloy was composed of non-desirable metals like Cu, Fe, Si or others. The latter could make cheaper alloys like 2000 series commercial aluminium as useful as other bit more expensive alloys like 7000 series.

At 1.6 $mA \cdot cm^{-2}$, the specific capacities were higher than the ones at 0.8 $mA \cdot cm^{-2}$. The latter measurements confronted the analysis performed to classic batteries, where the capacity decreased when the current increased. This unusual phenomenon could be related to competitive reactions between Al oxidation and self-corrosion, in the way that has been exposed during this work. The corrosion processes begin just by simple contact of the anode with the gelled electrolyte, giving aluminium hydroxide and hydrogen evolution as product. Figure 4.2.2.6 shows a schematic diagram of the processes taking place in the Al-air dry cell. The self-corrosion reaction, typed by a red point, is

spontaneous and no energy can be extracted. Once the discharge of the battery was activated, the Al anode started to oxidise, typed by a green point, providing the required electrons and generating $Al(OH)_3$, which was responsible of the end of the battery life by accumulation in the gel-electrode interface.

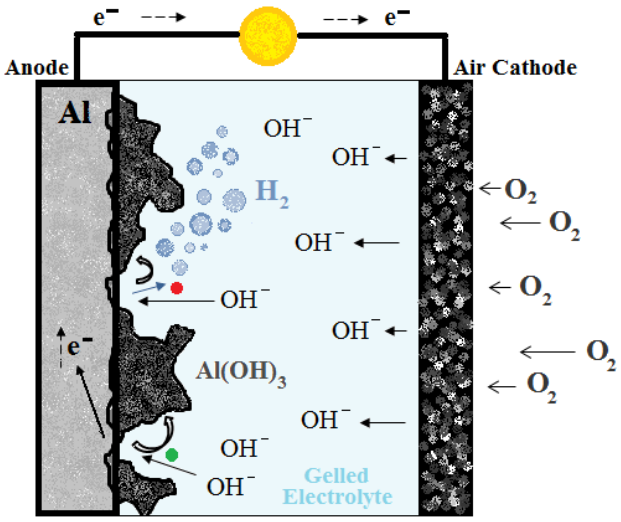

Fig. 4.2.2.6: Schematic diagram of the processes taking place in an Al-air battery with gelled KOH + ZnO electrolyte discharge.

Therefore, if there was a limit in the amount of aluminium hydroxide that could be accumulated in the interface, for a low requirement of electrons the extracted capacity was low, because a small percentage of the threshold amount of aluminate resulted from the Al oxidation and most came from corrosion. At higher currents, the amount of aluminate coming from oxidation grew, resulting in higher achievable capacity. Moreover, most of the Al molecules of the anode surface were oxidising for delivering electrons, so the anchorages for corrosion decreased displacing the H_2 generation.

The increase of the capacity at higher discharge currents took place up to a threshold because the own current increment involved a gain of resistance in the electrochemical process and the working potential of the electrodes fall. The discharging time, also, was directly related to the OH^- diffusion through the electrolyte. Therefore, once the concentration of OH^- on the surface of the gelled alkaline electrolyte was consumed by aluminium, a fast diffusion of hydroxyl ions was needed for higher current discharges.

This effect can be observed in Figure 4.2.2.7 for Al2024Clad, where the obtained capacities at 3.2 mA·cm^{-2} were lower than the ones at 1.6 mA·cm^{-2}; this comparison is shown in Table 4.2.2.1, some pages ahead. The value of the potential was also lower and presented more instability points.

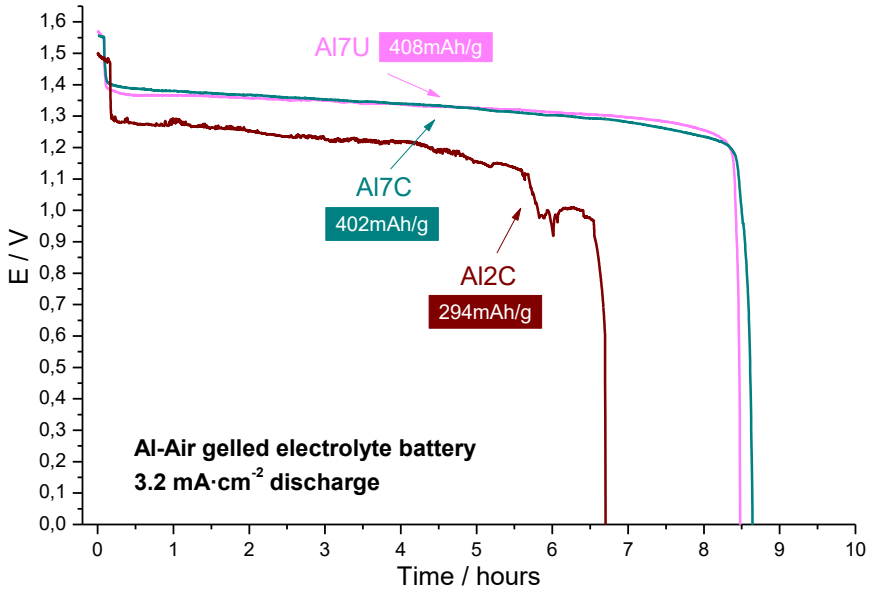

Fig. 4.2.2.7: Discharge of Al-air battery with gelled KOH + ZnO electrolyte at 3.2 mA·cm^{-2} with Al7U, Al7C and Al2C alloys as anodes.

Al7475Clad and Al7475 showed a quite flat potential evolution with higher specific capacities than the ones at 1.6 mA·cm^{-2}, demonstrating a better displacement of corrosion reactions at higher current ranges. Compared to Al2024Clad, Al7475 group alloys did not suffer from the shortage of hydroxyl ions in the electrolyte-electrode interface, because most of this OH^- ions where used for aluminium oxidation instead of aluminium self-corrosion.

The behaviour of the Al7475 was quite similar to Al7475Clad again. The differences between them was more pronounced at 0.8 mA·cm^{-2}, but at 1.6 and 3.2 mA·cm^{-2} the performance of both as anodes returned quite similar results. At 4.4 mA·cm^{-2} however, Al7475 achieved a longer discharge than the Al7475Clad alloy, with a better value of the specific capacity. This change in the trend could be explained by the dissolution of the impurity complex film (crust like alloying metal rich deposits) on the surface of the anode

at high current ranges. Once the discharge current exceeded a threshold, the galvanic couple was dissolved, no longer inducing the reduction of the alloying elements on the Al plate. This effect was proved in other works [12,13], where the purity of the aluminium was analysed for its use as anode. They concluded that there is a crossing point between the pure aluminium and lees pure Al oxidation behaviour, conditioned by the applied current. This crossing point determined from which current onwards was lees pure aluminium performing better as anode.

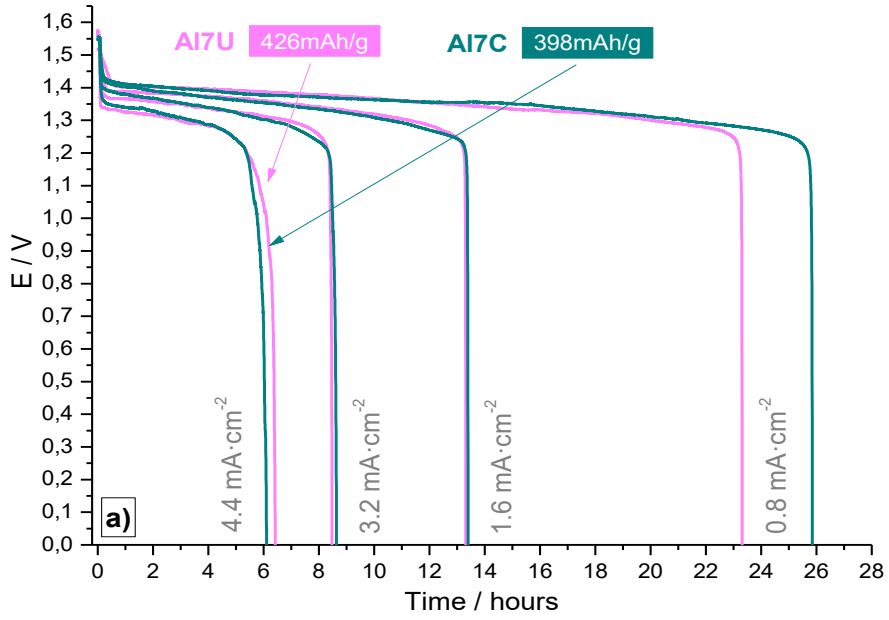

Fig. 4.2.2.8: Discharges of Al-air battery with gelled KOH + ZnO electrolyte at 0.8 to 4.4 mA·cm^{-2} with Al7U, Al7C alloys as anodes.

Figure 4.2.2.8 summarises the performance of Al7475Clad and Al7475 for the full range of currents measured in gelled KOH + ZnO electrolyte. The effect of the alloying elements (compared to the pure Al cover) can be clearly seen for the increasing current. At the lowest current measured, 0.8 mA·cm^{-2}, the Al7475Clad alloy outstripped the Al7475 in more than 2 hours of discharge. At 1.6 and 3.2 mA·cm^{-2}, the discharge times were quite similar, and, finally, for 4.4 mA·cm^{-2} the Al7475 performed a longer discharge of 6.5 h against 6 h of the Al7475Clad alloy. Therefore, it was found that for currents of 4.4 mA·cm^{-2} and higher in an alkaline gel electrolyte commercial Al alloy-air cell, Al7475

(without cladding) could provide longer discharge times than pure aluminium covered same alloy, or other alloys studied in this work.

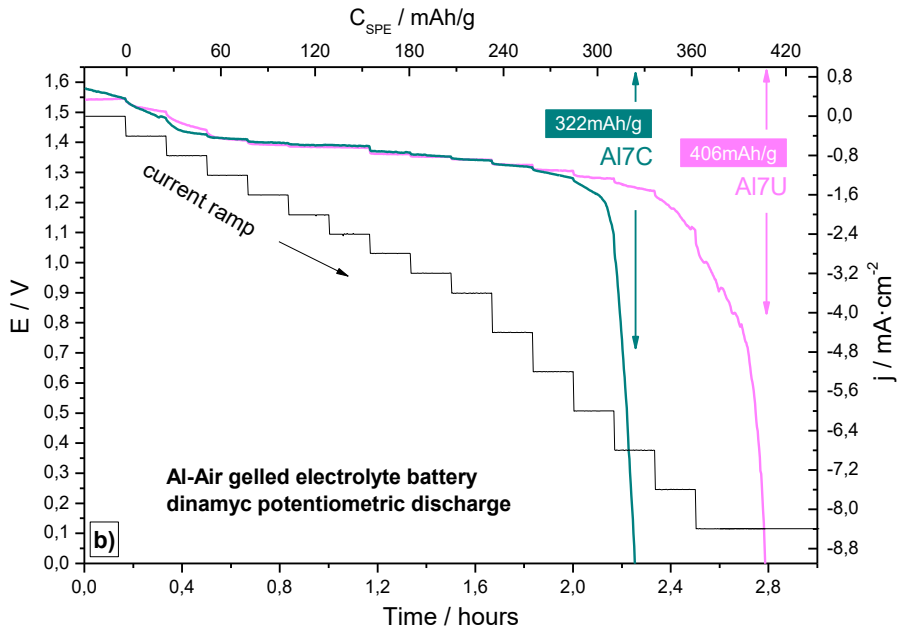

Fig. 4.2.2.8: Dynamic galvanostatic measurement of Al-air battery with gelled KOH + ZnO electrolyte from 0.8 to 8.4 mA·cm^{-2} with Al7U, Al7C alloys as anodes.

This fact was corroborated by a dynamic galvanostatic measurement of the Al7475Clad *vs* Al7475 alloys as anodes in Al-air battery. Increments of 0.4 mA·cm^{-2} were applied every 10 minutes until a discharging current of 3.6 mA·cm^{-2} was reached, and then the increments were of 0.8 mA·cm^{-2} every 10 minutes until the end of the battery life. The results can be observed in Figure 4.2.2.9. Al7475Clad-air battery reached a maximum of 6.8 mA·cm^{-2}, lower than the 8.4 mA·cm^{-2} achieved by Al7475-air cell, which showed an improvement of the specific capacity in the trial of 84 mAh·g^{-1}, from 322 to 406 mAh·g^{-1}.

Thus, at relatively high current rates Al7475 performed better than Al7475Clad and other commercial Al alloys, while at lower current ranges, pure Al cladded alloys presented higher performances, as shown in Table 4.2.2.1. This improvement was due to the lower influence of the galvanic corrosion between the alloying elements and Al at the higher explored currents, making way for the displacement of corrosion reactions

in favour of the oxidation of Al. And accordingly, allowing a better exploitation of the Al mass for achieving higher specific capacities. This finding could be key for commercial

Al-air cells with gelled KOH electrolyte, since it was proved that the accumulation of aluminate limited the battery life, and the use of pure aluminium was preferred at low current discharges, while Al7475 was found to be more successful for higher current trials.

Table 4.2.2.1: Specific capacity and maximum current loads for commercial Al alloy-air batteries with gelled KOH + ZnO electrolyte.

Al alloys	**0.8 mA·cm^{-2}** (mAh/g)	**1.6 mA·cm^{-2}** (mAh/g)	**3.2 mA·cm^{-2}** (mAh/g)	**4.4 mA·cm^{-2}** (mAh/g)	**Max. current load**
Al7U	228	316	408	426	8.6 mA·cm^{-2}
Al7C	256	331	402	398	6.6 mA·cm^{-2}
Al2C	234	328	294	-	-
Al2U	242	176	-	-	-
Al1U	46	-	-	-	-

Table 4.2.2.1: Specific capacity and maximum current loads for commercial Al alloy-air batteries with gelled KOH + ZnO electrolyte.

Al anode composition (%wt.)	**Electrolyte**	**Current (mA·cm^{-2})**	**E_{Cell} (V)**	**Capacity (mAh/g)**	**Assignee**	**Ref**
Al-2.26 Ag	KOH 0.6M + HPG (gel)	0.8	1.74	105	A.A. Mohamad	[14]
		1.6	1.68	58		
Pure Al mesh	KOH 9M + PAA 6% (gel)	0.7	1.31	64.4	Z. Zhang et al.	[15]
		2	1.30	112		
Pure Al powder	KOH 4M ethanol	0.7	1.32	236	J. Chen et al.	[16]
Al 2024	Aqueous 0.2M KOH	0.8	1.20	38.4	P.Ocón et al.	[17]
		1.6	1.15	54		
		3.2	1.05	97		
		6.4	0.95	121		
Al 7475	KOH 9M + PAA 6% (gel)	0.8	1.4	228	Present work	
		1.6	1.38	316		
		3.2	1.35	408		
		4.4	1.31	426		

The presented double-cathode cell design using A7475Clad or Al7475 alloys as anodes reached high results in terms of specific capacity compared to those in bibliography for Al-air alkaline electrolyte cells (some of them gelled), at medium-low current rates, see Table 4.2.2.2.

4.3. Sodium hydroxide electrolyte based commercial aluminium alloy-air high power battery.

The third approach for the development of a commercial aluminium alloy-air battery, was the use of a highly alkaline solution based in sodium hydroxide instead of potassium hydroxide. It is well-known that the ionic conductivity of KOH is higher than that of NaOH, and that is why most of the alkaline media based batteries use KOH as electrolyte (alkaline batteries, Zn-air, Ni-Cd, etc.). However, it was found that when some additives were added to NaOH electrolytes, the corrosion of aluminium can be minimised notoriously, and moreover, NaOH gives the chance to directly use the produced aluminium hydroxide during the discharge to feed the Bayer Process and subsequently the Hall-Heroult Process to completely recover new high purity fresh aluminium. When the $Al(OH)_3$ comes from the reaction in KOH electrolyte, it must be pre-treated to remove potassium.

The latter makes sense in the use of commercial aluminium alloys, cheap, abundant and even reused, for their use as an energetic vector, like hydrogen. Aluminium could be used as energy generation source in an Al-air battery with alkaline NaOH based electrolyte when energy is needed, while when there is an energy surplus, it could power the aluminium recovering from the $Al(OH)_3$ reaction product. This system presents some drawbacks as well as some advantages compared to hydrogen gas.

On the one hand:

- → Metallic aluminium can be easily transported and stored. And its high energy density makes low weights of this material deliver big amounts of energy.
- → Different aluminium alloy compositions can be used as anodes, so the purity is not a handicap (as is going to be demonstrated later).
- → Aluminium coming from its 2^{nd}, 3^{rd} or even higher life can be used as raw material for energy production. This means that old aluminium cans or windows, or even aluminium scrap can be used as anode, with no matter of how much times is being recycled before.

→ Metallic Al results no toxic, non-flammable, environmentally friendly and human compatible.

→ Its recycling and recovering from aluminium hydroxide is based in a well-developed and established industry, which makes the commercialisation and expansion of an Al based energy system viable with not so much infrastructure cost.

→ Renewable energy production exceed could be transform to aluminium as energy storage form.

On the other hand, some issues must be considered:

→ Voltage of the cell could be different depending on the aluminium alloy, so power electronics could be necessary to valance the system.

→ Operation cost could be medium to high because of the durability of the air cathode and continuous refilling of the electrolyte.

→ Bayer + Hall-Heroult processes consume big amounts of energy, so this "chemical" charging of the battery could present low cycling efficiency, as well as non-cost effectivity.

Considering all these points, this chapter of the research work is focused in the development of a NaOH based Al-air battery, with the aim of extracting as much energy as possible from commercial aluminium alloys.

From the previous chapter, where gelled potassium hydroxide electrolyte based batteries have been presented, the potentiodinamic discharge was taken as reference measurement for the electrochemical characterisation of the alloys.

A new electrolyte formulation was chosen from different experiments that are not going to be graphically presented, but explained, because these results are part of a patent of the company Albufera Energy Storage S.L., which financed the project where this work was carried out.

The electrolyte base was 4M NaOH, which is a standard concentration, very present in batteries or electrochemical related publications. This concentration was later checked

to ensure the best performance of the electrolyte. And to this electrolyte base some additives were added taking into account different experiments, publications as well as patents in this field.

The first additive was sodium citrate, which was found to complex the aluminium hydroxide formed during discharge of the battery, creating a matrix able to transport $Al(OH)_2^+$.

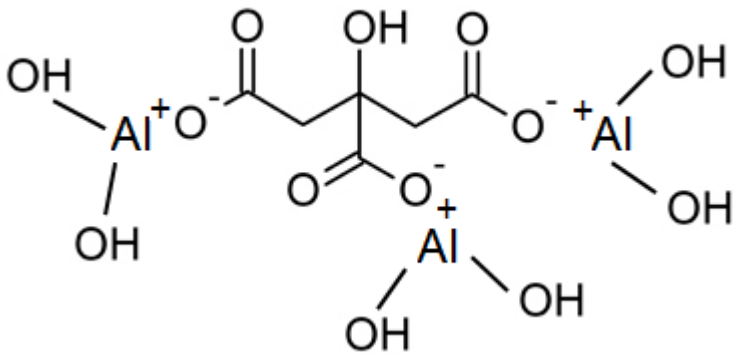

Fig. 4.3.1: Schematic diagram of citrate molecule complexing aluminium hydroxide.

This complex get located around the aluminium anode and facilitated the evacuation of aluminium hydroxide to inhibit the growth of the crust like aluminium hydroxide + alloying metals layer into the surface. The latter prevented the direct contact of alloying metals released in the electrolyte during discharge with the fresh aluminium anode, and so, prevented the galvanic corrosion between them. Consequently, the aluminium self-corrosion as well as hydrogen evolution get decreased. From older studies, it was proved that the concentration of sodium citrate in the electrolyte was directly related to the amount of aluminium hydroxide complexed. This was shown just by measuring the time elapsed for the first crust like surface at the same discharge conditions for different citrate concentration.

The second additive used was calcium chloride. Its solubility in alkaline electrolyte is very low so it got homogeneously dispersed, forming a whitish solution similar to that with ZnO in the beginning of this work. The use of calcium chloride was related to its capability to get reduced into the aluminium surface (like the effect of ZnO in KOH) and

prevent it from corrosion. Moreover, once the discharge reaction started, the electrolyte became more transparent, indicating that the calcium was deposited in the Al surface. Too high concentration of $CaCl_2$ created a too thick deposited layer into Al surface, not only preventing aluminium corrosion, but also Al oxidation, so the battery did not work.

And the last additive was NaCl, which was added to the electrolyte to increase the chloride concentration, which is well-known to attack native aluminium oxide layer in the Al anode, as well as the formed alloying metal clusters.

Al7475, Al7075, Al2024 and Al2024Clad were measured in this electrolyte. Al7475Clad presented in the last point of the work with interesting results, was not available at this point of the project, because the order of the results presented on this work is not the chronological order of when they were measured.

The objectives of this electrolyte formulation were to being able of develop a 10 Ah Al-air cell, with a discharging potential of more than 1 V, and able to deliver discharging rate of C/10 or even higher. This "C" discharge rate was invented by Coulomb: the "C" refers to the capacity of the cell, and the number refers to the amount of time to deliver this capacity. For example: if we take a 1 Ah battery, a discharge at 1C would be a discharge of 1 hour, so the current would be 1 A. In the same way, for this 1Ah battery a discharge at C/10 (Capacity under ten) would last 10 hours at a current of 100 mA, and a 2C discharge would take 30 mins (1/2 hours) at a current of 2 A.

A new cell casing was designed to allow bigger electrodes of 16 cm^2 of air cathode by both sides of an aluminium anode of 9 cm^2 by each face. The objective of 1 A current discharge, divided by 18 cm^2 of Al, resulted in a specific current of near to 60 $mA \cdot cm^{-2}$. This value was notably higher than the results presented before, and that´s why a new formulation was chosen with some specific additives.

For the first trials (before assembling the large size cell), a 4 cm^2 cathode and 3 cm^2 anode cell was tested (similar to that used in the first point of this work with 0.2 M KOH solution, but with the particularity than the cathodes were located by both sides of the

aluminium). Figure 4.3.2 shows a dynamic galvanostatic discharge of the cited commercial alloys in an Al-air battery with NaOH based electrolyte.

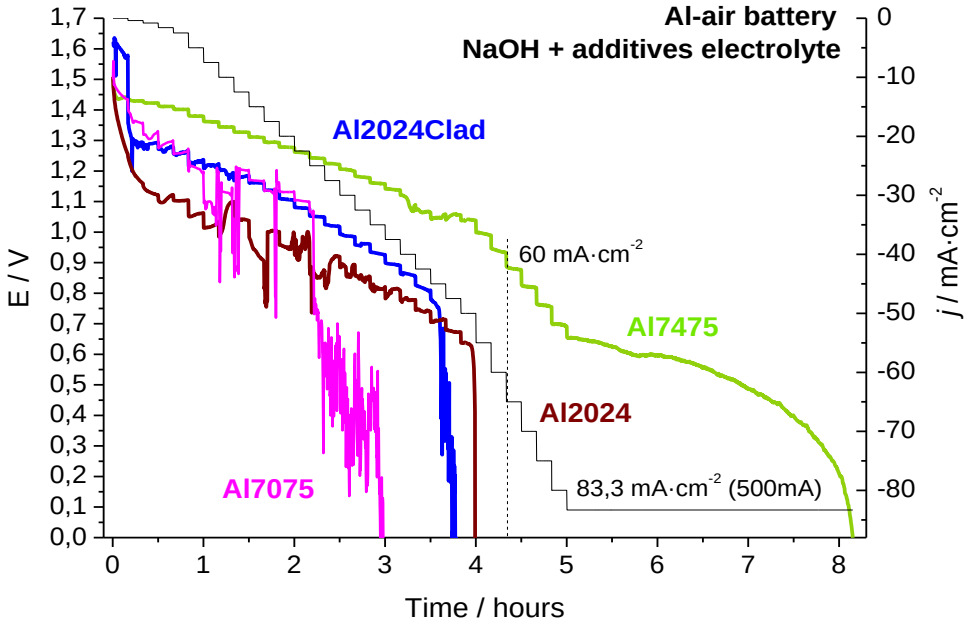

Fig. 4.3.2: Dynamic galvanostatic measurement of Al-air battery with NaOH + additives electrolyte from 0.5 to 83.3 mA·cm^{-2} with Al7475, Al2024, Al2024Clad and Al7075 alloys as anodes.

As can be seen the left horizontal edge shows the voltage of the cell during the experiment. And the right edge shows the specific current of the trial, which is represented by a stepped black continuous line. The current was incrementing every 10 minutes, first from 0.5 to 2.5 mA·cm^{-2} with steps of 0.5 mA·cm^{-2}; then from 2.5 to 50 mA·cm^{-2} with steps of 2.5 mA·cm^{-2} and finally from 50 to 83.3 mA·cm^{-2} with steps of 5 mA·cm^{-2}. The maximum measured specific current was 83.3 mA·cm^{-2} because of the own limits of the potenciostat-galvanostat station which reached 500 mA (for 6 cm^2 anode area). This type of test resulted very useful because it showed the maximum current for every anode, as well as which was the voltage response to an applied current. So, we could predict which was going to be the useful voltage of a cell at certain current discharge. The results obtained in this electrolyte formulation were aligned with the ones obtained with the different electrolytes based in KOH, being the Al7475 the alloy with the lower overpotentials and with the higher achievable maximum current. The Al7075, from the family of the latter one, performed a very instable potential evolution

with peaks related to the hydrogen evolution from self-corrosion. This worst behaviour could be due to the higher percentage of Fe and Si compared to Al7475 (0.5 and 0.4 *vs* 0.1 and 0.12, respectively). As explained before, these two metals are reported to create intermetallic compounds with the Al in the surface that act as favourable points for corrosion (these intermetallics reduce notoriously the overpotential for hydrogen evolution).

The curves obtained for the Al2024 family as well as the one for Al7475 alloy are analysed separately.

Figure 4.3.3 shows the potentiodinamic discharges of the Al2024 group-air batteries with NaOH based electrolyte.

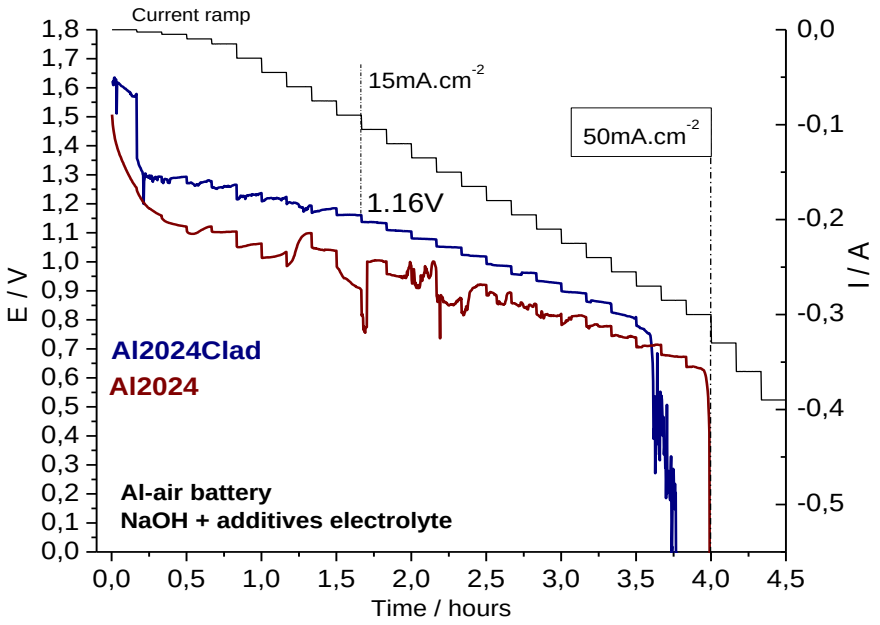

Fig. 4.3.3: Dynamic galvanostatic measurement of Al2024 group-air batteries with NaOH + additives electrolyte from 0.5 to 50 mA·cm^{-2}.

Al2024Clad-air battery delivered a maximum current of 280 mA, equivalent to 40 mA·cm^{-2}. The potential evolution was flat and increased constantly with the raise of the current. A first drop in the curve can be observed at low current levels which was related to the anode overpotential instead of the cathode (contrary to other experiments). This initial drop is also present in the Al2024 alloy. It is suggested that metals like Fe, Si or even Mn (0.5, 0.5 and 0.9 % weight for Al2024), that were also present in the Al7075, could aggravate in a more significant way the corrosion of Al in this new electrolyte

formulation than in the previous ones. Calcium present in the electrolyte can react with Fe, Al and Si to form Al-Ca-Si ternary as well as Si-Al-Fe-Ca quaternary intermetallic compounds in the surface of aluminium, breaking up the inhibition effect of the Ca, and adding lots of defenceless points against hydrogen evolution. The latter displaced the competition in favour of self-corrosion, displacing also the potential of the aluminium to more cathodic values.

In the case of uncladded Al2024 alloy this effect is even more noticeable, presenting a lot of irregularities during the discharge, higher hydrogen bubbling, and additionally a premature crust like accumulation around the anode was shown during the discharge. The latter indicated that the protective effects of the calcium or the citrate were been broken up, possibly because of the intermetallic commented before.

Even of this negative effect, this electrolyte formulation showed the capability to assembly an Al-air cell with a cheap and common alloy like the Al2024Clad, and to discharge it at 15 mA·cm^{-2} with an expected potential plateau of 1.16 V, which is a common voltage of other technologies.

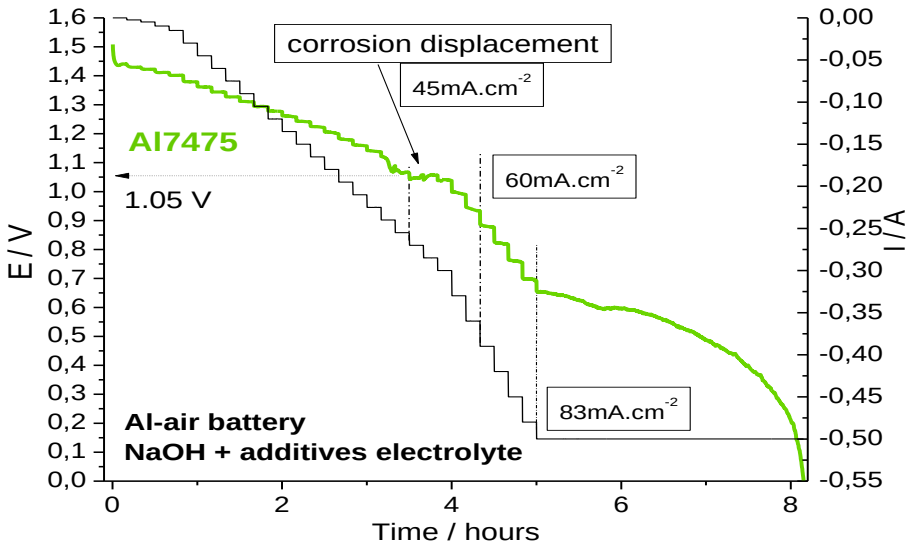

Fig. 4.3.4: Dynamic galvanostatic measurement of Al7475-air battery with NaOH + additives electrolyte from 0.5 to 83.3 mA·cm^{-2}.

Figure 4.3.4 shows the detailed discharge of the Al7475-air battery with the NaOH based electrolyte. The performance of this alloy was the best overcoming in a very notable way the Al2024 group alloys. This anode overpassed the objective of 60 mA·cm^{-2} for a

maximum current of 83.3 mA·cm^{-2} (500 mA), which was the maximum permitted by the measurement equipment. Additionally, when this maximum current was reached it performed a discharge plateau of more than 2 hours from 0.65 to 0.4 V.

A very important point was found in this test related to the corrosion of Al. When the discharge reached a specific current of 45 mA·cm^{-2}, the alloy as anode immersed in the electrolyte stopped producing hydrogen bubbles. The discharge continued for more than 4 hours (increasing the current), with hydrogen evolution. This was attributed to a total displacement of the corrosion in gain of aluminium oxidation. In fact, when the test was finished and the cell turned to OCP, bubbles were seen again.

It is proposed that could be a synergistic effect between Ca, sodium citrate and Zn coming from the alloy, that once reached a specific current, is able to maintain certain points of the anode continuously oxidising, while the resting points are protected. This effect is more clearly explained in a schematic way, see Figure 4.3.5.

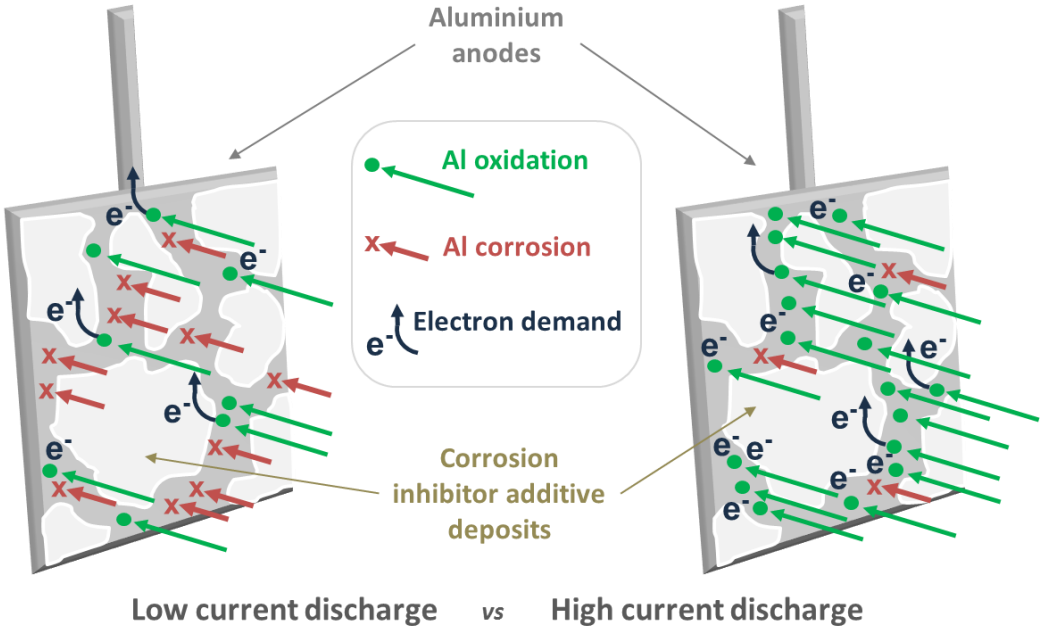

Fig. 4.3.5: Schematic diagram of the processes happening in aluminium anode surface at low and high current discharges: competition between oxidation and corrosion.

This phenomenon resulted quite interesting from an application point of view, because the cell potential for 45 mA·cm^{-2} was 1.05 V, which even if is not so much high, could be

useful by stacking cells in series. Additionally, without self-corrosion of the Al anode, there would be no Al active mass loss, no OH^- ion from the electrolyte consumption (so the pH will remain constant) and no water consumption from the electrolyte. The latter solves one of the issues presented at the beginning of this point of the work, related to the possible high costs of maintenance of a system based in this technology.

The high current discharge performed by the Al7475 made the reached specific capacity grow to incredible values compared to the ones presented up to this point of the work. Figure 4.3.6 represents the same discharge plot of the Al7475 in terms of specific capacity instead of hours.

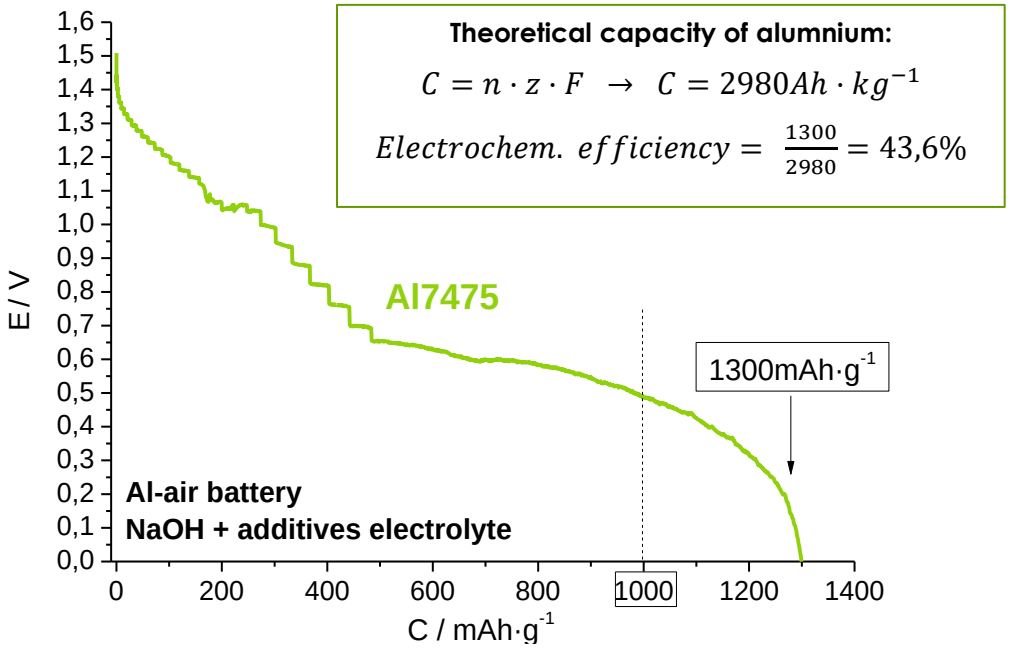

Fig. 4.3.6: Dynamic galvanostatic measurement of Al7475-air battery with NaOH + additives electrolyte from 0.5 to 83.3 mA·cm^{-2}in terms of specific capacity.

The reached specific capacity was 1300 mAh·g^{-1}, which compared to the theoretical aluminium capacity represents an electrochemical efficiency of 43.6 %. This energy extraction from aluminium resulted huge, and confirmed one of the advantages presented at the beginning, related to the use of Al as energy vector. The 1000 mAh·g^{-1}

specific capacity is signalled in the figure because it was one of the objectives to reach in the project, and it was far exceeded.

If we look at the cell behaviour at the objective of 60 mA·cm^{-2}, the voltage value was 0.9 V, close to the objective of 1 V. So it was decided to repeat the same experiment registering the individual potentials of each electrode to know which was the influence of each.

Figure 4.3.7, shows the potential evolution of each electrode and the Al-air battery during the dynamic galvanostatic discharge from 0.5 to 83.3 mA·cm^{-2}. The potential value for Al7475 anode was -1.27 V *vs* Ag/AgCl, the same than the one registered in polarisation measurements in 4 M KOH at 60 mA·cm^{-2}, which is a high electronegative value, with not so high overpotentials, considering that the OCP for this alloys was -1.60 V. So, the responsible of the low voltage of the cell was mostly the air cathode, which performed at a voltage of -0.390 V *vs* Ag/AgCl.

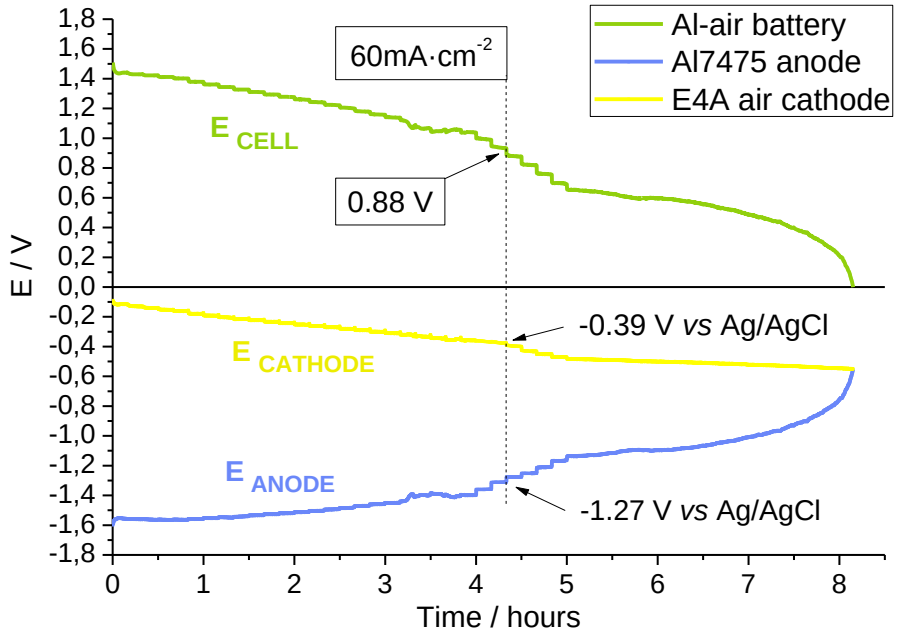

Fig. 4.3.7: Breakdown of electrode potentials in a dynamic galvanostatic discharge of Al7475-air battery with NaOH + additives electrolyte.

As presented in the introduction, other research groups and companies published much higher voltage performance for their air cathode based in Ag, Co or Ni-Co based spinels. These air cathodes could work at operating voltage values of even +0.600 V at high

currents. So, the operating potential of the cell at 60 mA·cm^{-2} could be as high as 1.9 V with the Al7475 commercial Al alloy anode and the NaOH based electrolyte formulation.

Once we had all this information about the cell performance *vs* high currents, it was assembled a cell for a galvanostatic discharge at continuous 60 mA·cm^{-2}. This cell was still the 3 cm^2 (by each face) aluminium anode cell, so the total current was 360 mA.

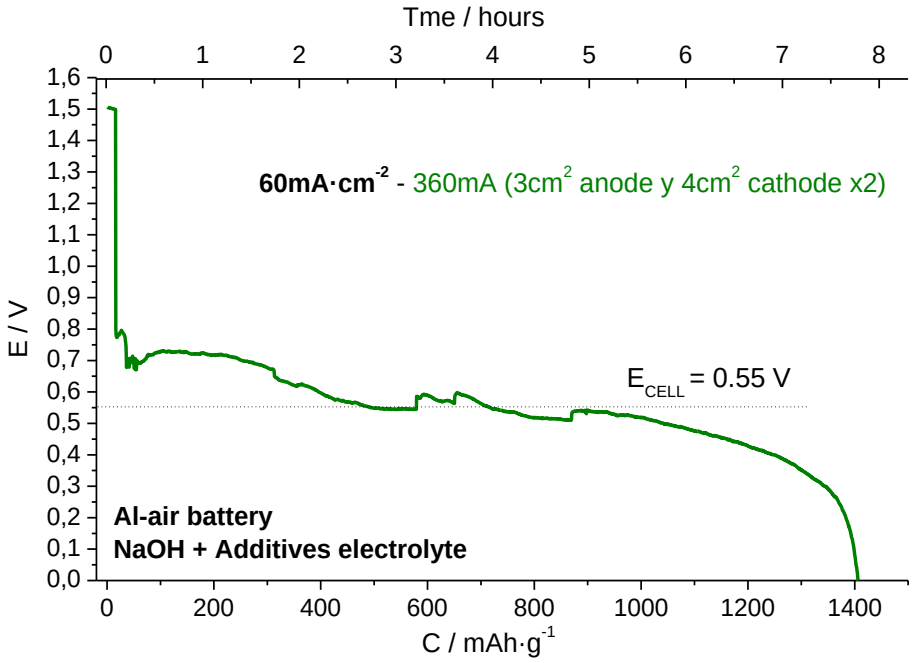

Fig. 4.3.8: Discharge plot of Al7475-air battery with NaOH + additives electrolyte at 60 mA·cm^{-2}.

The discharge potential of the cell was 0.55 V, lower than the 0.9 V registered during the dynamic galvanostatic test. The OCP for the cell was 1.5 V and when current discharge was applied voltage decayed 0.7 V. This result was surprising because it was quite lower than the expected result. The potential of the anode *vs* Ag/AgCl electrode was -1.15 V, similar to that measured in the previous tests (-1.27 V), so the high overpotential in this case was mostly related to the cathode behaviour. It is suspected that the latter could be because the dynamic galvanotactic test could had act as an activation period (starting from low current and progressively increasing) for the commercial air cathode, while in this case the cathode was directly polarised to such high current. However, if we look at the obtained specific capacities, the values were even higher than in previous tests,

achieving 1400 mAh·g^{-1} which is around of 50 % of electrochemical efficiency. The discharging time was near to 8 hours, less than the objective of 10 hour discharge.

Trying to solve the low working voltage of the cell, it was decided that the new cell casing design (for 9 cm^2 electrodes) should present less distance between the positives and the negative electrodes. This distance influences notoriously the overpotential of the cell so as shown in Figure 4.3.9 the distance was reduced a half of the previous design.

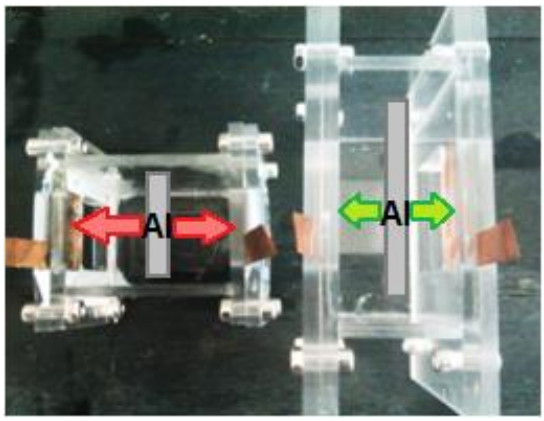

Fig. 4.3.9: Capture of Al7475-air battery cell casings, comparison of distance between electrodes.

So, with this new design and the higher area electrodes, a 1 A current discharge was tested for the Al7475-air battery.

The discharge of this big size Al7475-air battery performed a plateau in an average voltage of 0.9 V, 0.35 V higher than the previous tests with the small size cell. This result was very positive because it was quite near to the objective of 1 V. The obtained specific capacity was 1000 mA·cm^{-2}, which was lower than the previous ones, but this could had been because of the higher thickness of the large size electrodes, having an important percentage of the weight not being active. The cell discharge lasted for 8.2 hours, for a total capacity of the cell of 8.2 Ah, near to the objective of 10 Ah.

So, with the mix between the NaOH based electrolyte, commercial aluminium alloy Al7475 and cell design, the objectives of 10 Ah, 1 A (C/10 rate) discharge, 1000 mAh·g^{-1} and 1 V working voltage plateau, were near to be achieved. The use of a better air cathode could make the voltage of the cell improve in an important way, as well as the achievable maximum discharging current (Al7475 alloys showed good performance at

higher currents). Thus, these results proved the possibility of using Al as a fuel for Al-air batteries with NaOH based electrolyte, achieving high power discharges with high specific capacities.

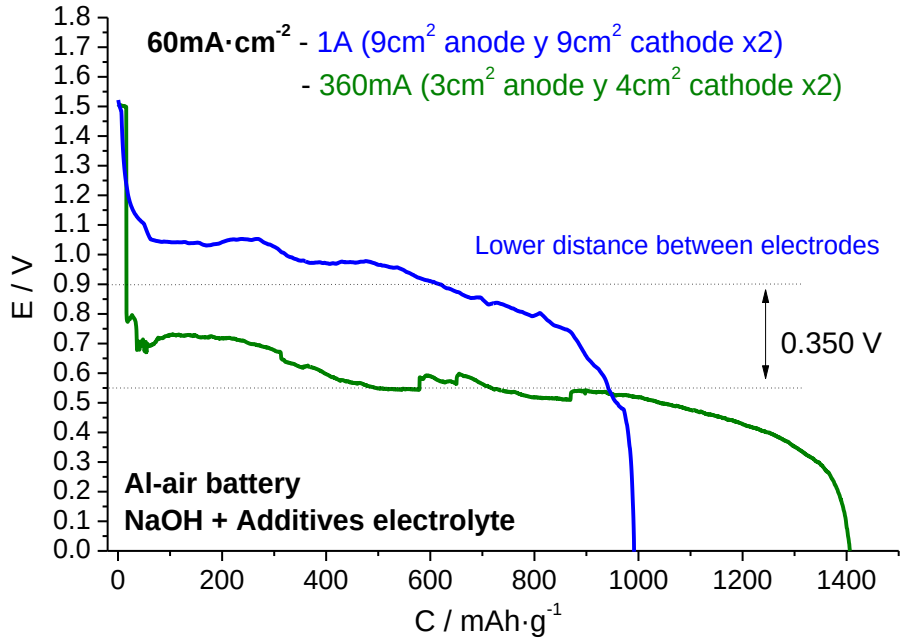

Fig. 4.3.10: Discharge plot of Al7475-air battery with NaOH + additives electrolyte at 60 mA·cm^{-2}, comparison between big and small size cells.

5. Chapter 2: Aluminium-air batteries with neutral pH electrolytes

This point of the work is focused in developing a neutral pH based electrolyte for its use in Al-air batteries. Why neutral pH? As presented before, aluminium in alkaline media suffers from a self-corrosion reaction that consumes active Al mass, water and hydroxyl ions from the electrolyte to from $Al(OH)_3$ and evolve H_2 gas. This parasite reaction makes the standby of an Al-air alkaline cell inviable because of the complete dissolution of the anode, or decrease in the pH of the cell. Additionally, other challenges related to the carbonatation of the alkaline electrolyte as well as, safety issues because of the high amount of evolved hydrogen and corrosive nature of the electrolyte, must be solved.

Saline batteries, as presented in the introduction, were invented many years ago, and nowadays are still in use, like the Mg-air seawater-activated battery. In the case of aluminium batteries, saline battery systems do not result in principle very attractive because of the low potential of the cells, issues related to the partial solubility of the reaction products and the poor performance of the ORR in neutral pH. For overcoming these issues, some efforts were done in the 80s for developing tailored Al alloys that could deliver more electronegative potentials, and higher specific capacities, and some patents were registered with these compositions.

The objective of this work is to use commercially available aluminium alloys as anodes, and so, these alloys are going to be tested in sodium chloride based electrolyte, even if the achieved cell potentials are low.

5.1. Sodium Chloride electrolyte based commercial aluminium alloy-air battery.

5.1.1. Characterisation of commercial aluminium alloys in sodium chloride electrolyte.

In the same way that is being done with the KOH based electrolyte in the first chapter, characterisation of commercial Al alloys in 2 M NaCl is presented in this point. 2 M was the chosen concentration, because it was a common research solution for electrochemical measurements [1,2]. The procedure was the same than the one presented before: hydrogen evolution, mass losses as well as potential evolution were registered at polarisation of 20 to 100 mA·cm^{-2}.

Contrary to what happened in alkaline solution, in neutral pH electrolyte there is no self-corrosion reaction, so by simple immersion of the alloy samples in the electrolyte, there was no corrosion behaviour, hydrogen evolution or Al mass loss. This results an important advantage in order to assembly a commercial cell.

However, during the discharge reaction of the battery, aluminium oxidation, water from the electrolyte is consumed and hydrogen is evolved as product, as explained in the equation 5.1.1.1.

$$\rightarrow Al + OH^- + 2H_2O \rightarrow Al(OH)_3 + H_2 \uparrow \qquad \text{eq. 5.1.1.1}$$

The assembly used for the characterisation was the same than the one for the KOH based ones. That allowed the measurement of the potential while the hydrogen evolution was being registered.

5.1.1.1. Hydrogen evolution at different current polarisations.

The studied alloys were the same than in the previous case, Al2024, Al2024Clad and Al7475.

→ Al2024:

Figure 5.1.1.1.1 shows the hydrogen evolution of Al2024 alloy at polarisation of 20 to 100 mA·cm^{-2}. As it can be seen, the volume of hydrogen evolved increased proportionally to the applied current. This results were logical, because the hydrogen generation was directly related to the oxidation of aluminium. If we look at the total amount of hydrogen evolved, for 100 mA·cm^{-2} the volume was near to 13 ml after 30 minutes. In the case of KOH electrolyte for the same alloy, at 80 mA·cm^{-2}, the volume was 15 ml. So, with this electrolyte, the amount of hydrogen evolved was less during the discharge of the battery, and during the standby was non-existent. This is clearly an important advance. Additionally, if we think about a standard specific current of 20 to 30 mA·cm^{-2}, the hydrogen evolves was just from 2 to 3 ml.

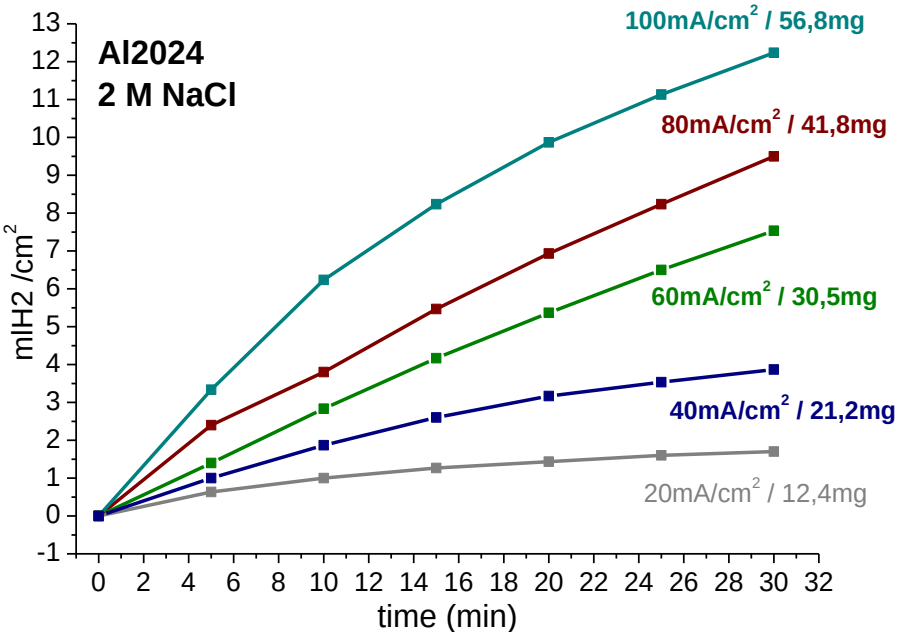

Fig. 5.1.1.1.1: Hydrogen evolution at 20 to 100 mA·cm^{-2} of Al2024 in 2 M NaCl.

→ Al7475:

Figure 5.1.1.1.2 shows the hydrogen evolution of Al7475 alloy at polarisation of 20 to 100 mA·cm^{-2}.

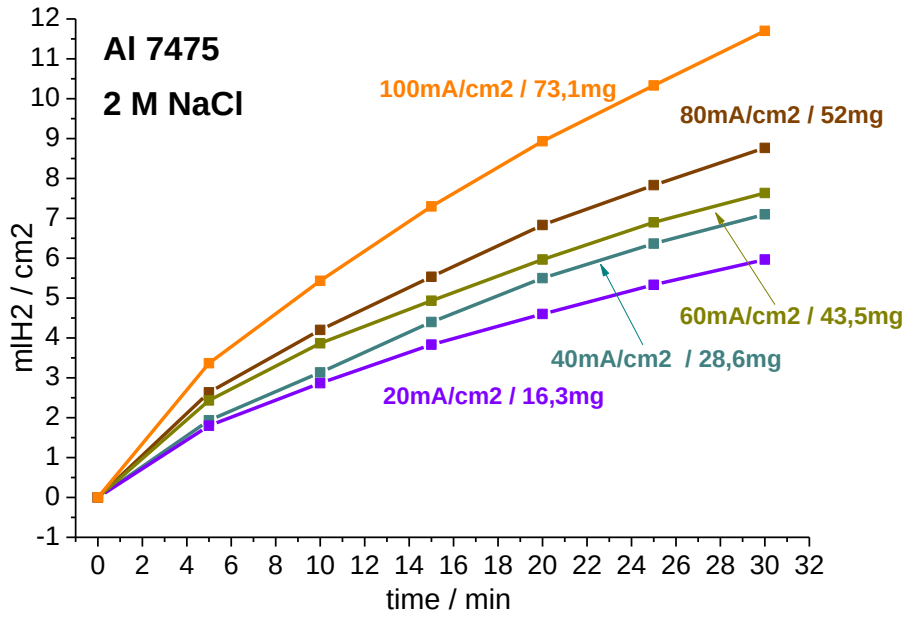

Fig. 5.1.1.1.2: Hydrogen evolution at 20 to 100 mA·cm^{-2} of Al7475 in 2 M NaCl.

For this alloy the evolution of hydrogen was even lower than the one for Al2024. There was no so much difference between 20 to 80 mA·cm^{-2} in term of evolved H_2 volume and weight loss, while at 100 mA·cm^{-2} the H_2 volume increased to 11.5 ml and the Al mass loss was notoriously superior to that at 80 mA·cm^{-2}. In comparison with the performance in KOH, the evolved H_2 was just a half part.

→ Al2024Clad:

Figure 5.1.1.1.3 shows the hydrogen evolution of Al2024Clad alloy at polarisation of 20 to 100 mA·cm^{-2}. For the Al2024Clad alloy the hydrogen evolution was the lower, as well as the consumed aluminium mass. This results were the same for KOH electrolyte, and they are related to the higher corrosion and oxidation protection rate of pure Al. The evolved hydrogen volume for the higher specific current was just 5 ml.

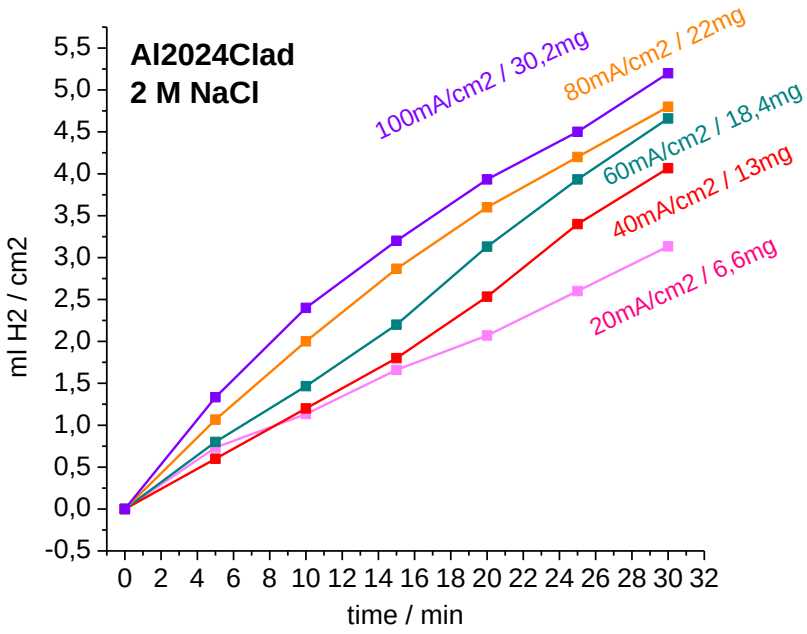

Fig. 5.1.1.1.3: Hydrogen evolution at 20 to 100 mA·cm^{-2} of Al2024Clad in 2 M NaCl.

The results for the three alloys were very promising, because the evolution of hydrogen was not so noticeable as in the case of alkaline based electrolytes. Just by simple visual inspection it was easy to differentiate the bubbling process, which was much more slow and once the test was ended, suddenly disappeared.

5.1.1.2. Mass loss at different current polarisations.

A table is presented with the recompilation of the weights of consumed aluminium during the polarisation measurements, see Table 5.1.1.2.1.

Table 5.1.1.2.1: weight loss of commercial aluminium alloy samples at different current polarisation in 2 M NaCl.

Alloy	***Specific current***				
	20mA/cm²	*40mA/cm²*	*60mA/cm²*	*80mA/cm²*	*100mA/cm²*
Al2024	12,4	21,7	30,5	41,8	58,1
Al7475	16,3	28,6	43,5	52	73,1
Al2024Clad	6,6	13	18,4	22	30,2

Aluminium consumption in mg

There were notable differences between the aluminium consumption for every alloy. Al2024Clad was the one with the lower mass consumptions as well as lower hydrogen evolutions, while for the other two the weight loss was higher. Al7475 presented similar consumptions to Al2024 till 80 mA·cm^{-2} but at 100 mA·cm^{-2} the result was shot up.

The increments in the amount of Al dissolved showed that the unique H_2 generation, as well as unique Al mass loss came from the anode oxidation, and no parallel corrosion reactions were taking place. That is easy to see because the amounts for every alloy doubled when the current was doubled or triple when the current increased by three.

5.1.1.3. Potential evolution at different current polarisations.

The evolution of the potential in NaCl electrolyte was a very important parameter because of the tips commented before. Compared to alkaline environment, were the oxidation potential of aluminium could be as high as -1.7 or -1.8 V *vs* Ag/AgCl, the same alloy in neutral media could present a OCP potential of less than -1 V. This situation difficulted the constitution of a battery with a high voltage performance.

→ <u>Al2024:</u>

Figure 5.1.1.3.1 shows the potential evolution of Al2024 alloy at polarisation of 20 to 100 mA·cm^{-2}. As predicted the potential for this alloys was very low compared to alkaline media. The OCP for Al2024 *vs* Ag/AgCl was just -0.640 V, less than a half of the potential in KOH. Once polarised, the plateaus were very flat and presented voltage values between -0.55 and -0.45 V for current between 20 and 80 mA·cm^{-2}. At 100 mA·cm^{-2} however, the overpotential increased considerably, being the voltage plateau of -0.32 V.

This values resulted very low, so a cell with 2 M NaCl electrolyte should present a low voltage and could operate just at low currents, unless the cathode presented a high voltage value and good response to high currents, which was difficult to happen.

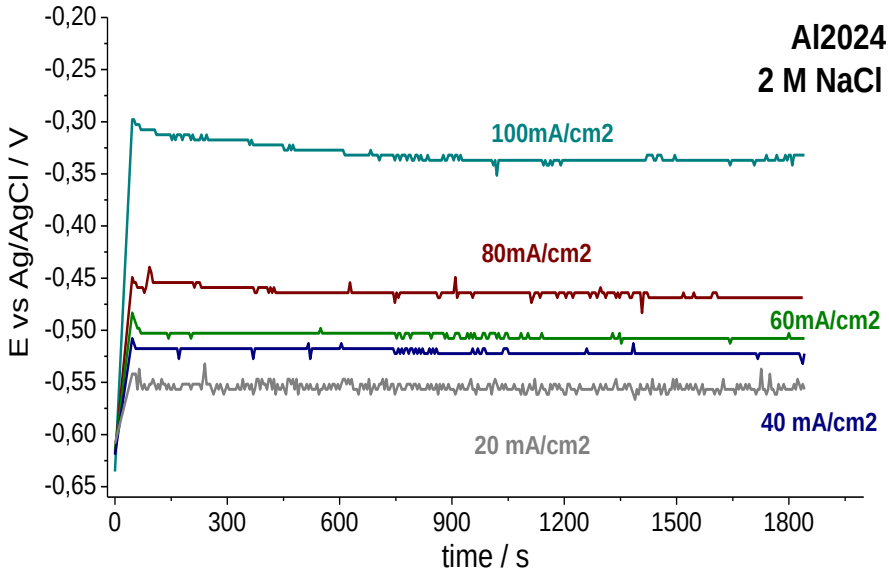

Fig. 5.1.1.3.1: Potential evolution at 20 to 100 mA·cm^{-2} of Al2024 in 2 M NaCl.

→ Al7475:

Figure 5.1.1.3.2 shows the potential evolution of Al7475 alloy at polarisation of 20 to 100 mA·cm^{-2}. In this case the OCP was more electronegative, with a value of -0.78 V.

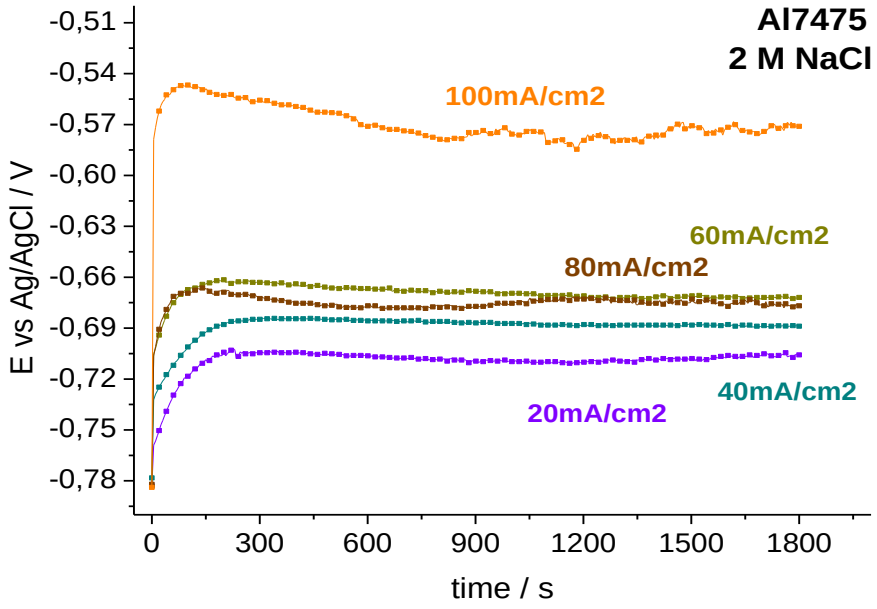

Fig. 5.1.1.3.2: Potential evolution at 20 to 100 mA·cm^{-2} of Al7475 in 2 M NaCl.

Additionally, the overpotentials when polarised were lower, presenting voltage plateaus of -0.7 to -0.66 V from 20 to 80 mA·cm^{-2}. Like in the previous case the voltage dropped to more positive values at the higher specific current, going up to -0.57 V.

This results were still not very flattering, but were better than the ones for Al2024 alloy, which´s OCP was more positive than the voltage plateau of this alloy at 80 mA·cm^{-2}. It was also a good new the flat evolution of the voltage during the tests, which indicated that the final battery could deliver very flat potential plateaus when discharged. This point is very critical in some electric devices that work in a certain voltage value, and low variation of this working potential could affect the normal operation of this devices or even damage them. So even if the resulting voltage of an Al-air cell with NaCl based electrolyte could be low, cells in series could be stacked until the desired voltage.

→ Al2024Clad:

Figure 5.1.1.3.3 shows the potential evolution of Al2024Clad alloy at polarisation of 20 to 100 mA·cm^{-2}. The OCP of this alloy was the higher with a value of -0.92 V, but contrary, once polarised the potentials drop to low values between -0.56 and -0.46 V at 40 to 100 mA·cm^{-2}, and -0.65 V at the measured lower current.

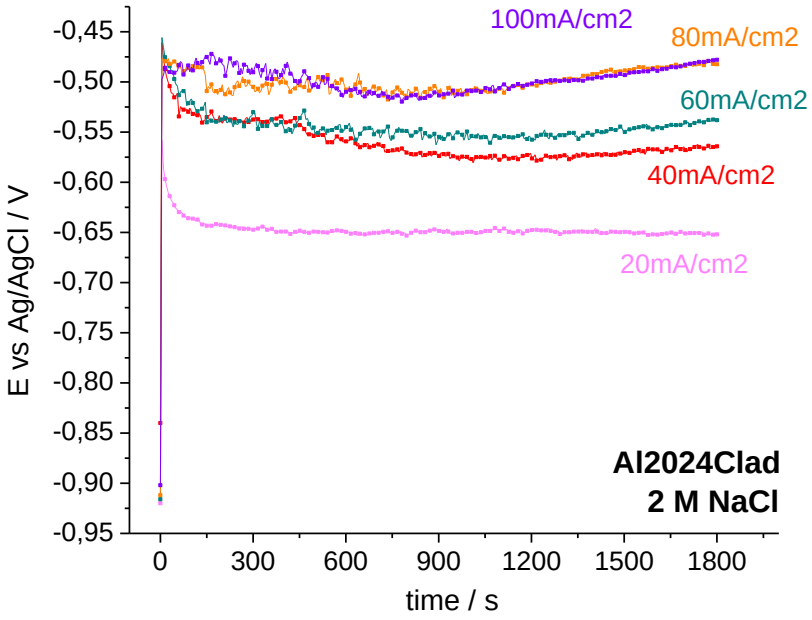

Fig. 5.1.1.3.3: Potential evolution at 20 to 100 mA·cm^{-2} of Al2024Clad in 2 M NaCl.

This results weren't very hopeful, but the advantages of not having corrosion, and the perspective of achieving high specific capacities was enough to try them in Al-air cell.

5.1.2. Sodium chloride electrolyte based commercial aluminium alloy-air battery performance.

For the constitution of the cells 2 M NaCl was the chosen electrolyte and E4A commercial air cathode from *Electric Fuel Ltd.*, the positive electrode. The cell casing used in these experiments were the same used with the NaOH electrolyte, composed of two air cathodes of 4 cm^{-2} and one anode of 3 cm^{-2} by each side. The effect of the electrode distance was not going to be considered even if it being proved to affect in a significant way to the working cell potential.

Al7475 alloy was the chosen commercial aluminium alloy from the previously characterised ones. From bibliography in this field, it was found that the Al1000 series alloys (high aluminium content) performed satisfactorily in chloride based solutions [18] so Al1085 alloy was tested as anode for Al-air batteries. First trials demonstrated that Al1085 alloy delivered more electronegative voltage values than Al7475 for specific current loads lower than 6 $mA \cdot cm^{-2}$, while at higher currents of 10 $mA \cdot cm^{-2}$ this alloys was not able to perform a discharge. The latter makes sense with the different results obtained along this work, being the pure aluminium the best performing anode for low currents, while once exceeded a current value (this limit was different for every electrolyte composition), Al alloys with different compositions demonstrated better performance.

Figure 5.1.2.1 shows the discharge plot of Al1085-air battery at 1 to 10 $mA \cdot cm^{-2}$ current with 2 M NaCl electrolyte. The OCP of the cell was 0.85 V, which is a very low value. Once the discharge began, the potential plateau at 1$mA \cdot cm^{-2}$ was 0.65 V for a specific capacity of 285 $mAh \cdot g^{-1}$. This values were poor but the number of discharging hours was high, near to 38 hours, compared to the values achieved in alkaline electrolytes, maximum 26 hours discharge with the gelled potassium hydroxide electrolyte.

At 6 mA·cm^{-2}, the plateau evolved from 0.55 to 0.45 V for a final discharge of 7.5h and 230 mAh·g^{-1} specific capacity. And at the highest current rate, the cell was not able to perform a clear plateau, and finally died.

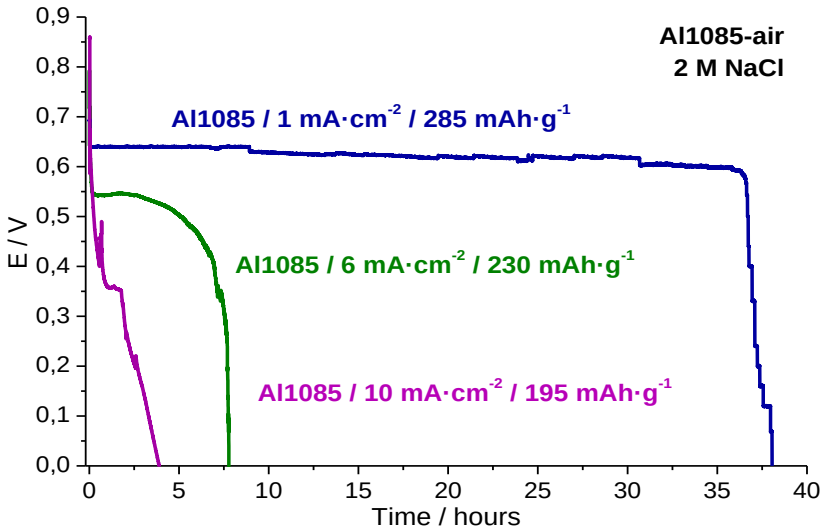

Fig. 5.1.2.1: Discharges of Al1085-air battery with 2 M NaCl electrolyte at 1 to 10 mA·cm^{-2}.

As mentioned before, for currents of 10 mA·cm^{-2}, Al7475 performed a clearer plateau and a much higher discharging time and specific capacity, see Figure 5.1.2.2. As can be seen the working voltage of the Al7475-air cell was very low, between 0.3 and 0.15 V. However, the discharging time was very high, as well as the achieved specific capacity of 540 mAh·g^{-1}.

The better behaviour of the Al7475 at higher current ranges *vs* Al1085 at lower current rates can be explained as the fact that alloying elements like Zn, Mg and Cu (present in the Al7475 alloy) lead to galvanic corrosion in the surface of the anode, that compete with the oxidation of the aluminium at low current rates. To the extent that Al is oxidised, the cited metals get released in the electrolyte originating galvanic pairs that induce the aluminium to corrode, competing with the anodic oxidation. This phenomenon is being presented yet for KOH based batteries, with the particularity that in these alkaline electrolytes, the galvanic pairs even aggravated in a more notable way the self-corrosion of Al, that is nor present in neutral media.

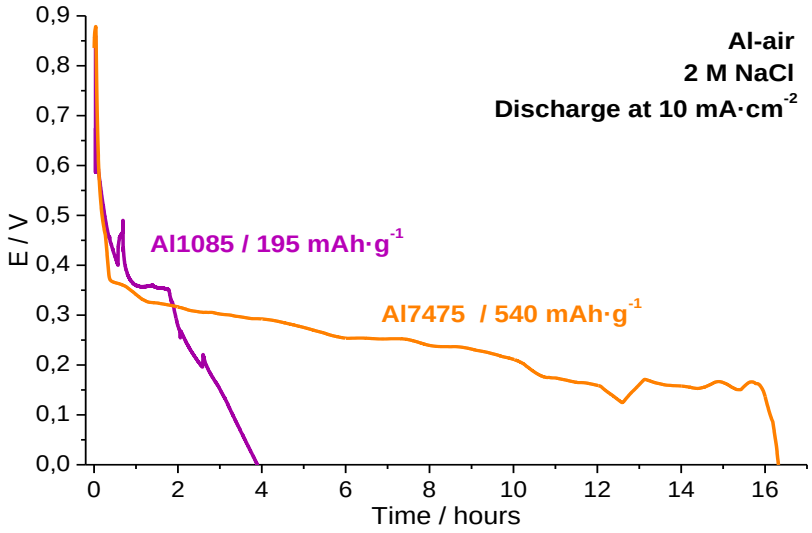

Fig. 5.1.2.1: Discharges of Al-air battery with 2 M NaCl electrolyte at 10 mA·cm^{-2}, with Al1085 and Al7475 anodes.

When the current density is greater, the galvanic pairs are not so dominant compared to Al oxidation, and the discharge performance is enhanced. Additionally, alloying Zn can drag Al to become oxidised, as was demonstrated previously in this work. Contrary, Al1085 alloy (high aluminium content >99.7%) performed better at low current rates due to a cleaner oxidation process, not impeded by secondary processes of the impurities. Fe and Si were found to be less critical for the Al behaviour in neutral media than in alkaline, because even of the intermetallic compounds formed in the Al surface, there is no spontaneous self-corrosion reaction that could take advantage of those weak points.

Even if these results seem to be very bad for the constitution of a viable battery, most of the voltage losses were found to be because of the bad functioning of the cathode. The anode potential at 10 mA·cm^{-2} registered for the Al7475 was -0.74 V, while the one for the cathode was -0.450 to -0.550 V. Normally, the potential of a useful cathode for a battery should be superior to 0 V, so with a well-functioning cathode, the working potential of the cell at this current should be at least 0.8 or 1 V. This voltage value could be even higher if it is considered the distance between electrodes, which in this case was not adjusted. So, a more compact cell design with a better air cathode could improve significantly these results.

Contrary to what we shown for alkaline electrolytes, the dead of the battery was not because of the total dissolution of the Al anode or because the pH decay to non-useful OH^- concentrations due to the self-corrosion. In this case, the end of the discharge was because of the accumulation around the anode of a jelly texture grey compound that impeded the diffusion of OH^- ions coming from the cathode.

As introduced before, aluminium hydroxide, which is a reaction product in alkane and in neutral pH, results completely insoluble in alkaline, while partially soluble in neutral and totally soluble in acid. So, in this NaCl electrolyte, once the aluminium began to oxidise and $Al(OH)_3$ started to be form as reaction product, it got accumulated around the anode and progressively formed a gel, that completely covered the negative electrode. Because of the partial solubility of this compound and its high adhesion to the Al surface (Al-$Al(OH)_3$-Al_2O_3 mix), it remained attached to the anode and adsorbed some water molecules to form H_5AlO_4, called aluminium hydroxide hydrate. This gel around the anode difficulted the arrival of hydroxyl ions until the anode couldn´t get oxidised no more.

Thus, for overcoming this situation a carbon treatment to the anode surface was proposed. The operation of this carbon treatment was to create a layer all over the Al surface with low adhesion to the formed $Al(OH)_3$, and enough porous not to impede the contact of the Al with the electrolyte.

5.1.3. Sodium chloride electrolyte based carbon treated commercial aluminium alloy-air battery performance.

The presented treatment was a very easy process that could be applied to any alloy. It consisted of a slurry of a carbonaceous material which was pasted into the electrode surface. The slurry was prepared by mixing 2 parts of carbonaceous material, 1 part of a binder and 7 parts of a solvent (by weight). The binder was PvDF (polyvinylidene fluoride), which is presented as a withe fine powder, and the solvent was NMP (N-Methyl-2-pyrrolidone). As carbonaceous materials CB (Carbon Black), PG (pyrolytic graphite) and rGO (reduced Graphene Oxide) were tested, all of them in powder form.

Once the paste was dispensed in the Al anode, the solvent was evaporated in an oven at 120ºC for 12 hours, resulting a thin homogeneous black layer covering the Al anode. For higher area electrodes, the ratio of the solvent was increased to get an ink instead of a paste, which was sprayed over the electrode. This technique resulted very easy and cheap.

Figure 5.1.3.1 shows the discharge behaviour of an Al1085-air cell with and without carbon treatment at 1 and 6 mA·cm^{-2}. For the first tries CB was the chosen carbon, because it results quite cheap, abundant and easily available. Al1085 alloy treated with CB at a current density of 1 mA·cm^{-2} performed two times longer discharge than the one without coating, resulting in a specific capacity of 630 against 285 mAh·g^{-1}. The cell potential was also slightly higher reaching a flat plateau at 0.7 V till the end of the discharge. This flat evolution was previously seen in the polarisation curves and results one of key points of this system.

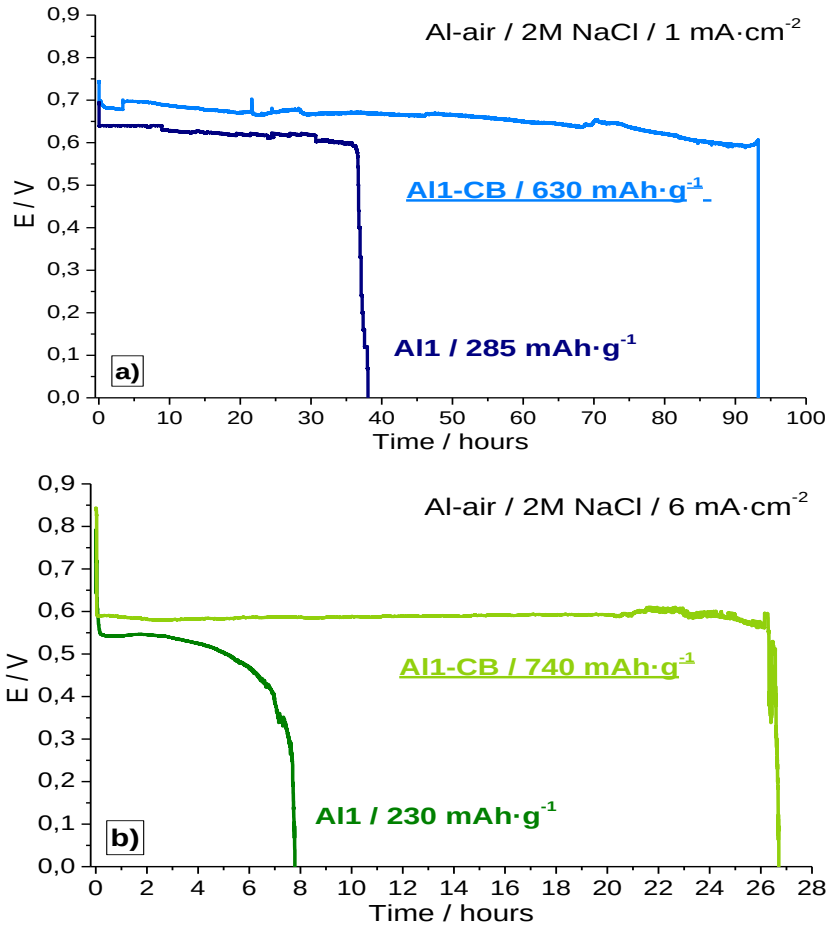

Fig. 5.1.3.1: Discharge plot of Al1085-air cell with vs without carbon cover in 2 M NaCl electrolyte at constant current of: a) 1 mA·cm^{-2}; b) 6 mA·cm^{-2}.

In the Fig. b) applied current density was 6 $mA \cdot cm^{-2}$ and it resulted in an even higher improvement of the discharging time (around three times longer). The potential of the cell evolved quite flat in 0.6 V and suddenly decayed because of the complete consumption of the electrolyte water according to the anodic oxidation reaction presented before, see eq. 5.1.1.1.

The final appearance of the cell was a completely crystallized $Al(OH)_3$ + NaCl mix covering both electrodes, because of the total consumption of the water. On the contrary, the performance of Al1085 without carbon treatment at 1 and 6 $mA \cdot cm^{-2}$, was impeded because of the total covering of the aluminium anode by the aluminate gel, as exposed before, without total water consumption.

Figure 5.1.3.2 shows a scheme of the comparison between the Al-air cell discharge with and without carbon treatment and how does it influence in the formation of the gel. The adherence of the aluminate into the CB layer results significantly lower than the one on metallic aluminium surface (Al-$Al(OH)_3$-Al_2O_3 mix). Due to this property and the higher density of the formed aluminium hydroxide hydrate + aluminium hydroxide mix, compared to the electrolyte, the gel tends to precipitate not rounding the anode, and not limiting the discharge of the battery.

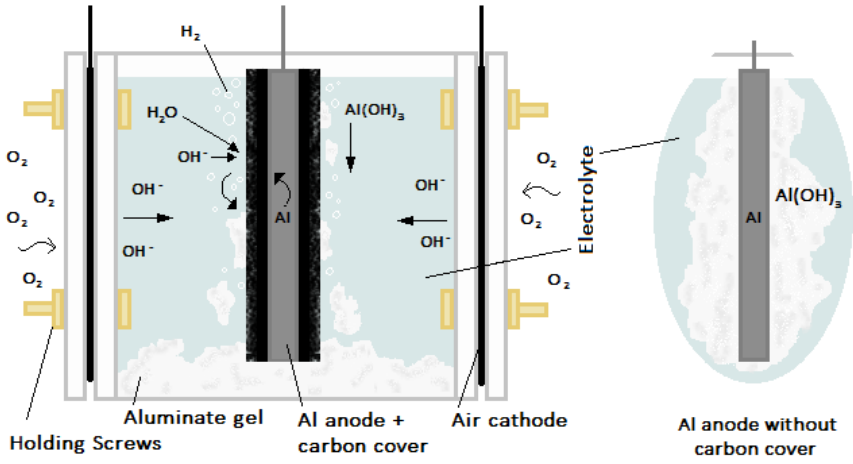

Fig. 5.1.3.2: Schematic representation of $Al(OH)_3$ accumulation in Al-air neutral pH cell. Anode behaviour with and without carbon treatment.

Through this method the partial solubility of the $Al(OH)_3$ remains unchanged, but it permits the sedimentation of the cited compound and so, in advanced cell designs the formed product could be extracted from the button of the cell continuously, limiting not at all the discharge behaviour. The extracted gel could be then treated to recover water and metallic aluminium as described S. Zaromb for a primary Al-air alkaline battery in the early 60s [19].

The effect of the carbon treatment was also proved for the Al7475-air battery at higher current of 10 $mA \cdot cm^{-2}$, see Figure 5.1.3.3. As mentioned before, the potential of the Al1085-air cell decayed quickly, performing a plateau of just 1 hour near 0.35 V. Nonetheless CB treated Al7475-air cell performed the higher specific capacity achieved in the NaCl electrolyte of 1210 $mAh \cdot g^{-1}$. Cell potential get stabilised at 0.4 mV for a plateau of 32 hours and a final drop to 0.2 V due to the release of an aluminium portion, and finally the discharge ended. Compared to that without carbon treatment the performance was 2 times longer and the potential evolution more stable. The latter proved the effectiveness of the proposed carbon treatment regardless of the employed aluminium alloy. In this case the water of the electrolyte was not completely consumed, and the reason of the battery dead was the break of the aluminium anode due to the high amount of Al mass consumed.

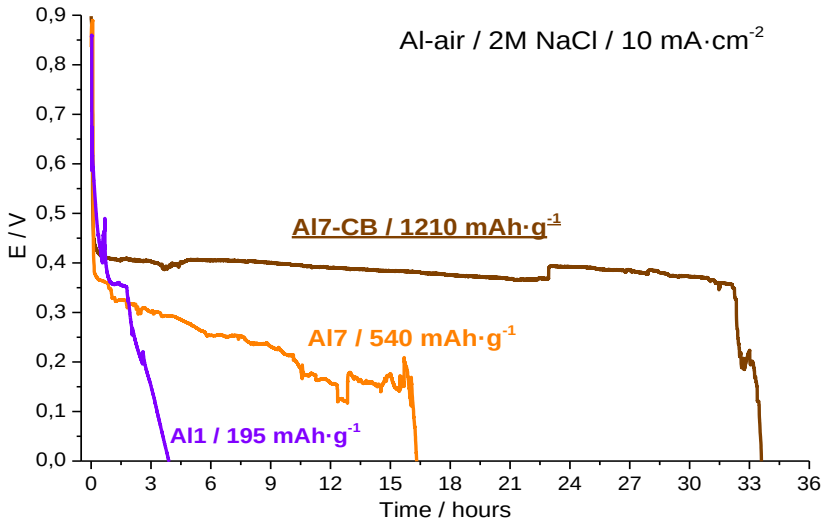

Fig. 5.1.3.3: Discharge plot of Al7475-air cell with vs without carbon cover in 2 M NaCl electrolyte at constant current of 10 $mA \cdot cm^{-2}$.

The better behaviour of the anodes with the carbon treatment was also proved by polarisation curves of the Al1085 and Al7475 alloys, see Fig. 5.1.3.4. These measurements were carried out at a scan rate of 1mV·s^{-1} from the OCP toward cathodic potentials. The current response was registered.

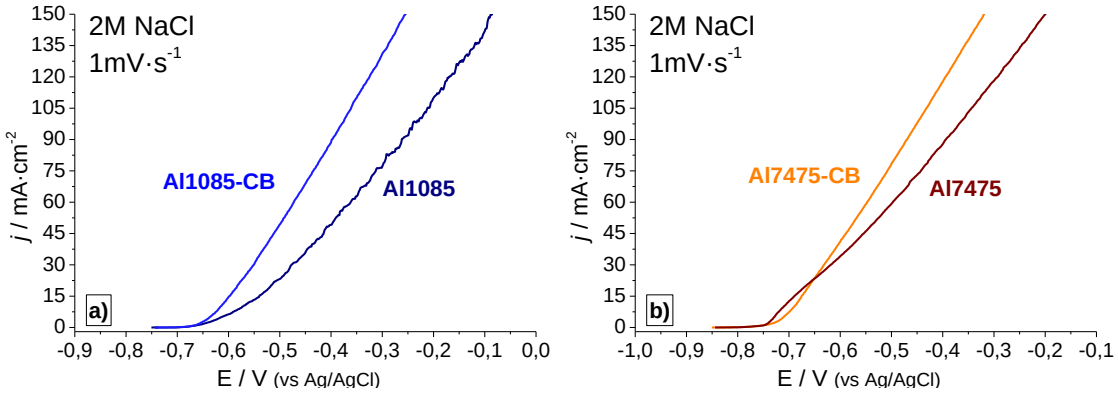

Figure 5.1.3.4: Polarisation curves, at scan rate of 1 mVs^{-1} and 298K in half-cell with and without carbon layer, of: a) Al1085; b) Al7475.

In both cases, Fig. a) and b), the current of carbon treated alloys increased rapidly. Nevertheless, in the case of the bare alloys, the potential of the Al was moved to more positive values for same specific current values. This behaviour is closely related to the accumulation of aluminate in the electrode surface, which finally causes a higher overpotential in the anode, and consequently in the Al-air battery.

The latter is clearly seen in the polarisation curve of the Al7475 alloy without treatment, that started delivering higher currents than the carbon treated one, but when the potential was -0.65 V there was a cross where the tendency changed. This change was due to the beginning of the gel formation around the electrode.

Table 5.1.3.1 reports a brief summary of different aluminium anodes studied by some investigation groups for Al-air batteries with neutral pH electrolyte. Tailored aluminium alloys seems to enhance in a notable way the performance of the cell, achieving discharges of 20 mA·cm^{-2} with high cell potentials above 1.2 V. Nevertheless, the price of the presented alloy results quite high and actually non-commercial. In the case of pure aluminium (5N), the behaviour of the cell is like the one with Al7475, however the price of this alloy results two orders of magnitude cheaper. A similar result for

commercial Al 1050 alloy is also reported, but discharging times and available currents are lower.

Table 5.1.3.1: Current densities, E_{Cell}, discharging time and price comparison of different Al-air neutral pH batteries in bibliography.

Al anode	Electrolyte	Current (mA·cm^{-2})	E_{Cell} (V)	Time (hours)	Price (€/kg)	Assignee	Ref
5N Al - UFG	2M NaCl	10	0.388	3*	>100	L. Fan et al.	[20]
5N Al - CG			0.399				
Al-Mg-Ga-Sn-Mn	2M NaCl	20	1.236	5*	>200	J. Ma et al.	[21]
Al-Mg-Ga-Sn			1.185				
Al-Mg-Zn-Ga-Sn			1.09				
Al 1050	NaCl	1	0.67	62	1.4	R. Mori	[18]
		2	0.64	28			
		3	0.58	7			
Al 1085	2M NaCl	1	0.65	94	1.2	Present work	
		6	0.6	26			
Al 7475		10	0.4	34	1.6		

*Partial discharge

The next steps of the work were trying to improve or to see the effect of other carbonaceous materials in the carbon treatment. As commented before, Carbon Black was the first used carbon, but PG (pyrolytic Graphite) and rGO (reduced Graphene Oxide) were also probed.

The preparation of the carbon ink/paste was the same, and the obtained coating presented similar mechanical resistance. Figure 5.1.3.5 shows the discharge behaviours of Al1085 and Al7475 treated with CB, rGO and PG at 1 and 10 mA·cm^{-2}.

Graphene treated alloys performed a quite similar profile to the ones with Carbon Black. In both cases, 1 and 10 mA·cm^{-2}, the discharging time was slightly lower due to a small variation in the thickness of Al plate and consequently the weight. The rGO covered anodes performed quite flat potential plateaus that could be related to: (a) the lower particle size compared to CB, that permit a good dispersion in NMP and the obtained paste resulted easier to dispense homogeneously in the aluminium anode; and (b) the more laminar structure of the material, that generates preferential paths for the chemical species inlet and evacuation.

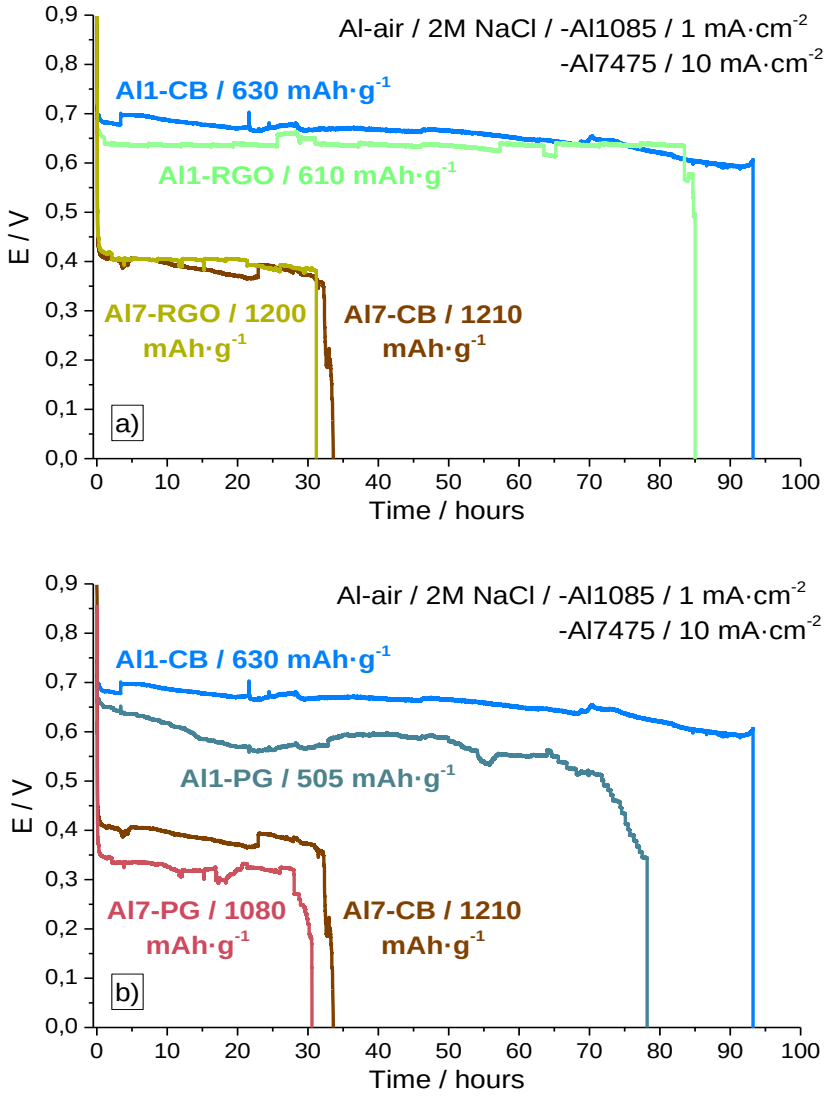

Figure 5.1.3.5: Discharge plot of Al1085 and Al7475-air cells with carbon treatment at constant current density of 1 and 10 mA·cm^{-2}, respectively: a) CB vs rGO; b) CB vs PG.

On the contrary, PG treated anodes demonstrated lower cell potential and specific capacity. This was found to be because of the high porosity of the material that gave rise to the accumulation of aluminate in the pores. In this way, even if the precipitation of the aluminate was possible, a little amount of $Al(OH)_3$ get fixed in the surface of the negative electrode hindering the arrival of hydroxyl ions and evacuation of new formed aluminate. Besides, PG resulted difficult to dispense or spray because its bad dispersion in the paste, and so, the obtained layer was thicker than the ones with CB or rGO.

A second pathway was also probed trying to enhance the performance of the carbon treatment: this approach consisted in the study of the ratio of binder in the paste. The principal function of the binder was to ensure a good physical adhesion of the paste in the Al surface, but the high amount used could be adding an extra resistance to the anode performance.

New proportions of carbon to binder, 4:1 and 9:1, were tested to ensure that the high initial binder content (2:1) was not limiting the movement of hydroxyl ions and the evacuation of aluminium hydroxide. First attempt with 9:1 proportion resulted unsuccessful. The carbon layer presented very low mechanical resistance and get detached just by manipulation of the negative electrode to assemble the cell. On the contrary the 4:1 proportion, allowed manipulation and presented similar resistance to scratching and adhesion to those of the initial ratio.

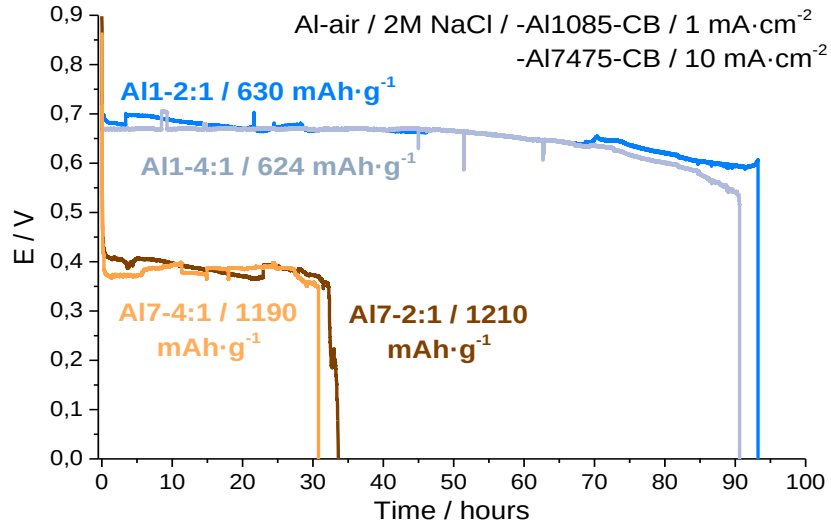

Figure 5.1.3.6: Discharge plot of Al1085 and Al7475-air cells with CB cover at constant current density of 1 and 10 mA·cm^{-2}, respectively: 4:1 vs 2:1 binder proportion.

Figure 5.1.3.6 shows the discharge behaviour of Al1085 and Al7475 treated with CB, 2:1 *vs* 4:1 proportion, at 1 and 10 mA·cm^{-2} respectively. There were no significant differences in the voltage plateaus and discharging times so it was concluded that the binder quantity was only affecting the adhesion and resistance of the cover. So, once reached a minimum proportion of PVdF in order to ensure the mechanical properties,

the electrochemical behaviour of the cell was not being affected by the binder percentage.

Once explored the pathways for optimising the carbon treatment, the binder proportion was fixed in 2:1 to ensure a maximum adhesion of the carbon layer and the carbonaceous material selected was CB. Despite the little advantage of the rGO *vs* CB, the price of the last resulted more than 100 times cheaper and the scalability more feasible. Considering the achieved results, it was decided to develop a new cell that could reach higher voltages for more realistic applications. A 3D printed 4s1p battery was designed, see Figure 5.1.3.7, to rise the cell potential up to 3.4 V in open circuit. The battery was based in the previous unity cells pattern but the positive-negative electrode proportion was reduced to 1:1 to ease the design. The four compartments were completely divided to avoid electrolyte transfer, and the upper side of the cell was silkscreened to ensure the isolation between the copper electrical contacts.

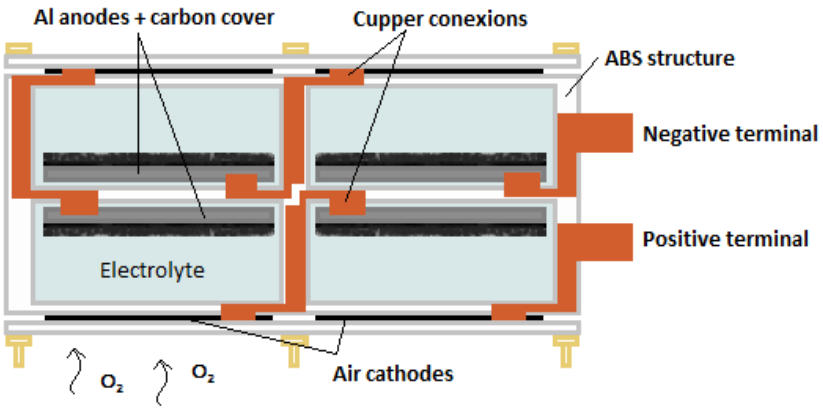

Figure 5.1.3.7: Schematic representation of 3D printed 4s1p Al-air battery.

CB treated Al1085 was the chosen anode for this battery because the selected current density for the test was 5 $mA \cdot cm^{-2}$ to achieve a high battery potential above 2V. Besides, the manipulation of the Al plate resulted easier because the high aluminium content, more malleable than Al7475.

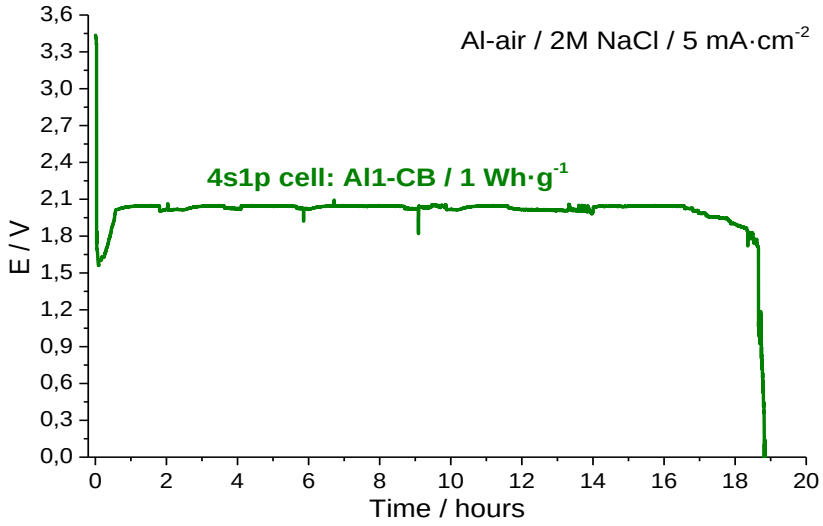

Figure 5.1.3.8: Discharge plot of 3D printed 4s1p Al1-air battery at a constant current density of 5 mA·cm^{-2}.

Figure 5.1.3.8 shows the discharge of the 4s1p battery at 5 mA·cm^{-2}, using Al1085 alloy as anode treated with CB carbon cover. The evolution of the battery potential resulted quite flat with a constant value of 2 V during 18 hours till a sudden final decay. This battery achieved a specific capacity of 480 mAh·g^{-1} per gram of aluminium in a discharge of 5 mA·cm^{-2}, which corresponds to an energy of 1Wh·g^{-1}.

Resulting battery potential did not correspond to the theoretical data achieved with the unity cells at 6 mA·cm^{-2}. It was expected that the total cell potential once polarized at 5 mA·cm^{-2} to be at least 2.4 V. The latter is related to losses because of the electric contacts and the worst operation of the air electrodes in a proportion 1:1 to anodes, without oversizing. However, this cell was just a coarse approximation to a more realistic saltwater activated battery, with the unique aim of proving the viability of the system.

So, we can affirm that the mix between the double cathode configuration, the neutral chloride based electrolyte and the carbon treatment on aluminium commercial alloys could be a good approach for the developing of commercially available seawater activated Al-air batteries. This mix presented some advantages like the non-corrosive nature of the electrolyte, and possibility to storage the Al anode in contact with the electrolyte; the high specific capacity of the used aluminium; and the flat potential

evolution of the cell, which makes it very successful for certain electronic devices. On the other hand, some issues must be surpassed: the low potential of the cell, which could be improved using tailed alloys, better air cathodes and better cell designs (less distance between electrodes); the exhaustion of the electrolyte water, what makes necessary a refill every certain time; and, the medium-low power rate, able to deliver a maximum of 10 $mA \cdot cm^{-2}$ in the case of the materials used in this work.

The latter along with the simple 4s1p 3D printed battery structure, and easily reproducible and scalable methods could give raise to the development of simple and robust sea water activated commercial batteries.

6. References

[1] D.R. Egan, C. Ponce de León, R.J.K. Wood, R.L. Jones, K.R. Stokes, F.C. Walsh, Developments in electrode materials and electrolytes for aluminium–air batteries, Journal of Power Sources. 236 (2013) 293–310. doi:10.1016/j.jpowsour.2013.01.141.

[2] M.A. Rahman, X. Wang, C. Wen, High Energy Density Metal-Air Batteries: A Review, Journal of the Electrochemical Society. 160 (2013) A1759–A1771. doi:10.1149/2.062310jes.

[3] J. McBreen, E. Gannon, The electrochemistry of metal oxide additives in pasted zinc electrodes, Electrochimica Acta. 26 (1981) 1439–1446. doi:10.1016/0013-4686(81)90015-3.

[4] J. Cheng, Z. Zhang, Y. Zhao, W. Yu, H. Hou, Effects of additives on performance of zinc electrode, Transactions of Nonferrous Metals Society of China. 24 (2014) 3551–3555. doi:10.1016/S1003-6326(14)63500-7.

[5] Z. Zhang, C. Zuo, Z. Liu, Y. Yu, Y. Zuo, Y. Song, All-solid-state Al-air batteries with polymer alkaline gel electrolyte, J. Power Sources 251 (2014) 470-475.

[6] Y. Li, H. Dai, Recent advances in zinc–air batteries, Chem. Soc. Rev. 43 (2014) 5257–5275. doi:10.1039/C4CS00015C.

[7] M.L. Doche, F. Novel-Cattin, R. Durand, J.J. Rameau, Characterization of different grades of aluminum anodes for aluminum/air batteries, Journal of Power Sources. 65 (1997) 197–205. doi:10.1016/S0378-7753(97)02473-7.

[8] Q. Li, N.J. Bjerrum, Aluminum as anode for energy storage and conversion: a review, Journal of Power Sources. 110 (2002) 1–10. doi:10.1016/S0378-7753(01)01014-X.

[9] Nisancioglu, K, Corrosion of aluminium alloys, Proceedings of ICAA3. 3 (1992) 239–259.

[10] S. Gustafsson, Corrosion properties of aluminium alloys and surface treated alloys in tap water, (2011) UPTEC K 11028

[11] J. B. Wang, J. M. Wang, H. B. Shao, X. T. Chang, L. Wang, J. Q. Zhang, C. N. Cao, the corrosion and electrochemical behavior of pure aluminum in additive-containing alkaline methanol–water mixed solutions, Materials and Corros. 60 (2009) 269-273

[12] Y.-J. Cho, I.-J. Park, H.-J. Lee, J.-G. Kim, Aluminum anode for aluminum-air battery - Part I: Influence of aluminum purity, Journal of Power Sources. 277 (2015) 370–378. doi:10.1016/j.jpowsour.2014.12.026.

[13] I.-J. Park, S.-R. Choi, J.-G. Kim, Aluminum anode for aluminum-air battery – Part II: Influence of In addition on the electrochemical characteristics of Al-Zn alloy in alkaline solution, Journal of Power Sources. 357 (2017) 47–55.

[14] A.A. Mohamad, Electrochemical properties of aluminum anodes in gel electrolyte-based aluminum-air batteries, Corrosion Science 50 (2008) 3475-3479

[15] Z. Zhang, C. Zuo, Z. Liu, Y. Yu, Y. Zuo, Y. Song, All-solid-state Al–air batteries with polymer alkaline gel electrolyte, J. Power Sources 251 (2014) 470-475

[16] C. Li, W. Ji, J. Chen and Z. Tao, Microfluidic Aluminum-air Cell with Methanol-based Anolyte, Chem. Mater. 19 (2007) 5812–5814

[17] M. Pino, C. Cuadrado, J. Chacón, P. Rodríguez, E. Fatás, P. Ocón, The electrochemical characteristics of commercial aluminium alloy electrodes for Al/air batteries, Journal of Applied Electrochemistry. 44 (2014) 1371–1380. doi:10.1007/s10800-014-0751-6.

[18] R. Mori, Capacity recovery of aluminium–air battery by refilling salty water with cell structure modification, J. Appl. Electrochem. 45 (2015) 821-829.

[19] L. Bockstie, D. Trevethan, S. Zaromb, Control of Al Corrosion in Caustic Solutions, Journal of The Electrochemical Society. 110 (1963) 267. doi:10.1149/1.2425727.

[20] L. Fan, H. Lu, J. Leng, Performance of Fine Structured Aluminum Anodes in Neutral and Alkaline Electrolytes for Al–Air Batteries, Electrochim. Acta 165 (2015) 22-28.

[21] J. Ma, J. Wen, J. Gao, Q. Li, Performance of Al–0.5 Mg–0.02 Ga–0.1 Sn–0.5 Mn as anode for Al–air battery in NaCl solutions, J. Power Sources 253 (2014) 419-423.

CONCLUSIONS

7. Conclusions

In this work the study of commercial aluminium alloys as anodes for aluminium-air batteries is being performed. Different types of electrolytes, alkaline pH, neutral pH and non-water based, have been presented. The obtained results can be concluded as follows:

- With 0.2 M KOH + ZnO electrolyte specific capacities of 120 $mAh \cdot g^{-1}$ were achieved in discharges up to 12.8 $mA \cdot cm^{-2}$ with the Al2024 alloy.
  - → The competition between aluminium oxidation and aluminium self-corrosion in the Al surface was enunciated and explained.
  - → Al mass consumption, as well as pH decay because of self-corrosion was found to be limiting factor of this system.

- With the gelled KOH + ZnO electrolyte specific capacities up to 430 $mAh \cdot g^{-1}$ were achieved in discharges up to 8.4 $mA \cdot cm^{-2}$ with the Al7475 alloy.
  - → The corrosion inhibition effect of ZnO was exposed, as well as how galvanic pairs between Al and metallic alloying elements influence the discharge behaviour.
  - → Aluminium hydroxide accumulation in the gel-electrode interface was found to be limiting factor of this system.
  - → Pure aluminium cladded Al7475Clad alloy was found to perform larger discharges at low current rates, while Al7475 uncladded performed better at higher current rates. This was found to be because of the dissolution of the galvanic pairs ones reached certain current value.

- With the NaOH + additives electrolyte the higher specific capacities up to 1400 $mAh \cdot g^{-1}$ were reached in discharges of 83.3 $mA \cdot cm^{-2}$ with the Al7475 alloy.

→ This electrolyte formulation presented a high corrosion inhibition behaviour, as well as successful properties for an Al based energy storage system infrastructure.

→ The complete displacement of self-corrosion was found at currents superiors to 45 $mA \cdot cm^{-2}$ in this electrolyte, and additives were found crucial for aluminium hydroxide crust dissolution.

→ An 8.2 Ah battery was assembled, able to discharge at C/10 rate (1A), with a voltage near to 1 V.

→ The distance between electrodes was found to be an influential factor in cell voltage.

- With 2 M NaCl electrolyte high specific capacities of 1210 $mAh \cdot g^{-1}$ were achieved at discharges of 10 $mA \cdot cm^{-2}$ with the carbon treated Al7475 alloy.

  → Hydrogen evolution in neutral pH electrolyte was found to be notably lower than in alkaline pH, and during standby of the cell there was no H_2 bubbling.

  → Accumulation of aluminium hydroxide around the anode was found to the be limiting factor of this system, and a carbon treatment was proposed to avoid this issue.

  → The carbon treatment multiplied in three times the discharge of Al-air batteries for achieving high specific capacities.

  → Carbon Black was found to present the best price to performance ratio in the carbon treatment, and the ratio of the binder was found not to influence the electrochemical behaviour.

So, as final conclusion:

The use of cheap and abundant commercial Al alloys in Al-air batteries could be the key for an aluminium based energy storage infrastructure, supported by the large know-how of Al industry.

ANNEXES

8. Annexes

Publications and patents related to this work.

→ M. Pino, C. Cuadrado, J. Chacón, P. Rodríguez, E. Fatás, P. Ocón, The electrochemical characteristics of commercial aluminium alloy electrodes for Al/air batteries, Journal of Applied Electrochemistry. 44 (2014) 1371–1380.

→ M. Pino, J. Chacón, E. Fatás, P. Ocón, Performance of commercial aluminium alloys as anodes in gelled electrolyte aluminium-air batteries, Journal of Power Sources. 299 (2015) 195–201.

→ M. Pino, D. Herranz, J. Chacón, E. Fatás, P. Ocón, Carbon treated commercial aluminium alloys as anodes for aluminium-air batteries in sodium chloride electrolyte, Journal of Power Sources. 326 (2016) 296–302

→ P. Rodríguez, J. Chacón, E. Fatás, P. Ocón, M. Pino, Celda electroquímica de aluminio-manganeso, Patent number: ES2540171 A1, (2015).